On the Improvement of Positioning in LTE with Collaboration and Pressure Sensors

Kevin P. McDermott

Thesis submitted to the Faculty of the
Virginia Polytechnic Institute and State University
in partial fulfillment of the requirements for the degree of

Master of Science
in
Electrical Engineering

R. Michael Buehrer, Chair
Vuk Marojevic
Carl Dietrich

May 6, 2015
Blacksburg, Virginia

Keywords: localization, collaborative position location, communications, geolocation, UTDOA

On the Improvement of Positioning in LTE using Collaboration and Pressure Sensors

Kevin P. McDermott

ABSTRACT

The ability to find the location of a mobile user has become of utmost importance. The demands of first responders necessitates the ability to accurately identify the location of an individual who is calling for help. Their response times are directly influenced by the ability to locate the caller. Thus, applications such as Enhanced 911 and other location-based services warrant the ability to quickly and accurately calculate location. The FCC has also put in place a timeline for indoor location accuracy requirements that must be met by the mobile communications service providers. In order to meet these requirements, there are many means of performing indoor geolocation that require research; in this thesis two specific methods of identifying the location of a user will be investigated.

In the first part, the indoor localization of a target, whose exact location is unknown, in a LTE network is studied. In this problem the time difference of arrival of the LTE uplink signals sent from the target to an observer are used as the means to estimate the target position. The two-dimensional location of a user is then estimated through the use of a nonlinear least-squares algorithm. To improve this approach, a cooperative localization technique in uplink LTE is proposed in which the User Equipment (UE) communicates with base stations as well as other handsets. Through simulated results it is shown that utilizing collaboration can improve location estimation and outperform non-collaborative localization.

In the second part, the indoor localization of a target, focusing on its third dimension or elevation, is studied through the use of barometric pressure sensors in mobile handsets. Finding the third dimension of location, or the correct height above the ground level which equates to the floor in a building that a UE is on, cannot be performed with two-dimensional measurement models. For this problem, the pressure sensors are used to accurately find an immediate pressure measurement and allow for the altitude of a handset to be calculated.

This altitude can be translated into an estimation for a specific floor of a building given the use of a ground floor pressure reference. Through simulation results it is then shown that the accuracy of third dimension or indoor-floor localization can be improved with the use of collaborative pressure sensors of other mobile handsets.

Dedication

This thesis is dedicated to my parents, Todd and Leslie McDermott. I would not have been able to reach where I am today without your love and support. You are both a true inspiration and I thank you for pushing me to always be my best. Love you always and forever.

Acknowledgments

Firstly, I want to acknowledge and thank my advisor Dr. Michael Buehrer for his vision and support ever since my junior year of my undergraduate studies at Virginia Tech when I joined the BS/MS program. Through his guidance and dedication, I was able to achieve my Master's degree.

I also want to thank my brother, Kyle McDermott, for lending a hand and pushing me to be better even when he thought he wasn't capable.

Finally, I have to thank my truly indispensable fellow students and friends at Virginia Tech who were always willing to help including Reza Vaghefi, Matt Carrick, Javier Schloemann, SaiDhiraj Amuru, Chris Headley, Daniel Jakubisin, Jeffrey Poston, Daniel Ridenour, Cody Hicks, Hilda Reynolds, and Matt Critz.

Contents

List of Figures

Tables

Abbreviations

3GPP	3rd Generation Partnership Projecct
AECID	Adaptive-Enhanced-Cell ID
A-GNSS	Assisted-Global-Navigation-Satellite-System
ALE	Adaptive Line Enhancer
AOA	Angle-of-Arrival
CRLB/CRB	Cramér-Rao Lower Bound / Cramér-Rao Bound
CRS	Cell-specific Reference Signal
DFT	Discrete Fourier Transform
DOA	Difference-of-Arrival
D2D	Device to Device
E-CID	Enhanced-Cell ID
ENodeB/eNB	Evolved Node B
E-SMLC	Evolved Serving Mobile Location Center
ETU	Extended Typical Urban model
GNSS	Global Navigation Satellite System
GPS	Global Positioning System
HVAC	Heating, Ventilating, and Air Conditioning
IFFT	Inverse Fast-Fourier Transform
IOT	Interference-over-Thermal
LMA	Levenberg-Marquardt algorithm (LMA)
LMU	Location Measurement Unit

LOS	Line-of-Sight
LTE	Long Term Evolution
MEMS	Micro-Electro-Mechanical System
ML	Maximum Likelihood
NLOS	Non-Line-of-Sight
NLLS	Nonlinear Least Squares
OTDOA	Observed-Time-Difference-of-Arrival
PRS	Positioning Reference Signal
QPSK	Quadrature Phase-Shift Key
RF	Radio Frequency
RMS	Root Mean Square
RSS	Received Signal Strength
RSTD	Reference Signal Time difference
SC-FDMA	Single Carrier Frequency Division Multiple Access
SINR	Signal to Interference Noise Ratio
SRS	Sounding Reference Signal
TA	Time Advance
TDOA	Time-Difference-of-arrival
TOA	Time-of-Arrival
UE	User-Equipment
U-TDOA	Uplink Time-Difference-of-Arrival

Chapter 1

Introduction

Determining the location of mobile handset or cellphone, known as user-equipment (UE) according to the 3rd Generation Partnership Project (3GPP), is highly useful in today's society for a variety of reasons. Location-aware technologies have applications in many aspects of commercial, public safety, and military sectors. Some specific applications include animal-tracking, proximity-based advertising, and emergency call services and new applications are becoming apparent with each passing day. While location-based services can be performed with a variety of methods, the ability to perform geolocation (also known as localization or positioning) techniques in a Long Term Evolution (LTE) network has taken precedence given the widespread use of the particular cellular network. The main driving factor of being able to geo-locate a UE on a LTE network is its requirement as a part of the nationwide emergency number system, referred to as Enhanced 911 (E911) calls, in which all US mobile carriers are required to find the location of a cellphone to within a specified accuracy.

This work follows what is considered the primary application of geolocation; meeting E911 requirements. The main scenario assumed here is an emergency scenario in which there is at least one mobile device inside a multi-story building and this mobile device needs to be quickly and accurately located. It is assumed that within the immediate surrounding area there is at least three to four functional, cellular base station and emergency response personnel capable of responding to the building with their own cellular devices. The methods proposed for localization of the unknown mobile are discussed and compared later in this paper as well as recommendations for those most likely to function in real world applications.

The most accessible and commonly accepted positioning system, widely used across cellphones, is a part of the global navigation satellite system (GNSS) known as the global positioning system (GPS). While the accuracy of this system outdoors is difficult to compete with, its poor performance indoors paves the way for cellular-based localization; determining the location of a handset with the network and no external sources such as GNSS [34]. Mobile phones have come to be used primarily indoors, in an environment where UEs are not always capable of associating with a sufficient number of base stations or, known as Enhanced Node Bs (ENodeBs) in 3GPP terminology, and are thus unable to determine their location with a high level of certainty. As a result and as a means of rectifying this highly prevalent issue, cooperative localization has become a growing area of research.

In cooperative localization, devices work together in a peer-to-peer manner in order to make measurements and discover their nearest neighboring devices [3]. The enabling technology that establishes communication with nearby neighbors with minimal involvement from the network is known as Device-to-Device (D2D) communication. Through this technology, direct radio links are allowed between cellular users for data communications. Discovery of neighbors is accomplished by listening to uplink transmissions from other cellular users and then establishing a link with active users. D2D is currently being researched by industry standards bodies such as 3GPP as well as private industry such as Qualcomm. Since this technology is still being researched it is not fully implemented in cellular devices as a part of the LTE infrastructure [39]. There is great motivation for this technology from the perspective of mobile-service providers partially as a result of the new mobile handset, position-accuracy requirements established by the U.S. Federal Communications Commission (FCC) [4]. There is also interest in D2D from other industries that may look to use the technology for proximity services such as content distribution and location-aware advertisement in a social as well as e-commerce sense[39, 40]. Following the implementation of D2D, its potential will be quickly realized. By utilizing this innovative technology, devices with unknown location will be able to make measurements with other known-location references which can include handsets rather than being limited to just network-radio base stations.

In this work, research is conducted into a cooperative localization technique for LTE systems in which the UE communicates not only with ENodeBs, to perform UTDOA measurements, but also with other UEs. Single source localization will be the focus, meaning that there is only one, primary UE with an unknown position to be located. However, other UEs will exist in the network environment such that cooperative techniques can be performed. All of the devices and base stations will communicate with each other and exchange information in order to improve the localization accuracy in the network. Ultimately, it will be shown that cooperative localization can significantly improve the localizability in the network through computer simulations where 3GPP simulation assumptions are considered. Additionally, a study of barometric pressure sensors in a mobile device will be presented to address the potential of inclusion for a third dimension calculation. Being able to locate a handset in three dimensions is critical in many applications and, thus inclusion of a means to determine altitude is imperative. Several techniques are analyzed and explained where pressure sensors are utilized to distinguish UE location within a building, resolving which floor the user is actually on. This approach is feasible due to the unique relationship between pressure and altitude; pressure increases as altitude decreases and vice versa. Ultimately, through the use of a weather station and pressure sensor references, the floor on which a UE is located can be estimated.

1.1 Measurement Models

In this section, the different types of network-based measurements generally used for sensor or UE localization will be described. In cellular localization there are typically a small number of ENodeBs (whose locations are fixed and known) alongside many UEs whose locations are unknown and need to be determined. In this case the measurement models are utilized to discover a single source localization and 2D, X-Y plane coordinates. The basic techniques that are either range based or angle based are as follows.

1.1.1 Received-Signal-Strength

To estimate the distance between two nodes, the average power transmitted is measured after the signal is received at one end. This technique requires at least three reference nodes in order to determine the 2D location of one node [56]. There is often a lack of knowledge of certain parameters of the link, in the case of Received-Signal-Strength (RSS), and the exact transmit power as well as the pathloss exponent tend to be points of error. The major sources of error in RSS are shadowing and multipath signals, but the relative signal strengths (using one ENodeB as a reference) assists with reducing estimation error [1].

The average received power (in dB) at the *ith* anchor or node, P_i, under the log-distance pathloss and log-normal shadowing, is modeled as [33]

$$P_i = P_0 - 10\beta log_{10}(\frac{d_i}{d_0}) + n_i, i \in C \tag{1.1}$$

where P_0 is the reference power at reference distance d_0 (which depends on transmit power), β is the path loss exponent, d_i is the true distance between source and the *ith* anchor, and n_i is the log-normal shadowing term modeled as a zero-mean Gaussian random variable with a corresponding variance σ_{dB}^2. The standard deviation of shadowing is reported in dB units and is typically between 4 and 12 dB [32]. Moreover, σ_{dB} is related to the environment where a network placed and is constant with range [32].

1.1.2 Angle-of-Arrival

The circular radius is distinguished for each base station or ENodeB From this AOA can be performed, the location of the desired target can be found by the intersection of several pairs of angle direction lines, only needing two measuring units in order to obtain a 2-D position estimate [54]. In LTE, AOA measurements are standardized as the estimated angle of a UE with respect to a reference direction; being the geographical north, positive in a counter-clockwise direction [1]. This is depicted in Figure 1.1 below, adapted from [56].

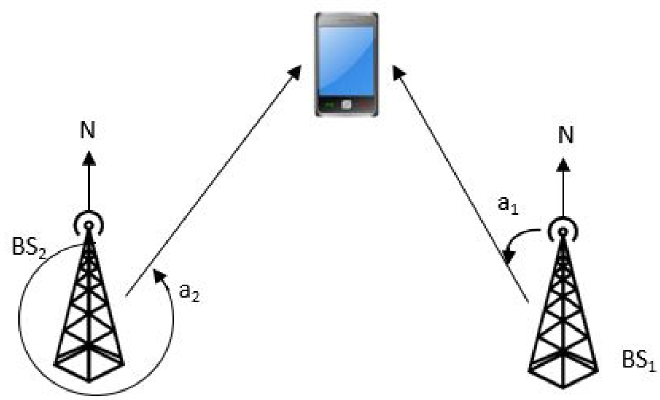

Figure 1.1: Estimation of the distance between a mobile and the base station using AOA

When estimated as a part of the uplink transmission, the ENodeB can estimate the angle utilizing the Sounding Reference Signal (SRS) [53]. While AOA does not need time synchronization, it does require complex hardware that can be affected by shadowing as well as path distance degradation [54]. Shadowing and multipath become a severe impact when trying to utilize this technique indoors. The AOA measurements can be modeled as [1]

$$\begin{pmatrix} x \\ y \end{pmatrix} = (R_{TA} + \Delta R_{TA}(\gamma - \frac{1}{2})) \cdot \begin{pmatrix} \sin(\phi + \Phi(\delta - \frac{1}{2})) \\ \cos(\phi + \Phi(\delta - \frac{1}{2})) \end{pmatrix} \tag{1.2}$$

where ϕ is the beam direction, Φ is the beam width, and the UE positions are represented by $(x\ y)^T$. The parameters γ and δ vary from $[0, 1]$. Overall, this technique is utilized in combination with other measurement techniques, which will be discussed later, in order to achieve handset localization .

1.1.3 Time-of-Arrival

The distance from an anchor or ENodeB to the UE is directly proportional to the propagation time, T_i. TOA is a technique that allows locating a UE by calculating the time of arrival of the signal from the UE to more than one ENodeB [56]. For 2-D localization, the TOA measurement must be made with a least three reference points. A simple depiction, adapted from [56] can be seen in Figure 1.2 below:

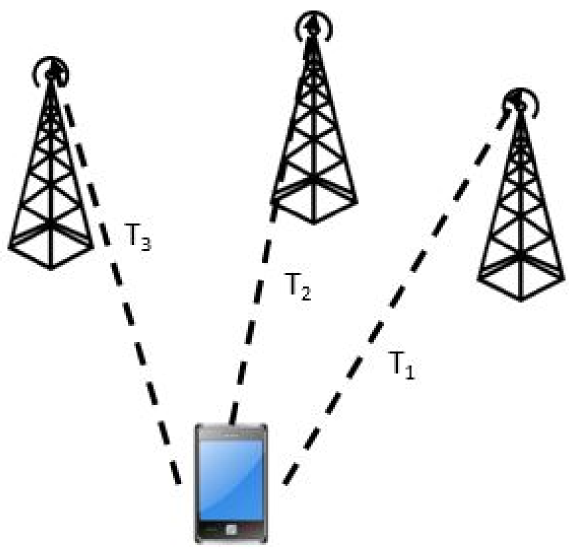

Figure 1.2: Time of Arrival from Three Anchors to a UE

The measurements are susceptible to delay and both transmitters and receivers need to be precisely synchronized which can be achieved by including a time stamp in the signal. Like AOA, measurements indoors are impacted by the difficulty to acquire a line-of-sight

(LOS) channel [54]. TOA can be estimated either by measuring the phase of the received narrowband carrier signal or by the direct measurement of the arrival time of a wideband narrow pulse [56]. Often a first-detected peak technique is utilized for TOA where τ_ω is the TOA of the first detected peak. The TOA estimated distance measured at the *ith* anchor is modeled as [41]

$$\hat{d_\omega} = c \times \hat{\tau_\omega} \tag{1.3}$$

where c is the propagation speed of the signal depending on the environment and ω represents the receiver's bandwidth. Distance measurement error is then calculated through [41]

$$\epsilon_{d,\omega} = |\hat{d_\omega} - d| \tag{1.4}$$

where d is the actual distance of a direct path between nodes.

1.2 LTE Geolocation Techniques

Within LTE standards several specific positioning techniques are supported which include: Enhanced Cell ID (E-CID), Assisted-Global Navigation Satellite System (A-GNSS) also sometimes referred to as A-GPS or Assisted Global Positioning System, Orthogonal Time Delay of Arrival (OTDOA), and (starting with Release 11 initiated technique) Uplink Time Difference of Arrival (U-TDOA).

The following describes these techniques in greater detail.

1.2.1 Enhanced Cell-ID

While this technique is based on Cell of Origin (COO), in which the position of the device is estimated using knowledge of the geographical coordinates of its serving base station or ENodeB, it has been redefined for LTE. On top of the coordinates of the ENodeB, E-CID also utilizes radio signal measurements [53]. Overall, E-CID exploits four sources of position information which include: the cell-ID and the corresponding geographical coordinates of the serving cell, the timing advance (TA) of the serving cell, the cell-IDs with their corresponding signal measurements of the cells (there are up to 32 cells in LTE), and the AOA measurements [1]. This technique is utilized in both cases of UE-ENodeB communication, as a part of the downlink as well as the uplink. The downlink procedure is performed between the UE and the Evolved Serving Mobile Location Center(E-SMLC) using LTE Positioning Protocol (LPP) and measurements are provided by the UE; known as UE-assisted or E-SMLC-based E-CID. The uplink procedure is performed using the LTE Positioning Protocol Annex (LPPa) with measurements from the ENodeB; known as eNB-assisted E-CID [38]. The UE-assisted measurement techniques include reference signal received power (RSRP), reference signal received quality (RSRQ), received signal strength indicator (RSSI), and UE Rx-Tx time difference. The network-assisted or ENodeB-assisted measurements include TA type 1 being (ENodeB Rx – Tx time difference) + (UE Rx – Tx time difference), TA type 2 being ENodeB Rx – Tx time difference, and uplink AOA [1, 38]. One of the methods of E-CID, applied to LTE yields the distance from the TA time measurement as [1]

$$R_{TA} = \frac{c \cdot TA}{2}, \tag{1.5}$$

where c is the speed of light. This method requires knowledge of the geographical cell, the locations of the ENodeB, and the distance between the ENodeB and the UE from the given equation with knowledge of TA. Another method of E-CID relies on signal strength to calculate distance. Knowledge of the network, specifically cell polygons, combined with the signal strengths of the UE are used. The effects of shadowing must be taken into account in this instance. Overall, E-CID has been improved upon from WCDMA implementations, as in LTE the timing advance precision is of the order of 10m. This technique is easy to implement but can have low accuracy resulting from the resolution of the size of the cell polygons.

1.2.2 Assisted-Global Navigation Satellite System

The global positioning system is considered the most successful positioning systems in an outdoor environment. However, stand - alone GNSS performance is affected by two main factors including the geometry of the satellites used and the error in the range or pseudorange measurement [1]. In order to estimate a unique location, a GNSS receiver must initially perform a search for and acquire at least four satellite signals; acquiring more signals is preferred. The task of the GPS receiver is to find the correct code phase and Doppler, detect the data bit edges, and perform navigation data demodulation. When in dense environments or without clear sky view(such as indoors), it is well known that GPS positioning accuracy is severely decreased due to poor coverage of satellite signals [54].

As an extension of GPS and through the use of newer mobile handsets which contain partial or full GPS receivers, A-GPS is implemented with a receiver that attempts to improve or eliminate some of the steps that a GPS receiver must conduct. In order to do so, assistance data is collected from a network of GPS reference receivers which are located at sites with favorable signal conditions where satellites can be continuously tracked. A simplistic model of an A-GPS network architecture can be seen in Figure 1.3 adapted from [56]

While tracking the satellites, the receivers transfer the information that they demodulate to the cellular network for further distribution to the GPS receiver in the cellular phone. By doing this, the demodulation may be avoided and the Doppler domain search time is reduced. The GPS receiver in the cellular phone gets access to complete navigation models and correction parameters while only having to calculate the coherent code and performing a Doppler search [57]. Therefore, the calculation capability is more accurate than GPS alone.

1.2.3 Time Difference of Arrival

This technique is used to locate a UE by comparing the difference of arrival times of a signal between multiple measuring units [54]. For this to work all ENodeBs must have synchronized

Figure 1.3: Assisted-GPS model

clocks, but the UE does not have to share the same clock [56]. While TOA compares the absolute time of arrival at multiple anchors, TDOA compares the differences between the arrival times. TDOA establishes a hyperbola with its foci located at the, typically, two or more reference nodes [56] and then the coordinates of the UE are a result of an intersection point of the hyperbolas. This method can be seen in Figure 1.4 adapted from [56].

The equation of the hyperboloid is given as [54]

$$R_{i,j} = \sqrt{(x_i - x)^2 + (y_i - y)^2 + (z_i - z)^2} - \sqrt{(x_j - x)^2 + (y_j - y)^2 + (z_j - z)^2} \qquad (1.6)$$

where (x_i, y_i, z_i) and (x_j, y_j, z_j) represent the fixed receivers i and j; and (x, y, z) represent the coordinate of the target. Some further mathematical techniques need to be utilized in order to calculate the exact solution. TDOA is also commonly estimated through the use of a cross correlation between measuring units. Through an integration over the time period of the same received signal, TDOA estimates can be resolved despite the presence of some signal delay as well as noise [54].

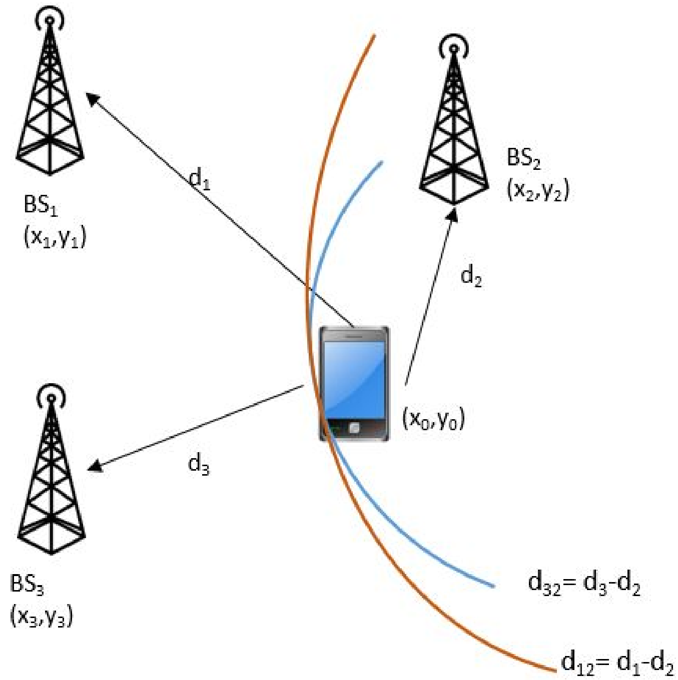

Figure 1.4: Time Difference of Arrival used to locate a mobile device

1.2.4 Observed Time Difference of Arrival

This technique only operates on UMTS networks and is a UE-assisted method based on reference signal time difference (RSTD) measurements (relative timing differences between two cells) conducted on the downlink [51]. Following TDOA, the position of the user is calculated by using the reception time at the UE. Further, OTDOA requires timing measurements from at least three ENodeBs with a good geometry in order to find the UE's position at the intersection of at least two hyperbolas established about the base stations [56]. Each hyperbola represents a pair of cells which correspond to a set of points with the same RSTD for the two cells [1]. It must be noted that the timing measurements are valid only given that the timing offset is known as well as the location of transmitter is known. A system of equations is generated from the, at least three, ENodeBs that when solved provide the distance measurements. There are many approaches to solve the system of equations including the approaches taken in [35, 36, 37]

In regards to the LTE resource grid, as a part of LTE Release 8, Cell-Specific Reference Signals (CRS), a pseudo-random QPSK sequence, were utilized for OTDOA. With Release 9, Positioning Reference Signals (PRS), still a pseudo-random QPSK sequence, were introduced as the CRSs were deemed insufficient for positioning and the PRSs provided a higher probability of detection in the radio frame [53]. OTDOA does not require synchronization between the base stations and the UE. On the other hand, alongside shadowing and non-line-of-sight (NLOS) propagation, detection capability can be a limiting factor for this method of localization [1].

1.2.5 Uplink Time Difference of Arrival

This technique is very similar to OTDOA except that it uses the uplink signal, from the UE to the base stations, for calculation rather than the downlink signal. In UTDOA, the uplink signals are used to measure the time difference of arrival between neighboring cells, requiring multiple receiver sites at different locations in range of the uplink signal [1]. UTDOA measurements can be performed at the ENodeB or at a Location Measurement Unit (LMU) which can be any sort of stand alone unit located either externally or internally to the ENodeB [66]. The position calculations in either configuration or implementation remain the same.

UTDOA has been included in the 3GPP LTE standards as a part of Release 11 and is setup differently from its downlink counterpart. In order to perform the position calculations a new, frequency-domain reference signal sequence, derived from a Zadoff-Chu sequence has been created; known as the Sounding Reference Signal (SRS). The SRS sequences occupy a selected part of the last Orthogonal Frequency Division Multiplexing (OFDM) symbol in a subframe. A major advantages of these measurements is that there is no need for demodulation at the LMU as the SRS sequence is known as well as the SRS bandwidth and periodicity. With power control in place to attempt to mitigate interference, hearability proves to be a disadvantage as transmitted signals from the UE may not be strong enough to be received at a large number of base stations and thus could prevent a UTDOA measurement [1].

1.2.6 Other Measurement Types

There are a variety of other types of measurement techniques used for localization considered in various publications. For instance, significant work has been done regarding RF Fingerprinting in which a user is located by placing RF measurements onto an RF map [1, 51]. The geographical maps can have detailed information regarding the RF topology and can be used to construct a 3-D map with accurate information regarding the cellular system in the area. As an extension to fingerprinting, adaptive enhanced cell ID (AECID) is done by adding several parameters to the RF fingerprint. In LTE, CIDs, timing advance information, and AOA are some of the parameters that are added to the radio map [1]. There are also several hybrid techniques that take advantage of different methods simultaneously to maximize estimation of localization [52].

1.3 Problem Statement

As mentioned earlier, this thesis will focus on two different aspects of handset localization. The two problems are addressed in this section.

In the first part an investigation is done into two dimensional localization with UTDOA and collaboration in LTE. It is assumed that the location of a user is unknown, and the aim is to determine it's location from noisy measurements obtained within the network without the aid of any external sources. UTDOA utilizes the time difference of arrival of uplink signals received at base stations in a LTE system. UTDOA has been investigated by several others in [27, 28, 29, 30, 52]. With the stringent E911 localization accuracy requirements from the

FCC, the performance of this technique needs to be improved. For this reason, the use of other handsets or users in the LTE network for collaborative localization is introduced.

In the second part of this thesis, a method for determining the third dimension for indoor localization is explored. Models have been created to relate altitude or height to pressure. A barometric pressure sensor can measure the air pressure and the corresponding altitude can be calculated. New mobile phones have barometric pressure sensors built in that are capable of recording and reporting the experienced pressure. There are several sources of error that affect the pressure sensor which need to be taken into consideration [22]. Here, pressure sensors are manipulated to show how to identify the floor a handset is located on.

1.4 Literature Survey

A brief survey of other pieces of work was performed in order to gather research pertaining to the subject material of this thesis. Measurement models and different techniques pertaining to their use in LTE are explored. Through this a comparison was able to be done in order to distinguish advantages and disadvantages between different techniques and methods. UT-DOA is the chosen method from the measurement models in this thesis and as such research in UTDOA for two dimensional positioning in LTE. Several papers described here utilize UTDOA in LTE for positioning. Ideas of how to expand the X-Y localization calculations to X, Y, and Z had to be brainstormed as well The means of finding the third dimension of location is explored in Ch. 2, but some three dimensional positioning papers are also described here.

The paper written by Wigren [24] develops a method for including altitude in the adaptive enhanced cell identity (AECID) positioning method whenever high precision A-GPS, OT-DOA or U-TDOA position measurements occur in a LTE network. Fingerprint positioning information includes cell IDs, received signal strengths (RSSs) from the serving and neighbor cells, time advance (TA) of the serving cell, as well as angle of arrival (AOA) information.

An initial U-TDOA position measurement in combination with the fingerprint positioning information are combined to then compute a 3GPP polygon which sets the boundaries of the cluster; all in a 2D plane. By including the measured altitude information, which is a part of A-GPS, OTDOA and U-TDOA reports in LTE, the polygons are abstracted into a 3D plane to provide a 3GPP ellipsoid point with altitude and uncertainty ellipsoid.

The paper by Marwan Mahmood Shakir [27], addresses U-TDOA using Chan's method for hyperbolic location and important factors which need to be taken into consideration for improved U-TDOA accuracy. The paper explains how U-TDOA is a useful technique that is superior in many ways to other location derivation techniques given it does not require special alterations to mobile networks. Also, with no specific antenna requirements and the ability to potentially work in situations with no LOS, it is displayed that U-TDOA can prove to be advantageous in time and money to TOA and Difference-of-Arrival (DOA) methods. Concluding, it is explained that the sampling rate and interference cancellation are the two major factors in determining position location when utilizing U-TDOA. When the sampling rate is increased PL estimation can be performed more accurately as time quantization error in U-TDOA estimates decreases as the sampling rate is increased [27]. Finally, with cross-correlation and parallel interference cancellation, the negative effect of the strong desired user signal can be canceled and other users' received signal quality can be improved.

There was a specific study done in Mosul City, Iraq, as an urban area of 3x3 km, comparing performance of U-TDOA and A-GPS and is shown in [30]. It must be noted that U-TDOA measurements were not provided by the city operator companies and that a simulation was used for the U-TDOA method. In the paper, position is determined from U-TDOA trilateration and then utilizing Chan's method [35] for solving the U-TDOA equations. Many factors and their influence on the accuracy of U-TDOA positioning are discussed; accuracy is displayed via root mean square (RMS) error. Ultimately, U-TDOA is shown to meet FCC requirements with accuracy of under 100m for urban areas, suffering mainly from multipath delay as well as geometric dilution of precision (GDOP).

One further paper by Mardeni [28], utilizes U-TDOA positioning with a pre-filtering function called adaptive line enhancer (ALE) to enhance the delay estimation performance of the cross correlation and ultimately improve the accuracy of TDOA. Mobile signals are received at pairs of base stations and then the nonlinear hyperbolic equations are used to obtain a unique localization. The pre-filtering on the pairs of received signals, being delays of one to the other, implements a normalized least mean square (NLMS) algorithm (normalizing the input signal with the input power) to de-correlate noise samples between the reference and input signals. This method claims to show a superior improvement in accuracy calculations over a conventional cross correlation without pre-filtering.

An exploration into improving LTE TOA-based indoor positioning is done in [41]. TOA positioning is calculated via cross-correlation peak detection, but the precision is deemed to low to be efficient for indoor environments. A new parabolic approach is thus taken to refine the coarse estimation of position without added complexity. Typically a parabola is fitted to the measured correlation. In [41], three cross-correlation samples are taken in the neighborhood of the coarse estimate which results in a parabola with a more narrow variance. When compared to the conventional approach, the parabolic interpolation introduced improves timing estimation.

Finally, in the literature regarding measurement techniques, a study has been done that deals with Observed Time Difference of Arrival (OTDOA) and a preliminary look into cooperative positioning in LTE [34]. The paper proposes UE collaboration as a means to improve the localizability in the network as well as the accuracy of position estimation. It is assumed that UEs can communicate with one another via D2D communication. The reference signals in LTE that are discussed for TDOA measurements are the cell-specific reference signal (CRS) and the positioning reference signal (PRS). Using a centralized algorithm for cooperative localization, a maximum likelihood (ML) estimator is utilized; achieving the Cramér-Rao lower bound (CRLB) and therefore being the minimum variance unbiased (MVU) estimator. Further, the minimization problem is solved via a Gauss-Newton algorithm which is linearized with the Taylor series approximation. Ultimately this OTDOA technique shows a

30% improvement in localizability by utilizing collaboration.

Using measurement models, localization needs to be achieved in not only two dimensions, but in the third dimension as well. A great deal of 3D localization techniques are accomplished through hybrid measurement models, typically including GPS, but this lacks the capability to function well indoors. The matter of horizontal and vertical indoor localization is addressed as independent algorithms in [42]. While the horizontal algorithm involves the subdividing of an area into unique signature ares that are associated with RSS measurements, the vertical algorithm is more unique. A basic building model is generated and then a coordinate system is set up in order to simplify the three dimensional coordinate system to a two dimensional system. One axis , Z, exists between an anchor on the top floor and an anchor on the bottom floor. The second axis, X is the distance between the roughly estimated user location or test point and the Z axis. With the distances between the base station and mobile receiver known the vertical position can be found. Typical RSS calculations are performed with power and gain parameters but the outdoor pathloss model is altered to account for the concrete between floors. This algorithm is extrapolated to a multi-anchor system that simulates real conditions and fluctuations of wireless signals; resolving the floor of the user in each instance.

Several other papers utilize a ray-tracing environment emulator in order to study channel characteristics in urban 2D and 3D environments [43, 44, 45]. This tool has been shown to make favorable predictions regarding received power, angle of arrival, and link performance. A specific ray-tracing tool developed by Bell Labs is used in [43]. This tool is trained with the geometry of buildings, angle of incidence, dielectric coefficients, wall thickness, and frequency and 3D antenna patterns. [43]. With all of this information, the 3D ray-tracing technique can simulate the physical environment and use wave propagation physics to predict radio signals with a high level of confidence. A method on how to achieve good indoor wireless coverage, taking account parameters in all three dimensions is shown in [43]. While 3D localization is not performed, the ray-tracing technique lends itself to being a useful tool for modeling a 3D environment and all of the related wireless parameters.

There are several studies in published technical papers regarding collaboration of user equipment in wireless sensor networks. A great deal of work, highly cited, was done by Patwari in [32, 33]. In [33] there is a focus on the accuracy of relative location estimation, but it establishes a network of reference devices (knowing their location *apriori*) and "blindfolded devices" (no absolute coordinate knowledge) in which all devices must estimate the range between themselves and their neighboring devices. The system requires the devices to be capable of peer-to-peer range measurement as well as the use of a distributed or centralized location estimation algorithm; using RSS and TOA. Ultimately this study proves that location estimation variance bounds or CRBs decrease as more devices are added to the network while also showing the ML estimator derived for RSS localization is biased and finding the global minimum is computationally complex. It was shown that localization with approximately 1 m RMS error can be achieved with TOA measurements and that these results can easily be expanded to three dimensions.

A further discussion of cooperative localization is done in [32]. This study, again, shows how to calculate the CRB on the location estimation precision for all sensor positions simultaneously (time delay is accepted), but does so with TOA, RSS, and AOA measurement techniques. Other information is included such as major sources of error: shadowing, multipath, additive noise, etc.; for each of the measuring techniques as well as a note on calibration and synchronization for each situation. Furthermore, the advantages and disadvantages are compared for centralized and distributed algorithms. This work motivates further research into cooperative localization and its potential for use in accurate location calculations.

1.5 Thesis Outline

An introduction of the thesis has been given in Chapter 1. A background of measurement models as well as LTE geolocation models was given along with an exploration into literature and research performed in the associated areas of this thesis: UTDOA, LTE indoor geolocation, 3D geolocation, and collaborative localization. Chapter 2 investigates UTDOA of LTE signals utilizing the Sounding Reference Signal. Both the link and network layer system parameters are defined along with the pieces of the uplink transmission scheme. Then the method of calculating the range error for location estimation and the algorithm used to predict the location through the use of base stations as well as other UEs for collaboration are also explained.

Chapter 3 of this thesis develops the investigation into the use of barometric pressure sensors in mobile handsets for altitude resolution inside of buildings. First, the relationship between pressure and altitude is established along with all of the variables that can alter pressure both inside and outside of a building throughout the day or course of the week. Then the inclusion of barometric sensors and their behavior as a measuring unit is explained. With this understanding, a series of test cases are proposed which exercise the pressure sensor in different methods attempting to find the best method of resolving the floor location of a mobile handset in a building.

Chapter 4 of this thesis will detail simulation and test scenario results for UTDOA and pressure localization. Given the system setup and development of an uplink signal, the Signal-to-Interference Noise Ratio(SINR) based on hearability is shown. With the connections between the unknown UE and ENodeBs as well as other UEs in the network established, localization can be performed. The results of the location estimate through collaboration is presented and its efficiency as well as improvement is addressed. Then the initial analysis of the pressure sensor used for experimentation is shown and the results of the test cases for utilization of a pressure in a mobile handset are displayed and discussed. Each of the test cases have their own advantages or disadvantages, but some instances prove more accurate as well as efficient than others. Of all the scenarios, one method is proposed as the best and most feasible option for resolving third dimension location or the floor on which the user is located on.

Chapter 2

UTDOA Localization with Collaboration

2.1 Introduction

The need for a nationwide emergency number and the capability to route the call to the nearest public safety responder while providing the calling number and location has been recognized for more than five decades. With the advent of and exponential prevalence of wireless phones, this emergency service had to be integrated with mobile phones. However, following "anytime, anywhere" communications, a specific location is not always tethered to the mobile phone [50]. As a result, the area of and research done in wireless positioning has become an even larger concern with the need to meet the Federal Communications Commission Enhanced-911 location accuracy requirements; updated in February 2014. Public Safety Answering Points (PSAPs), locations responsible for answering calls to 911 for emergency services, need to be able to pinpoint the caller and transfer this information to the appropriate response teams. Knowing that the majority of 911 calls are made from mobile phones, the ability to accurately locate a mobile phone has become and will continue to be of significant importance to emergency service teams. With accurate localization of users, police officers, firefighters, and medical personal are capable of performing their job more effectively and efficiently.

The LTE standard mentions several cellular-based positioning techniques which include: E-CID, A-GNSS, and OTDOA. Extensive research and work has been done on these methods to allow for their inclusion as a feature within every day handsets. They have all met the challenges that an LTE positioning method has to overcome. Each of the positioning techniques must be able to maintain measurement accuracy when experiencing conditions such as fading and cell timing offset [55]. There also has to be an underlying reliable protocol exchange between the base-stations or network and the mobile devices. Further, end-to-end performance needs to be acceptable; the overall system performance which includes positioning accuracy and response time need to optimized. Finally, as an all-encompassing factor, performance in real world conditions needs to be considered as it is the most important metric for determining both user satisfaction as well as adherence to FCC mandates for E911 [55]. Overall, the cellular-based positioning techniques have been fully established but they are not without their flaws; unable to overcome all of the challenges of a cellular-based positioning method.

It was agreed by 3GPP to look into network-based positioning for inclusion into the LTE positioning methods. Uplink or network-based positioning is performed when measurements are not focused at the end-user but rather at a Location Measurement Unit or any stand alone unit located either externally or internally to the ENodeB [66]. This sort of positioning has come to display several advantages that have helped prove its worth amongst the cellular-based techniques. Andrew Solutions summarized these advantages and pushed for 3GPP work on UTDOA [7]. With no UE involvement in the actual position calculation, there is a built-in deterrent to detection, jamming, or spoofing from the UE perspective. With the majority of work done at the LMU, a high processing gain can be achieved which allows for improved hearability, detection, and participation of base stations for timing measurements [7]. Network-based positioning opens the door for future location calculation methods that have no impact on the UE.

In this work the exact position of the target UE is not known. We show that the position location estimator must solve a nonlinear least-squares (NLLS) problem in order to accurately estimate the x and y coordinates of a UE. In order to perform collaborative position estimation, it is further assumed, that D2D communication can be established between active UEs in the network. In a typical wireless network, there is no synchronization between UEs and ENodeBs. However, for the simulations it is assumed that each of the target UEs will transmit the same SRS sequence without coordination and that there is to be no interference between one another. Only one target UE and its SRS sequences will be processed in the network at a time.

The remainder of this chapter details the link layer and network layer simulations necessary for performing estimation location with UTDOA in LTE. As a part of the link layer, the means of creating the sounding reference signal is explained and how it is then mapped to the LTE resource grid. Then the calculation of expected range error given a particular SINR is explained. The network layer simulation, utilizing the SRS, establishes an LTE network of users and base stations to then use a nonlinear estimator to estimate the location of the desired user.

2.2 Link Layer Simulation

2.2.1 Reference Signals

Reference signals are typically included in OFDM frames as a part of LTE for measuring TOA. Their place in the resource grid is known and as such they are a reference point on uplink or downlink transmissions. While cell-specific reference signals and positioning reference signals are included in downlink transmissions as a part of LTE Release 8 and further, a new reference signal was introduced for uplink transmissions; the sounding reference signal (SRS). This reference signal was first introduced as a part of LTE Release 8 and is used to measure uplink channel quality over a specific section of bandwidth to assist with scheduling and link adaptation [5]. The SRS is always located in the last OFDM symbol in the second slot of a sub-frame and is not tied to the user payload which makes it have less impact on scheduling. It has come to be used for estimating uplink timing for UE positioning as it has to ability to change periodicity, bandwidth, frequency position, and power [8]. Once all of these parameters are set and maintained at a E-SMLC, the SRS is ideal for performing UTDOA and locating a UE in the X and Y plane. The SRS parameters can be discovered by all neighboring ENodeBs and then location measurements can be made.

Specific SRS parameters were chosen for the purposes of the simulation performed in this work. Following the baseline assumptions in [9] and then also the work of 3GPP in [13] allowed for the parameters seen in Table 2.1 to be reached. Some primary assumptions for the simulation are that the reference signal is known to all cooperating sites in the network and the sites know the SRS bandwidth as well as the periodicity. Group hopping as well as sequence hopping are not considered for this simulation making the group number, $u = 0$, and the base sequence number within the group, $v = 0$. Several parameters that are necessary for SRS sequence generation are based upon the channel bandwidth. Given that the channel bandwidth is 10 MHz, the number of uplink resource blocks is 50 following Table A.2.2.1.1-1 in [14]. The main seeding variables $m_{SRS,0}$ and N_0 are designated by "higher layers" according to [13] but were chosen to be $m_{SRS,0} = 48$ and $N_0 = 1$ from Table 5.5.3.2-2 for this simulation [13]. The length of the base sequence, M_{sc}^{RS}, is then assumed to be $3N_{sc}^{RB}$ or greater at all times. There are eight separately configured SRS sequences for each UE and are represented by eight cyclic shifts, $\alpha_{\tilde{p}}$, according to Eq. 2.1 from [13]

$$\alpha_{\tilde{p}} = 2\pi \frac{n_{SRS,\tilde{p}}^{cs}}{8} \tag{2.1}$$

where $n_{SRS}^{cs} = \{0, 1, 2, 3, 4, 5, 6, 7\}$ and $\tilde{p} \in \{0, 1, ...N_{ap} - 1\}$ and N_{ap} is the number of antenna ports used for the SRS transmission [13]. All eight shifts of each base sequence are created in the simulation, but the first sequence with the first cyclic shift, when $n_{SRS}^{cs} = 0$, is the only sequence utilized for simulations in this work. The base sequence starts as a Zadoff-Chu sequence whose length is $N_{RS}^{ZC} = 283$ being the largest prime following the value of $m_{SRS,0}$ and $M_{sc}^{RS} = 288$ [13]. The Zadoff-Chu sequence is utilized for its characteristic of having constant amplitude and zero auto-correlation. These two properties are verified and displayed in Fig. 2.1 and Fig. 2.2. Different users in the network can possess the same Zadoff-Chu sequence, but their SRS sequence would be cyclically shifted in order to appropriately overlay in the LTE resource grid. Ultimately, following the various root equations, the reference signal sequence is defined as in Section 5.5.1 of [13]

$$r_{u,v}^{(\alpha)}(n) = e^{j\alpha n}\bar{r}_{u,v}(n), 0 \leq n < M_{sc}^{RS} \tag{2.2}$$

where each α is a different cyclic shift of the base signal sequence $\bar{r}_{u,v}(n)$ and M_{sc}^{RS} is the length of the reference signal sequence [13]. The method of defining $\bar{r}_{u,v}(n)$ can be seen in Section 5.5.1.1 of [13]

The mapping of the SRS sequence to physical resources is done following [13]. Given the simulation parameters, the SRS is mapped to the full frequency bandwidth of the last OFDM symbol. Therefore the data sequence is zero-padded to 600 modulation symbols. At this point the entire SRS is ready for the rest of the processing in the transmitter.

2.2.2 LTE Uplink Transmission Scheme

With the data bits mapped into modulation symbols, an uplink transmission scheme has to be applied by the transmitter. Single Carrier Frequency Division Multiple Access (SC-FDMA) is used in uplink transmission of LTE to improve the peak-to-average power ratio as well as other disadvantages that are associated with standard OFDM [46]. SC-FDMA applies an N-point discrete Fourier Transform (DFT) mapper which transforms the modulation symbols in the time domain into the frequency domain. This allows for multiple subcarriers to carry each data symbol which allows for spreading gain or frequency diversity gain [47]. Then, like

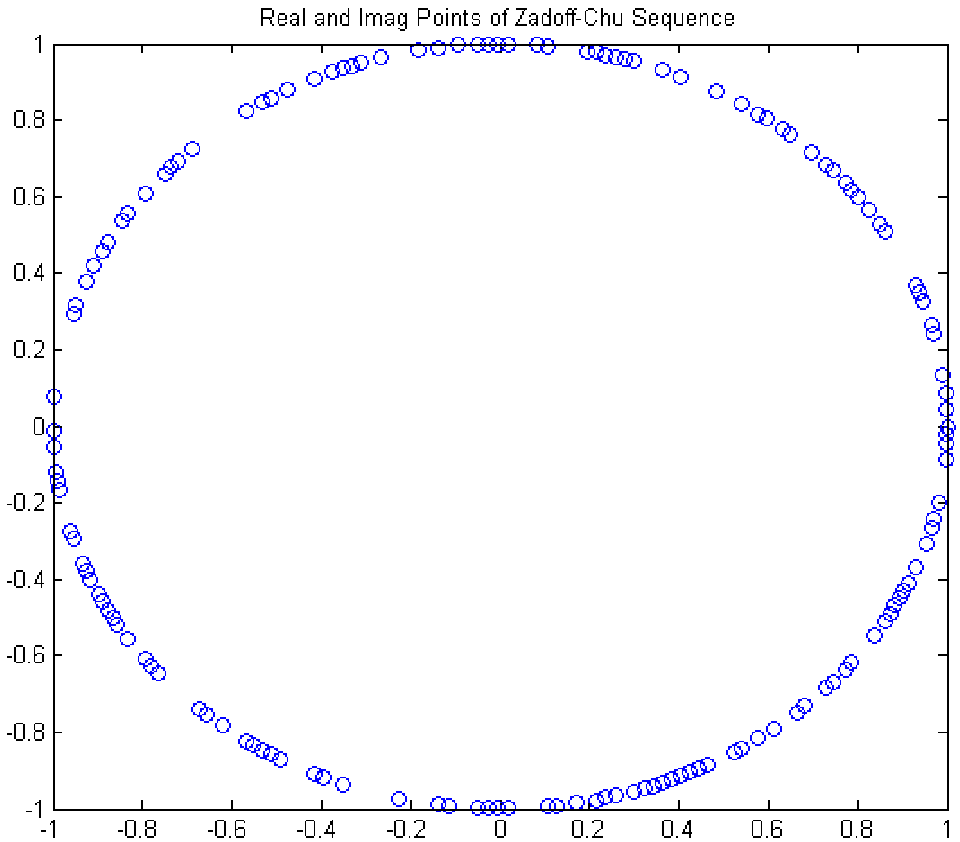

Figure 2.1: Amplitude of Zadoff-Chu Sequence

OFDM, an inverse fast-Fourier transform (IFFT) is used to retrieve the time samples before the sequence is passed through the channel.

Following the 3GPP specifications, the channel employed in this simulation is a Rayleigh fading channel. To simulate the worst-case scenario given a 500 meter inter-site distance, the Extended Typical Urban model (ETU) model is used. The profile for this model can be seen in Table 2.2. The 'rayleighchan' function within Matlab, seeded with the ETU tap delays as well as other required variables, was utilized for this simulation. It must be noted that this function had to be altered in order to allow for a causal system. As a part of the fading delay profile, no path gains or impulses are expected to occur before time, $t = 0$. The taps and path gain profile output of the original 'rayleighchan' function can be in 2.3. From

Figure 2.2: Autocorrelation of Zadoff-Chu Sequence which is the Basis of SRS

this figure, it is seen that path gains occur at negative values of time which is impractical in this simulation. In order to accommodate for this, the entire delay profile had to be shifted 20 symbols or 1 μs to ensure that the taps were appropriately placed in time. With the shift, the resulting taps and path gain profile can be seen in 2.4. All of the path gains, occurring where there are solid circular markers, occur at $t = 0$ or later. The range errors resulting for the tap profile, in the noncausal case, can be seen in Fig. 2.5. The range errors from the altered and utilized tap profile can be seen in Fig. 2.6. Both sets of range error were calculated given the same parameters, the only alteration was the causality fix.

Table 2.1: Summary of Link Layer Simulation Parameters

SRS Parameter	Assumptions
System Bandwidth	10 MHz
Center Frequency	800 MHz
Sampling Frequency	20 MHz
FFT Size	1024
Accumulations	50
Modulation	QPSK
Number Uplink RBs	50
Cyclic Prefix	Normal
Number of UL Symbol/RB	7
Number of Antenna Ports	1
Number of Layers	1
M_srs	48
Channel Fading Model	ETU
Cell ID	0
Cell Group	1

Table 2.2: ETU Case I Tap Delay Profile

Excess tap delay (ns)	**Relative power (dB)**
0	–1.0
50	–1.0
120	–1.0
200	0
230	0
500	0

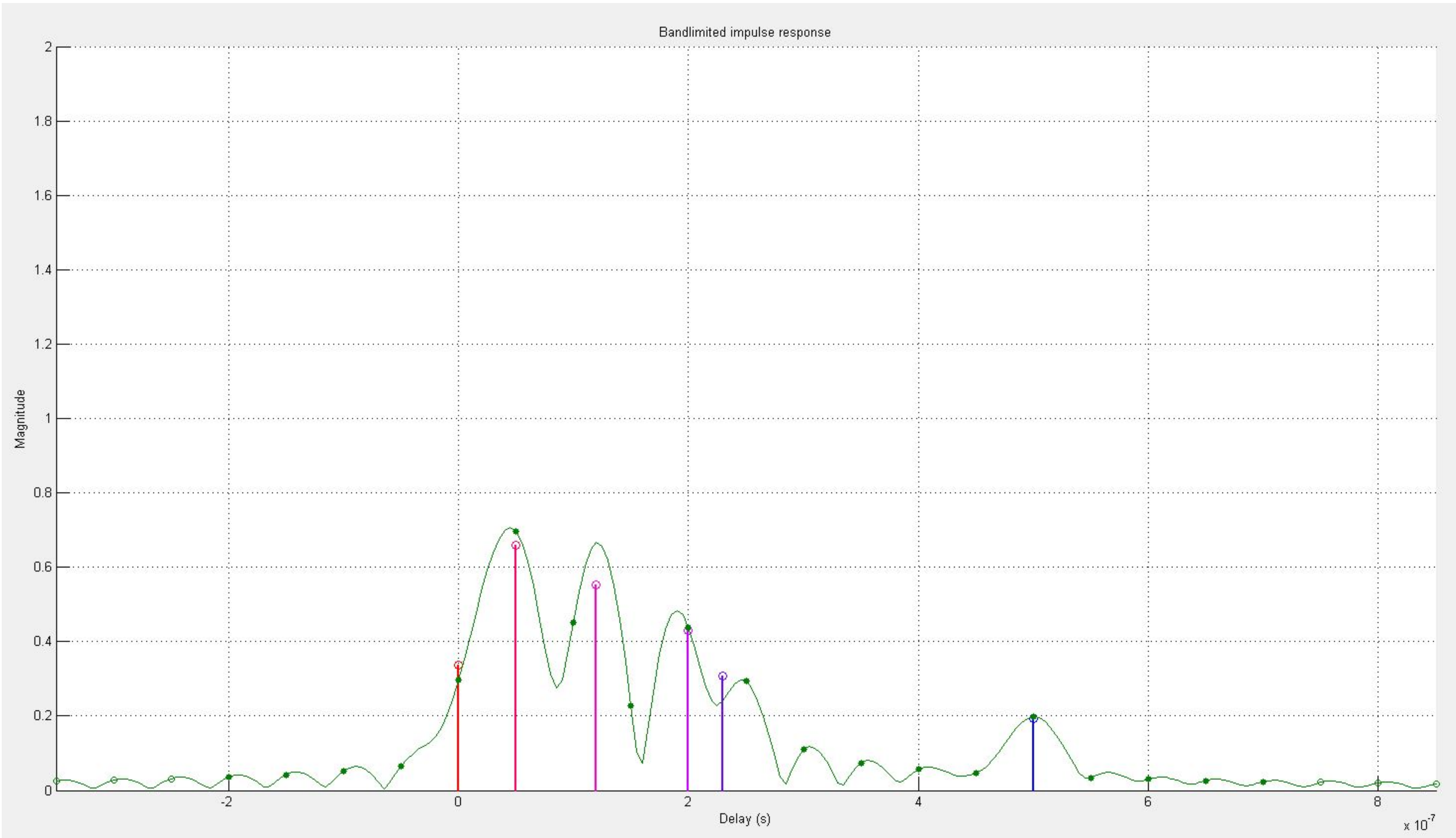

Figure 2.3: ETU Case I Rayleigh Fading Model with Noncausal Taps

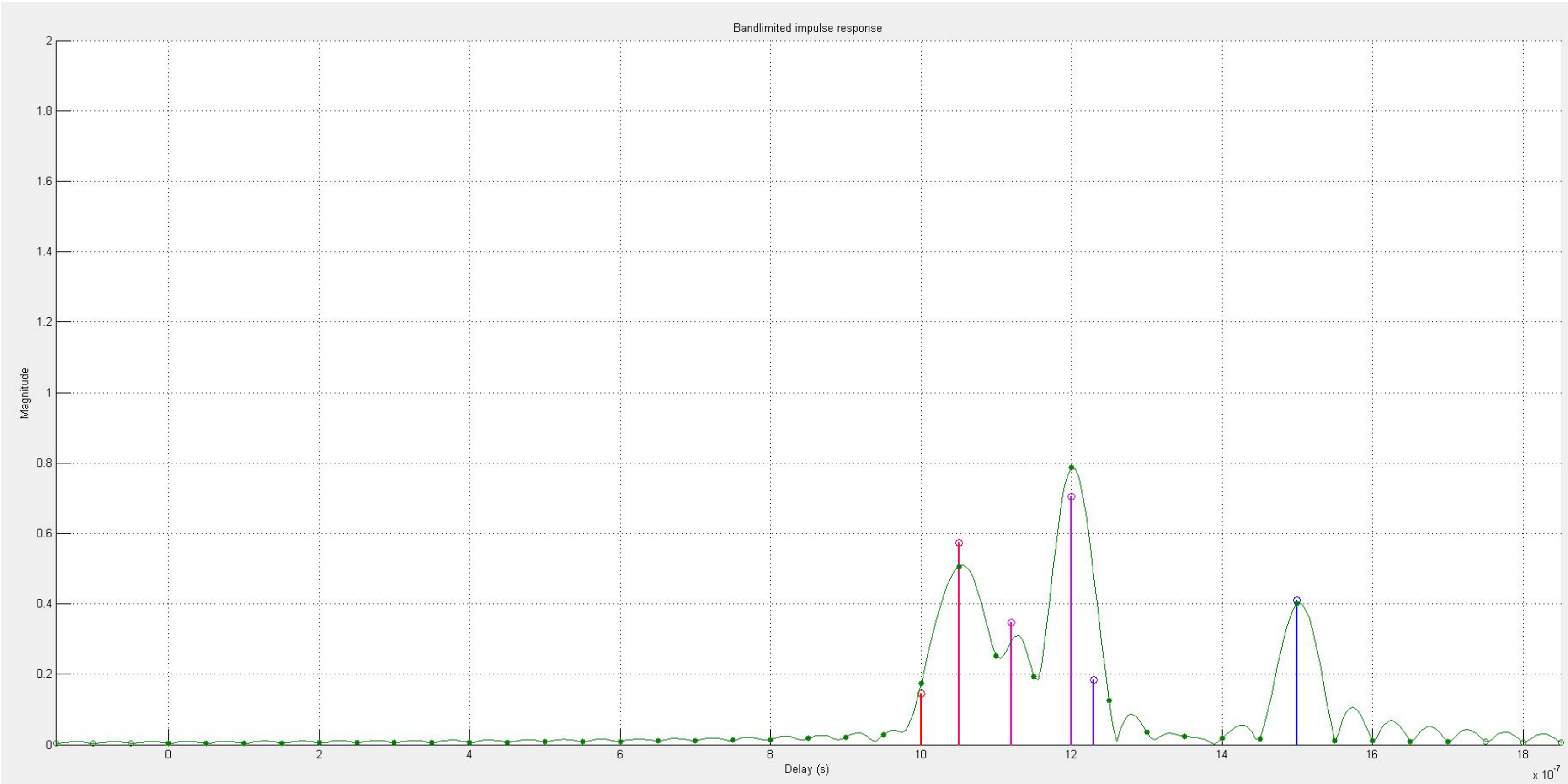

Figure 2.4: ETU Case I Rayleigh Fading Model with Causal Taps

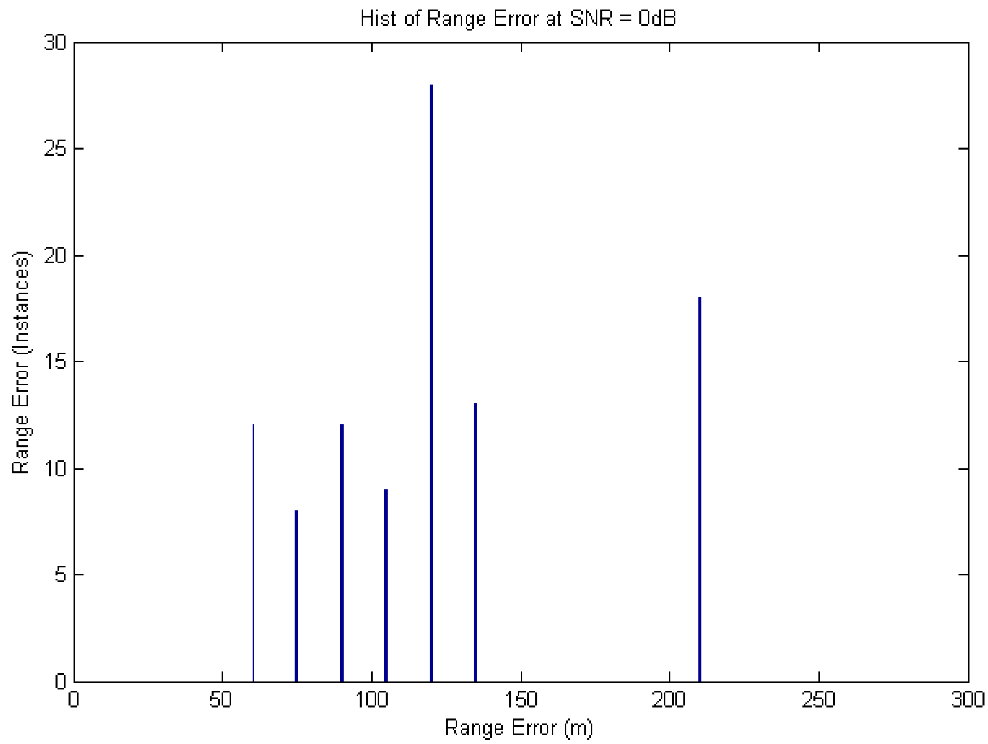

Figure 2.5: Resulting Range Measurements for Rayleigh Fading Model with Noncausal Taps

2.2.3 UTDOA Estimation

In order perform position estimation through UTDOA, a signal must be sent from a UE to several base stations. All of the base stations who are capable of communicating with a particular UE will receive this signal. There is a particular time-stamp with each received signal. With no synchronization, the individual clocks of the targets and anchors can drift and will not necessarily be aligned. As a result, the recorded time at the moment of transmission of the signals from the UE to each of the base stations cannot be directly compared. All of the times of arrival need to be compared at one LMU in order to perform UTDOA. All measurements are collected at the LMU where they can be analyzed and the locations of all of the UEs in the network can simultaneously estimated. The location estimation can be performed by the UEs and reported to the LMU. This method of localization is char-

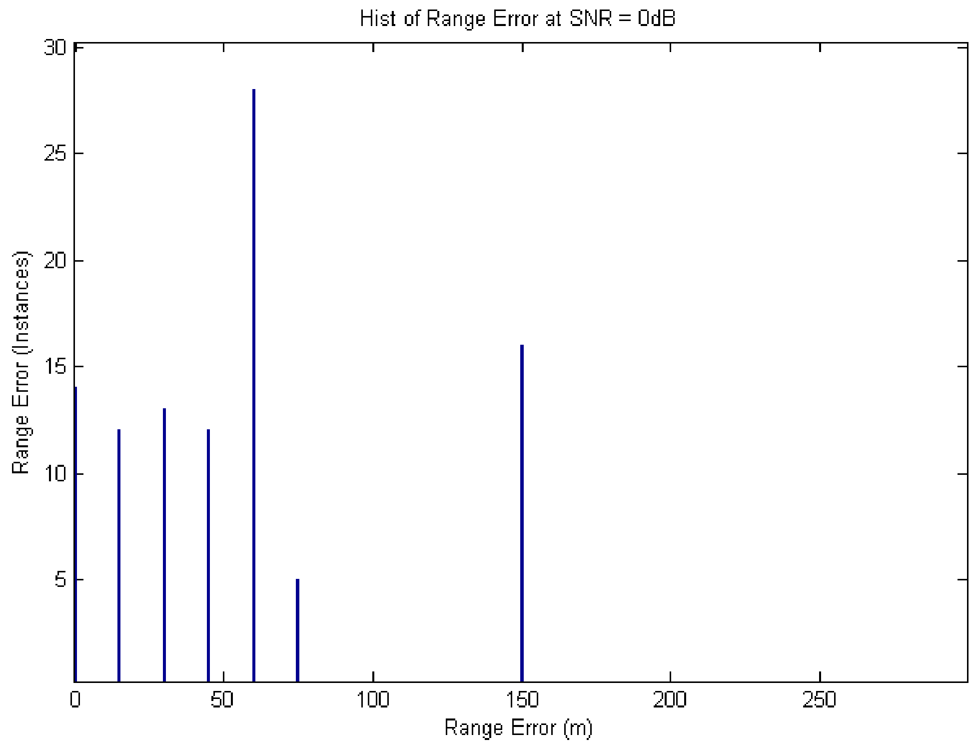

Figure 2.6: Resulting Range Measurements for Rayleigh Fading Model with Causal Taps

acterized by the use of a distributed algorithm. For this study, having all processing done at the LMU, a centralized algorithm is used and hence provides more accurate results than the cases where distributed algorithms are used [34]. It must also be noted that for this algorithm, demodulation of the signal at the LMU is not needed. As a result of the SRS sequence being known between the UE and the LMU, the timing measurement accuracy is not affected by the demodulation performance of the signal at the LMU [11].

Following the generation of the SRS sequence and its transmission through the Rayleigh fading channel to satisfy ETU Case I, a correlation can be performed. For this simulation and following 3GPP, processing is not performed at the LMU until 50 SRS sequences have been received or accumulated [9]. The correlation technique is utilized to resolve a range error in the differential between the pre- and post-channel sequence transmissions. It must be noted that the correlation is performed at one centrally located LMU by comparing the original sequence and the received sequence. By finding the maximum peaks in the correlation, a time of arrival range error can be calculated from the uplink signal accumulations.

As mentioned, every SRS sequence is located in the same location in the LTE resource grid and the sequence utilizes one OFDM symbol. After being mapped and having the FFT performed, each SRS sequence is held within 1168 symbols. This size of the entire sequence is dictated by the size of the FFT (1024) and the size of the cyclic prefix (144). After all 50 sequences are accumulated, the spacing between SRS sequences is ideally 1168 symbols and the full length of the transmitted sequence is 58400 samples. The sequence is extended to 58420 with the 20 additional symbols to ensure causality. With 50 accumulations of the pre-channel and post-channel SRS sequence, the correlation is performed by comparing the energy levels across the spectrum. The 50 accumulations of the post-channel sequence are compared one at a time with the pre-channel chain of sequences in the form of a sliding window. Additional sequences of the post-channel samples are added to the correlation until all 50 are being correlated and then the correlation is performed by reducing the post-channel accumulations. Due to the sliding-window manner of the correlation the entire correlated sequence is double the length of the 50 accumulated SRS signals or 116800 samples. The results of a such a correlation can be seen in Fig. 2.7. For clarity, the max peak is marked in Fig. 2.7 and is located at 58420 samples. No range error will occur if after all 50 sequences are correlated, the maximum peak of energy exists at 58420 samples. The index of this sample in the correlation corresponds to a perfect overlap of both sequences of 50 SRS accumulations and a range error of 0 m.

With the addition of noise in the channel, the ideal spacing is not always maintained and thus an error in range can result. The range error is calculated using Eq. 2.3 and is given in meters.

$$RangeError = |(X - \gamma) * (1/f_s) * c| \tag{2.3}$$

where X is the index of the maximum value or peak from the correlation of SRS sequences, γ is the length of the accumulated pre-channel SRS sequence including the fix for causality, f_s

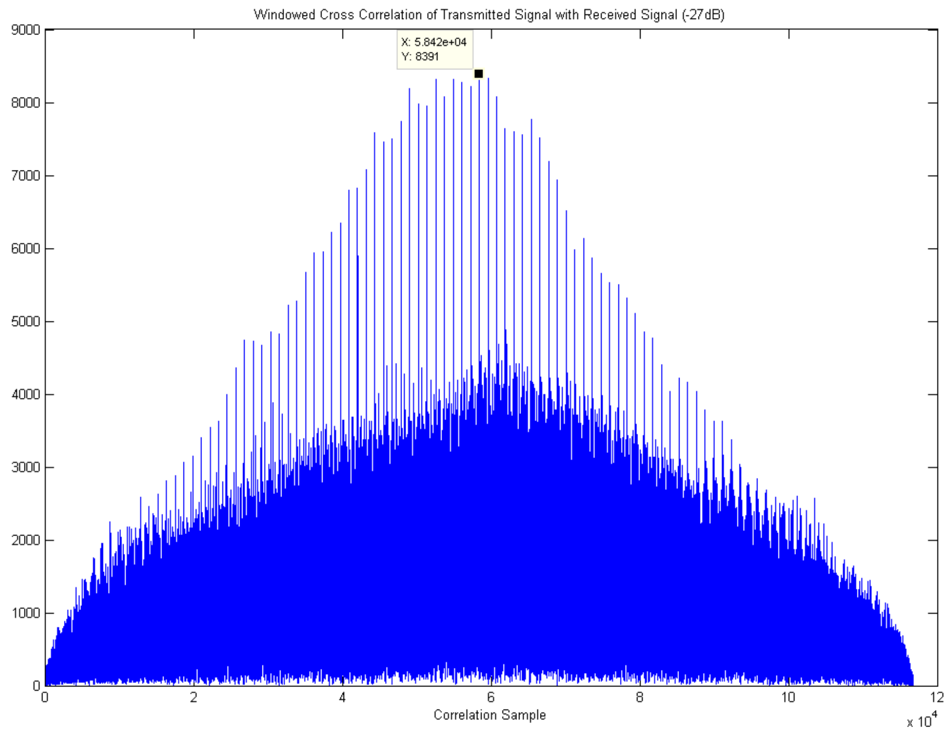

Figure 2.7: Ideal Results from Full Cross Correlation of SRS Sequences in Low SINR

is the sampling frequency, and c is the speed of light. The absolute value of the range error is taken as a negative range error would only indicate a different direction in the geometry, but this is not a concern. If the correlated peak is detected earlier or later in time, the absolute range error is the value of concern.

This simulation, calculating range error, is run for 1000 iterations over a range of SNR values from -27 dB to +25 dB. This range is chosen based upon the connectivity threshold of ENodeBs being set at -27 dB. At low SINR values, the associated normalized noise added to the signal resulted in erroneous peak detections. Looking at the cross correlation in Fig. 2.8 it can easily be seen that location of the max peak has shifted from that of the one seen in Fig. 2.7. When a peak is chosen to be the max when it is actually not within the boundaries of the ideal cross correlation peak, the resulting range error, being a result of the sample delay time multiplied by the speed of light, is over 17 km. A range error of this magnitude will occur whenever a peak is chosen that is delayed 1168 symbols or more; beyond the time separation of one full SRS sequence. Given that a full receiver is not being implemented, such a range error is considered to be erroneous and it exceeds the entire length of the network (Fig. 2.11) by several times.

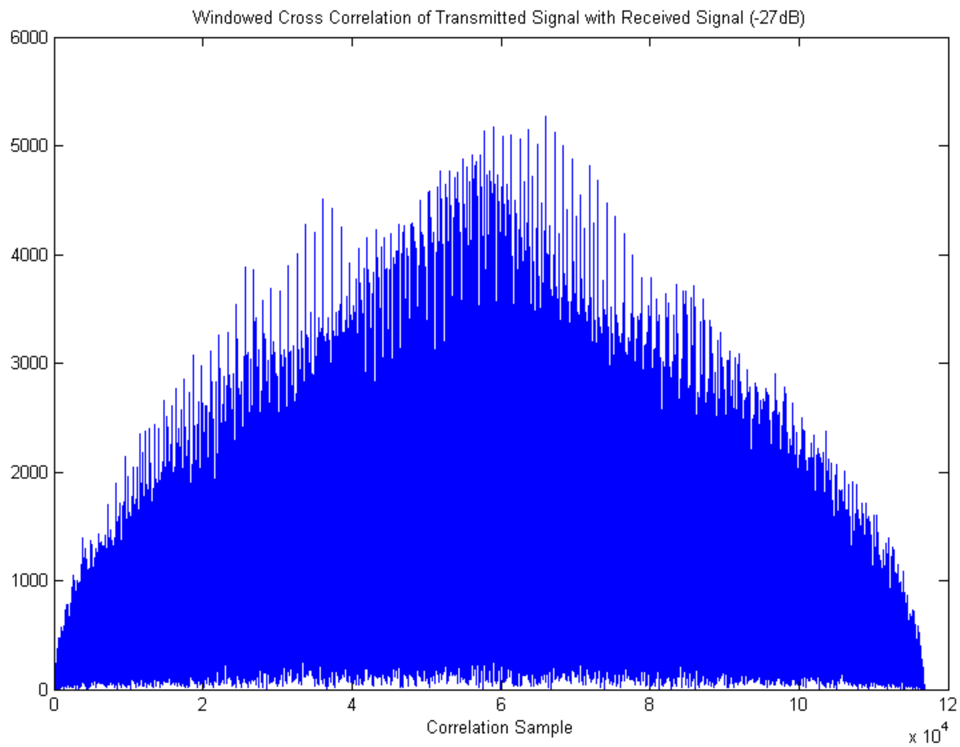

Figure 2.8: Results from Full Cross Correlation of SRS Sequences in Low SINR with Large Range Error

In order to avoid the wrong peak detection, a window was applied to the correlation of the SRS sequences. Given 50 accumulations of the SRS sequence, the ideal peak location, resulting in 0 m of range error, is known and can be windowed. To allow for a shift in the location of the peak about the ideal location in time, the window is centered about the SRS sequence and extends for 500 symbols on either side of the sequence to allow for at most 17.5 km in error. The resulting correlation window which prevents erroneous symbol detection can be seen in Fig. 2.9. The figure displays the window over which the max peak

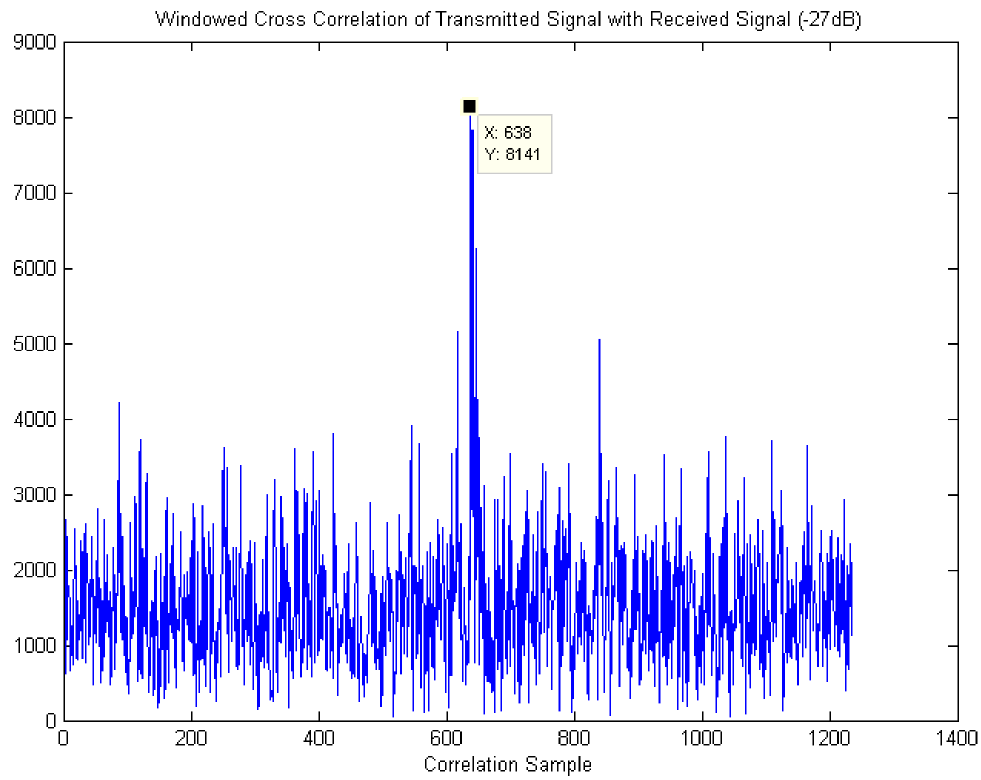

Figure 2.9: Result of Windowing the Cross Correlation of SRS Sequences in Low SINR

is searched for in the correlation. The windowed set of the correlation was generated from the same SNR settings (-27 dB) as was displayed in Fig. 2.7 and Fig. 2.8. From this. it is clear that the desired SRS sequence peak will be detected and an unfeasible error will not occur. Fig. 2.9 also displays an ideal peak detection; having the peak at sample 638 in the simulation window. Accounting for the windowed amount of samples and using Eq. 2.3, the corresponding range error for this figure is 0 m. An example of a 150 m range error can be seen in Fig. 2.10. The peak detected in Fig. 2.10 is at 648 samples which when adjusted for the windowing (adding 57782 samples to shift the index back) resolves to a 150 m TOA range error.

Ultimately from the link layer simulation, a range error lookup table was constructed for use in the network layer simulation. The base stations which connect to the unknown UE are

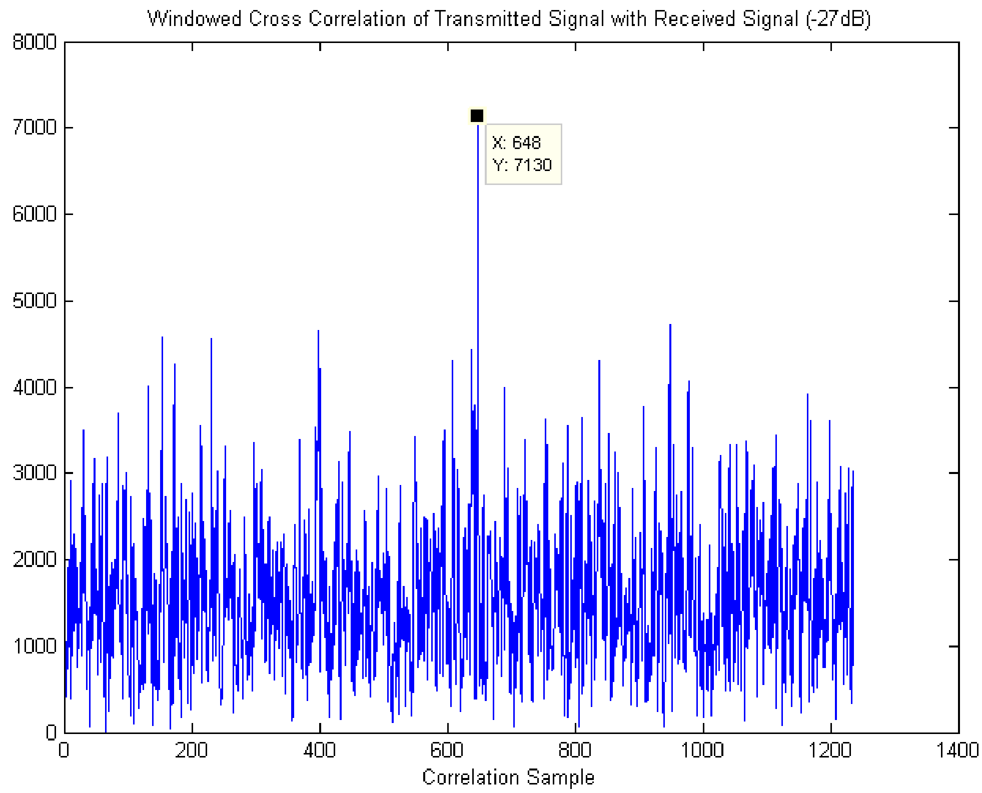

Figure 2.10: Result of Windowing the Cross Correlation of SRS Sequences in Low SINR with Error

associated with a random TOA range error that corresponds to the SINR of their received signal. With the range error lookup table complete, the link layer and SRS sequence can be associated with the rest of the uplink simulation.

2.3 Network Layer Simulation

2.3.1 Simulation Parameters

The simulation parameters were selected based on the 3GPP assumptions for UTDOA in [9]. Table 2.3 summarizes the specific parameters used in the network layer simulations.

The configuration of the simulated LTE network is shown in Fig. 2.11. There are 19 ENodeBs in the network and they are depicted with solid triangles. Each ENodeB has a 3-sector antenna with the pattern defined in Table 2.3. The UEs are randomly placed throughout the entire network. Once the UEs are placed, their SINR needs to be determined for each link based on the used reference signal (SRS). For each ENodeB, the SINR from ENodeBs and other UEs are calculated. If the SINR at the ENodeB terminal is higher than a specific threshold, the corresponding link is assumed to be present. The connectivity threshold was set at -27 dB for ENodeBs and -6 dB for UEs. The interference for calculation of SINR between the UE and all base stations was modeled after 3GPP specifications in [10] and can be seen in Fig. 2.12. This interference model assumes a realistically high load where 80% of the required resource blocks are scheduled in each of the serving and neighboring cells. While such data traffic is uncommon in an actual case, it is important, for worst-case analysis, to characterize the severe interference case in order to test the performance of localizing system [10]. As seen in Fig. 2.12 the approximate peak of the interference-over-thermal (IOT) distribution was assumed to be 8.2 dB for this simulation. The interference was then modeled through the use of a randomly distributed normal variable to most accurately model the 3GPP specification seen in [10].

Table 2.3: Summary of Network Layer Simulation Parameters

Parameter	Assumption
Cell	Hexagonal grid, 19 cell site
Inter-Site Distance	500 m
Pathloss Model	L = 128.1 + 37.6*$\log_{10}$R
Penetration Loss	20 dB (Case 1 & 3)
Shadowing Std	8 dB
Shadowing Correlation	0.5 (Between sites), 1 (Between Sectors)
Antenna Gain	15 dBi (3 sectors per site)
Antenna Patternn	$A(\theta) = -\min[12(\theta/65°)^2, 20]$ dB
ENodeB Power	46 dBm
UE Power	23 dBm
UE Noise Figure	9 dB

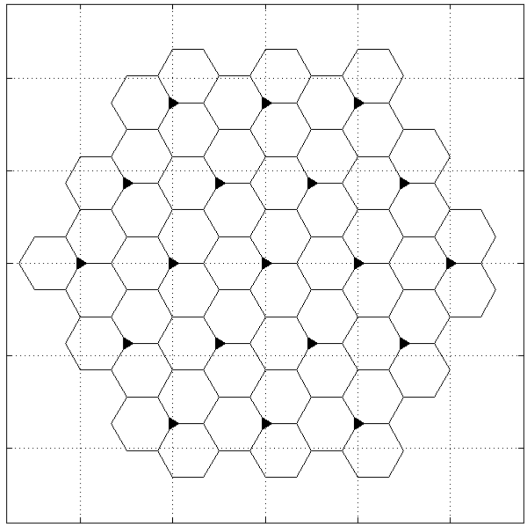

Figure 2.11: Configuration of the simulated LTE network. The locations of ENodeBs are represented by solid triangles. The UEs are randomly placed in the network. The inter-site distance is 500 m.

2.3.2 Nonlinear Position Estimator

In order to estimate the location of a UE given connections to a variety of anchors, an optimization algorithm from Matlab, 'lsqnonlin' is utilized using the Levenberg-Marquardt algorithm (LMA). This algorithm solves nonlinear least squares curve fitting problems; the problem that arises from the distance equation between an anchor and a UE with unknown X and Y coordinates for the UE. In UTDOA, The squared distance between the mobile and the ith base station is given as [30]:

$$\begin{aligned} R_i &= \sqrt{(X_i - x)^2 + (Y_i - y)^2} \\ &= \sqrt{(X_i^2 + Y_i^2 - 2X_i x - 2Y_i y + x^2 + y^2)} \end{aligned} \tag{2.4}$$

where X_i and Y_i are the *ith* location coordinates for the *ith* connected base station and x and y are the unknown UE's coordinates. Several of these distance measurements are needed in

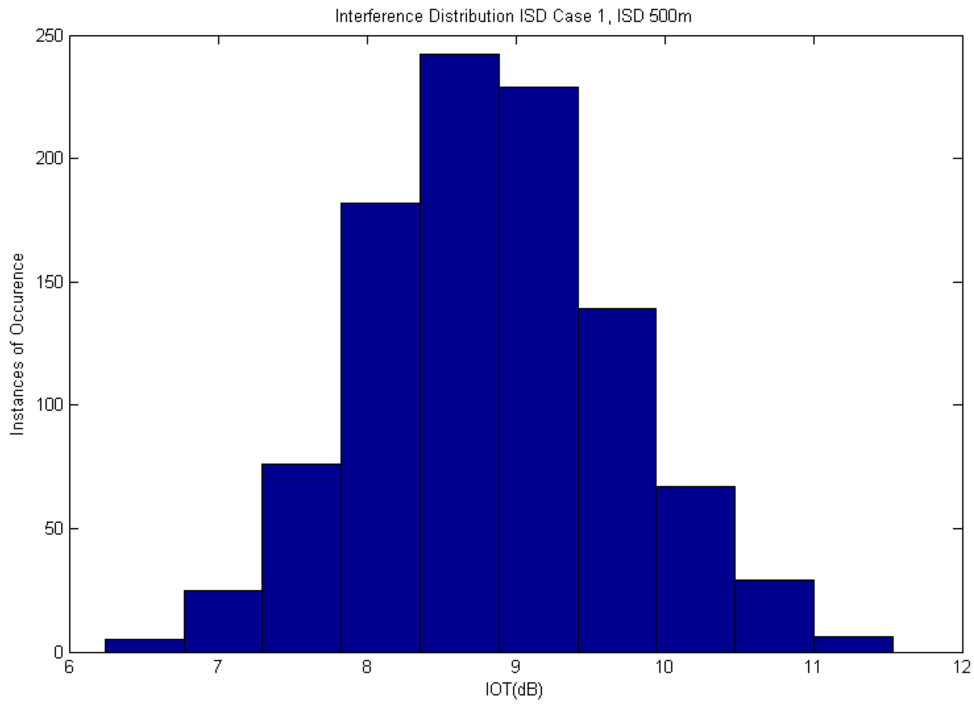

Figure 2.12: 3GPP Specified Interference over Thermal (IOT) Distribution for ENodeBs in Uplink Transmission

order to accurately estimate the x,y location of the target UE. Further, the position equation that is utilized for localization from the distance equation is given by [49]

$$f_i(x, y) = \sqrt{(x - X_i)^2 + (y - Y_i)^2} - \sqrt{(x - X_0)^2 + (y - Y_0)^2} \tag{2.5}$$

where x and y are still the the unknown UE's coordinates and X_0 and Y_0 are the coordinates of the reference node. The following equation gives the NLLS estimator for non-collaborative TDOA [49]

$$\hat{\theta}_{NLLS} = \arg\min_{[x,y]^T} \sum_{i=1}^{N_m} (z_i - f_i(x, y))^2 \tag{2.6}$$

where $i = 1, ...N_m$ and N_m is the number of reference nodes. Then $z_i = f_i(x, y) + \eta_i$ and η is the noise at the ith estimation.

In order to fit a parameterized function to the given location data points, the Levenberg-Marquardt algorithm reduces the sum of the squares of the errors between the function and the measured data points through a hybrid of the gradient descent method and the Gauss-Newton method [48]. Through the iterative reduction of the sum of the squares, the Levenberg-Marquardt algorithm is capable of converging to a set of data points when the parameters are either close or far from the original value. The algorithm will perform

> "more like a gradient-descent method when the parameters are far from their optimal value, and acts more like the Gauss-Newton method when the parameters are close to their optimal value." [48]

With parameters close to the optimal value, the algorithm tends to converge faster than if the parameters are far. The nonlinear distance equations between the target UE and all of the connected anchors takes the form seen in:

$$min_x||f(x)||_2^2 = min_x(f_1(x)^2 + f_2(x)^2 + ... + f_n(x)^2) \tag{2.7}$$

The Levenberg-Marquardt algorithm is executed for five iterations from the perspective of each unknown UE in the network; attempting to minimize the error of the location estimate given all of the connected anchors and their distance equations to the target. With each iteration a set of estimated coordinates is reported and can then be compared to the known location of the target to determine the error.

The location estimation results of the algorithm from the computer simulation are explained in Chapter 4.

Chapter 3

Pressure Sensor Utilization for Localization

3.1 Introduction

The earth's atmosphere exerts pressure on the earth's surface. Atmospheric pressure measured by a barometer is commonly referred to as barometric pressure. This pressure can be portrayed as a column of air that exists on top of the earth's surface and the column decreases or increases in size as elevation increases or decreases, respectively [62]. Thus, barometric pressure is inversely related to elevation and can be used to estimate elevation. Pressure can vary both vertically as well as horizontally; affected by several variables. Common practice uses the atmospheric pressure at sea level as the base reference. Other measured pressures can be referenced to this base to determine the offset. Regardless of elevation, the earth's weather patterns also affect the local atmospheric pressure conditions; high pressure being associated with sunny weather and low pressure bringing storms. As outlined in the previous section, pressure measurements will be considered as a means to determine the vertical plane element of the target phone's location; specifically the floor that the phone is located on. According to the International System of Units, pressure is measured in pascal (Pa). The unit of pressure generally used for atmosphere is the hPa or millibar (mb or mbar) where $1hPa = 1mbar$; hPa and other variants of Pa will be used in this work. The nature of barometric pressure in the outdoor environment is susceptible to several variables, the primary one being the real-time weather conditions. For the baseline, the standard temperature and pressure at sea level is 288.15K and 101.3 kPa respectively. Blacksburg, Virginia, the location used for these evaluations, is approximately 2100 ft above sea level [63]. This suggests that the Blacksburg standard pressure, altered for height, should be approximately 93.9 kPa holding all other variables constant and based upon the following equation [64]:

$$h_{alt} = \left(1 - \left(\frac{P_{sta}}{1013.25}\right)^{0.190584}\right) \cdot 14533.45 \tag{3.1}$$

where h_{alt} is the altitude (ft) and P_{sta} is the station/site/measured pressure (hPa). Based on the local weather conditions, the air pressure outside will vary and can be below or above the base reference of 101.3 kPa given a low or high pressure system. For example, a low pressure system is usually associated with rainy conditions in the area and will cause the pressure to drop. Furthermore, there is a large discrepancy between the outdoor pressure and the pressure of an indoor environment. The pressure inside a building is what will be considered since we are interested in indoor geolocation.

There are several variables that induce vertical air pressure differences in a building including stack effect, fan pressurization, wind cycling, barometric cycling, and thermal cycling [65]. While buildings are designed to maintain a certain pressure within the structure and manage the differences between the outside environment and the indoors, the main portion of the building envelope in which the effects of pressure differences occur can be observed in the construction cavities. In these spaces, which exist between support layers and exterior walls of the building, the effects of pressure differences are present and these extend inwards into the building. Stack effect is a temperature-driven phenomenon that occurs when warmer indoor air rises in the building and ultimately escapes. In association with this, there is a reverse air-pressure difference at the base of a building in which cold air leaks in or infiltrates.

Fan pressurization is realized via mechanical systems such as ventilation and humidification systems. It is created by building HVAC (heating, ventilation and air conditioning) systems to overcome undesired environmental influences such as stack effect. The HVAC system causes a slight over-pressurization of a building to try to reduce the infiltration of outdoor air at the ground level. Stack effect and fan pressurization will tend to induce pressure differences of +10 Pa to +50 Pa; corresponding to an altitude change between 2.7 ft and 13.8 ft [65].

The other three effects causing indoor pressure differences are tied more directly to time and the local weather conditions. The wind speed in the open air is likely to change from day to day and these changes can increase or decrease the indoor air pressure based on the number and location of openings in the exterior of a building. With a uniform number of openings around the building, the indoor pressure will tend to be lower than that of the exterior pressure [65]. If the building is sealed with no windows that can open, this affect is significantly minimized. Barometric pressure varies with weather conditions and, like wind pressure, affects the interior of a building through pressure on the outside surfaces. While the pressure outside can change rapidly depending on an incoming weather front, micro changes of the indoor barometric pressure of $\pm$ 50 Pa can occur up to 50 times an hour [65]. Using Eq. 3.1, this alteration of 50 Pa will display an approximate vertical measurement variation of approximately 14 ft. This proves to be a nontrivial variation and a value that can directly impact the calculated floor that the UE is located on. Therefore this must be taken into account for indoor pressure sensors. Following the wind and the actual pressure in the outdoor environment, the third affect is temperature which also plays a significant role in altering the pressure inside a building. Variations of temperature on the exterior surfaces of a building will cause compression and expansion of the actual structure depending on whether the temperature decreases or increases, respectively. These alterations in the exterior of the building due to temperature variations can further allow air to escape or enter the building also affecting the pressure. Ultimately, all of these pressure differences induce air leakages and can cause minor alterations to the indoor pressure environment as well as damage to the building over a long period of time in which cycling goes unchecked. Stack effect and fan pressurization are known to be the largest causes of indoor to outdoor pressure differentiations.

In order to more accurately predict the indoor pressure on a daily basis, the causes of alterations in the outdoor pressure are also worth analyzing. While the altitude of a location will alter it's pressure; there are more variables that impact the horizontal pressure of an area. These factors will help address how wide of an area can expect to have the same pressure. The variables that directly impact horizontal pressure are grouped into thermal and dynamic causes [25]. Much like vertical pressure, temperature will alter the pressure over an area. As the sun heats the earth and thus the air, the volume of the air will expand and decrease its density. When this occurs, the warm air will rise and the surface pressure will decrease. In much the opposite affect, surface pressure will increase when the air gets colder. While temperature changes when moving away from the equator, pressure does not evenly increase. The reason for this is the dynamic causes of horizontal pressure variation; the rotation of Earth and it's patterns of circulation [25]. Ultimately, the patterns of temperature and Earth's rotation need to be constantly analyzed and mapped to deduce the distribution of horizontal pressure of an area. These maps, still referencing everything to sea level, have *isobars* which are lines drawn on maps to show areas of equal pressure [25]. Through the use of these maps it is also possible to predict weather patterns; being used by meteorologists and geologists every day.

As good practice, it can be assumed that the pressure of an area is changing whenever wind is present. Wind is a response to differences in pressure and is associated with a pressure gradient or the differences of pressure between two locations [25]. A pressure gradient force is the root of this phenomenon as it is induced from the difference in pressure and triggers air movement or wind. In the horizontal sense, the pressure of an area of a few square miles will tend to be the same; truly distinguished by pressure gradients on meteorological maps. In the vertical sense, the pressure will alter approximately 3.6 kPa per 1000 ft [26].

3.2 Literature Survey for Pressure Aided Localization

Phones are now capable of taking a variety of measurements, equipped with an array of sensors, and then utilizing the information for purposes such as localization. As stated previously, people are now dialing 911 more from mobile phones rather than land-lines and their ability to be located in such times is of utmost importance. The sensors that are now present in phones are an ongoing area of research as they can be a useful tool for assisting in this endeavor. Some such work has been performed by [15]; directed towards the emergency call system in the U.S. and it's focus on caller's location through a targeted floor localization system. The approach taken to provide a floor-level accuracy of positioning with minimal infrastructure support involves the use of multiple sensors found in today's smartphones. The sensor array that is utilized includes the Inertial Measurement Unit, a three-axis accelerometer, a three-axis gyroscope, and a three-axis magnetometer. The sensors are used to provide measurements for the implementation of analysis modules which compute the user's location. These analysis modules track the user throughout a building, monitoring travel via stairways, elevators, and escalators; any means of vertical movement inside of a building. Working in tandem with the sensor array, the other portion of this localization approach involves deploying beacons sparsely throughout buildings. The majority of analysis and computation is done within these beacons while the phone is the tool to provide specific measurements. The users' phones receive building information upon entering on a certain floor of a building and then the phones are provided with corrections to their location as they travel through the building through the use of the analysis modules.

The interest in phone sensors for localization has become greater and greater as these sensors have become standard features. The variety of sensors and their capabilities are endless. One particular sensor has garnered a lot of attention and is the focus of the work done here; a pressure sensor.

An initial study of barometric pressure sensors and their capability for aiding indoor localization efforts was done in [16]. Several pressure sensors, in different phones, were compared and experimented with. It was seen that pressure varied with time, location, and between devices. Despite these variables, height alterations were detected with ease and thus a route for its use. A predictor was put in place to report when a change in floors occurred based upon pressure differences. Overall, through the analysis of the difference in pressure, it is claimed that the exact number of floors that have been changed can be detected with almost 100% accuracy given some fingerprint information. It is also stated that it is difficult to use the pressure sensor to determine the actual floor of the user; given absolute pressure varying across devices and the existence of multiple entrances in a building.

The weather of the area in which a pressure reading is taken greatly affects those measurements. In order to estimate altitude, [18] proposes the utilization of weather station temperature and pressure information. Each piece of information is constantly monitored; temperature is updated hourly and pressure is updated more often. By monitoring and correcting the smartphone pressure reading according to the current sea-level pressure and temperature, altitude was able to be estimated with an average error of 1-2 m. The same estimation accuracy with pressure sensors (Bosch BMP085) was achieved by [19]. 3D localization was performed using wireless sensor nodes and a MLS algorithm for 2D position estimation and then adding information on pressure to the algorithm for the third dimension. The estimation error for the 3D positioning was 12 m or less; noting that the inclusion of pressure data did not truly improve the positioning accuracy with the use of the specific MLS algorithm. Approximately 60 Pa of noise was seen in the pressure sensors due to acoustic waves. The use of pressure sensors alone was shown to not be enough for floor identification due to several sources of error including: the nature of atmosphere pressure, inaccuracy of base station placement, and variations in the wind and the air temperature [19].

Work done by Bollmeyer and others in [21] uses highly sensitive pressure sensors in order to distinguish minute (in centimeters) alterations in altitude. While these sensors are not currently used in smartphones, several observations were made in the paper regarding barometric pressure sensor accuracy. The need to monitor as well as compensate for humidity and temperature changes for accuracy sake in medical situations is highlighted in this work. Real-time, continuous measurements are not needed in this application which allows for filtering and averaging of data to improve the estimated altitude. Further, the work of [20], where pressure sensors improve altitude information for GPS systems through differential barometric measurements, is adapted for the medical application. In order to perform a differential calculation, at least two pressure sensors are needed. To address the sensor offset and be able to calibrate it out, these two sensors are located in the same environment and they make measurements at the same time. One sensor is held at the point of calibration and the other is then moved, referring back to the reference point pressure to resolve altitude and also account for the various sources of error.

Much like the use of other sensors as was seen in [15], research has been done with pressure sensors working with infrastructure to perform localization. Many such systems are setup as a fingerprint-based localization technique and can be seen in [16, 17]. The issue with such systems is that real deployment is both complex as well as expensive. To address these issues, [17] has leveraged crowdsourcing of smartphones with pressure sensors to build barometer fingerprints; naming the technique Barometer based floor Localization (B-Loc). These fingerprints, contained on cloud servers, have pressure values for each floor of a building and are used to locate users' floor levels by associating pressure values within the map. When a user enters a building, using some specified mobile client software, B-Loc builds the barometer fingerprint map and then collects real-time barometer readings from the user's phone. An activity recognition algorithm is in place as a part of B-Loc to track the users as they move between floors. The B-Loc system is able to handle multiple users' barometer readings through a calibration algorithm that removes drift and establishes any user as a reference when they have the highest confidence value or highest probability of correct calibration. The cloud server propagates the calibration factor as needed across users in the same location. With all users calibrated and transmitting their real-time pressure readings, a clustering algorithm is put in place to create and update the fingerprint map. Ultimately, phones associate with the pressure reading on the map that most closely matches their own.

3.3 Barometric Pressure Sensors in Mobile Handsets

As a part of mobile handset construction, many models are emerging with pressure sensors included in their design. The main manufacturer of these Micro-Electro-Mechanical Systems (MEMS) barometric pressure sensors is Bosch; having shipped more than 120 million pressure sensors in 2013 for use and implementation in the majority of smartphones [59]. Knowing the intended future use of the pressure sensor in a mobile handset to be for height calculation, Bosch Sensortec has addressed several technical questions originating from the FCC regarding the wireless location accuracy for E911. The company believes that the current barometric pressure sensors, following the requirement established by the FCC, (as of May 2014) will

> "allow for altitude determination of equipped mobile devices to within 3 meter accuracy for at least 67 percent of calls within three years, and for at least 80 percent of calls within 5 years" [59].

The BMP180 sensor, manufactured by Bosch, can be found in several mobile handset models including the Samsung Galaxy S4 and is capable of measuring ambient pressure with an absolute accuracy of approximately 0.12 hectopascals (hPa) which translates to approximately 1 meter of change at standard sea level. Bosch states that with the inclusion of their sensors, with such accuracy, the FCC 3 meter target of accuracy can be met in phones. Further, Bosch claims that their sensor can maintain a 1 meter accuracy when transitioning between the outdoors and an isolated indoor environment, usually a building with HVAC systems. Bosch further states that the sensor must make a series of precise measurements outdoors for a suitable reference for the indoor pressure calculation [59].

For Bosch pressure sensors and all others, there exist two primary categories of sensor error that need to be taken into consideration. The first and foremost is relative measurement error which is inherent to the pressure sensor. This limitation of the hardware results in absolute pressure variations even within a stationary phone and cannot be calibrated out but instead has to be budgeted for [2]. The other source of error is sensor drift characterized as sensor degradation over time that makes measurements offset from the original calibrated state. Even when a mobile handset is stationary, the pressure can drift and can report a 1.4 m or approximately 4.6 ft change in height after a short time duration of 15 minutes [16]. Fortunately, this can be calibrated out if there is an accurate and frequent reference measurement that is available at a known altitude in some air environment [2].

In order to calibrate, the actual relationship between the measured pressure and elevation needs to be taken into consideration. While it is known that pressure experienced on a body will change depending on the altitude, there are other underlying variables. The relationship is described by Bernoulli's Equation, seen in Eq. 3.2 [61]

$$P_1 + \rho g y_1 + \frac{1}{2}\rho v_1^2 = P_2 + \rho g y_2 + \frac{1}{2}\rho v_2^2 \tag{3.2}$$

where ρ is the air density and g is gravity. The variables y_1, v_1, y_2 and v_2 represent the height and air flow velocity of region 1 and 2, respectively, through which the fluid or air in this case, transitions. P_1 and P_2 represent the pressures of region 1 and 2. To simplify this equation for the purpose of this study, it is assumed that the velocity of the air on each floor is approximately 0; thus, $v_1, v_2 = 0$. Also, if pressure is considered to be atmospheric pressure at all times, establishing a building as a homogeneous system, then ρ is also constant. Through manipulation of the equation, a difference in pressure can be written as ΔP which equals $P_1 - P_2$. This leaves a difference in height ($\Delta y = y_1 - y_2$) and the two constants, ρ and g on the right side of the equation such that Eq. 3.2 is simplified to

$$\Delta P = -\rho g(y_1 - y_2) = -\rho g \Delta y \tag{3.3}$$

With this equation, and while assuming gravity and the density of air can be considered constant values, it is established that there is a linear relationship between height and pressure. Analysis of the pressure measurements from a mobile handset can thus be considered to display the same increasing or decreasing behavior from day to day based on altitude. However, this does not prevent an actual change in baseline pressure in a building; still being affected by the variables mentioned earlier.

Following this, it must be noted that the main deficiency with Bosch sensors (as well as those made by other manufacturers) is the use of the pressure sensors without appropriate calibration. Pressure values are held in reference to the actual standard pressure that exists when at sea level. If sensors are not calibrated at sea level, which is considered standard pressure, then any measured pressure by the sensor will need to have an offset applied or a re-calibration. The method of rectifying this offset relies on finding the local barometric pressure and temperature. These need to be known at the same time that the altitude is being determined on the mobile device. A reference for local pressure and temperature is typically taken from a nearby weather station with known vertical position above sea level. This sort of calibration will not be performed by everyday users with their mobile handsets, and indoor measurements cannot be taken simultaneously with measurements at a weather station. The issue of how to properly establish a reference value for pressure readings is a question yet to be answered. Further, utilizing the pressure sensor in a manner to establish a third-dimension estimate for localization in the vertical (Z) plane is something that is investigated here.

3.4 Barometric Pressure Tests and Potential Use Cases

As a means of locating a mobile device indoors, a barometric pressure measurement from the phone in question can be a part of the transmitted information to a telecommunications service provider's terrestrial base station (ENodeB) or any other local RF anchor. This pressure reading could be used to assist in determining the location of the handset in the vertical plane. However, due to the fluctuations of weather conditions affecting real time barometric pressure and the other aforementioned variables, an indoor pressure measurement and its corresponding altitude calculation would not be directly related nor could it be referenced to the ground level pressure outside of the building. While UTDOA localization will provide a two dimensional, X-Y plane location, the third dimension is still in question. Utilizing barometric pressure readings as a method in which this third dimension, the vertical height above ground level, can be calculated and reported, with a reasonable level of accuracy, is to be investigated here.

As indicated, many current models of mobile smart phones incorporate a barometric pressure sensor. In order to test the accuracy and consistency of this type of sensor, several experiments were conducted in which a mobile handset was used to record pressure readings on different floor levels of a building as well as outside at ground level of this same building. To ensure consistency with the experiments, all pressure sensor data was gathered in the Durham Hall building on the Blacksburg campus of Virginia Tech. This building has four floors allowing for various heights and corresponding pressure readings to be collected. The majority of tests were conducted using a Samsung Galaxy S5 from T-Mobile (G900T) which contains a STMicroelectronics LPS25H MEMS pressure sensor. According to its specifications, the LPS25H pressure sensor has a relative accuracy over pressure of ± 0.1 hPa while operating at room temperature, see Appendix **??**. This translates to a relative accuracy of ± 2.92 ft or approximately ± 0.9 m for altitude given Eq. 3.1. While Bosch explains the use of the BMP180 sensor with ± 1 m accuracy in their comments to the FCC, other sensors with equivalent or better accuracy should be interchangeable for such a situation regarding localization. Thus the use of the STMicroelectronics LPS25H is considered to give comparable results to those of the Bosch Sensortec sensor.

To gather comparative data, experiments were conducted with several other handsets of the same and also varying models. The handsets included in the experiment were a single Samsung Galaxy S4, two other Samsung Galaxy S5s, and one HTC One M8. The Galaxy S4 contains the Bosch Sensortec BMP180 with a relative accuracy of ± 0.12 hPa which corresponds to a ± 3.5 ft relative accuracy in altitude at room temperature. The HTC One M8 contains the Bosch Sensortec BMP280 which performs with the same relative accuracy of pressure as the BMP180. Specific device details can be seen in Appendix 6.

With the goal of determining the exact floor a handset is located on, several scenarios were conceived to test the ability of a pressure sensor to accurately measure the pressure and translate that pressure to an altitude of a handset. Every scenario assumes that the UE in question is able to report its X-Y plane geographical coordinates through U-TDOA as well as report its pressure readings. The first scenario relies on only having the UE present in the building and on the floor where it is to be discovered. The local weather station information measuring the outdoor environment can be obtained at the time of the test scenario, but the UE itself has no knowledge of this pressure information. The second scenario entails calibrating to the measured pressure and altitude of a local weather station. The altitude of the ground floor of the building must also be known in this case. The third scenario involves utilizing infrastructure in order to assist in localization. Barometric pressure sensors are located on each floor and the UE trying to determine its location would calibrate to these sensors. The final and proposed use scenario involves a single UE that has memory of its pressure readings as a means of reference. The handset will be able to establish a first floor pressure reading and then calculate and report its altitude relative to the measurement taken upon entering a building. The final scenario has the unknown UE on a floor of the building and then additional UEs throughout the building to act as collaborators. The collaborating UEs will be able to report their estimated location as well as pressure reading. The local weather station reference can also be obtained. The primary focus of this test will have a collaborating UE located on same floor to compare pressure readings with that of the unknown UE and attempt using their independent pressure differential to determine the third dimension, the vertical location in question through an average between the devices. With this variety of tests, an appropriate method of calculating the altitude and, thus floor, of a UE to be located will be determined.

3.4.1 Error Model of the Pressure Sensor

As mentioned previously, the majority of testing was conducted with a T-Mobile Galaxy S5 mobile handset which contains a STMicroelectronics LPS25H barometric pressure sensor. In order to ensure that the pressure sensor contained within the phone was a viable option for such testing, error models had to first be produced to deduce whether the STMicroelectronics pressure sensor actually displays the accuracy that it's specifications state.

First, the physical distance that separates the floors of the Durham Hall building at Virginia Tech was measured at 14 ft. Then the pressure inside of the building was recorded using the target phones from the same locations at different floors levels for five minutes at a time at a sample rate of 5 ($\frac{samples}{s}$) to provide approximately 1500 pressure measurements per location. Pressure sensor data was recorded while the mobile handset was held at waist height; ensuring that the physical separation when moving floor to floor would be 14 ft. Assuming this natural position of a handset also lends itself to the outcome of the data and its relation to a real life situation. With such a position of the mobile, when altitude is calculated, there is room for error in both the positive (upwards) or negative (downwards) direction that can be accepted before the calculated floor is incorrect. In regards to other error, inherent in the pressure sensor, this test was performed across different days to collect a significant number of samples and to test the pressure sensor as the weather changed outdoors which, as mentioned, alters the indoor pressure as well.

Once all of the barometric pressure data was compiled, the corresponding altitudes had to be calculated using Eq. 3.1. All of the data from a respective floor and particular day was combined such that a common mean and variance could be found across the floor. With this information, a "ground" reference could be established. In a situation in which the pressure sensor needs to be utilized to determine the floor it is located on within a building, the elevation of the ground floor will not be the same in every building nor will it be the same day-to-day. As such a ground-floor will be entirely relative to the building the mobile handset is in. To find the difference in altitude, the lowest floor on which measurements were taken is used as the ground reference floor. It is also known that the distance between floors in the test building is constant and 14 ft. The deviation from the actual height change is found by subtracting differences in calculated altitude which will be considered measurement error. Ultimately, the knowledge of the pressure on the ground-floor will help identify the floor the handset is on; this will be discussed later. The error was modeled relative to changes in altitude. In other words:

$$Error = \alpha - \bar{x} - (14 \cdot n)\,[ft] \tag{3.4}$$

where α is the calculated barometric altitude from the pressure sensor readings; $\bar{x}$ is the mean of the calculated barometric altitude of the ground-floor reference; and n is the number of floors away from the ground floor. It must be noted that 14 is a constant given the calculations are done when floor separation is 14 ft as in Durham Hall. Eq. 3.4 will give the difference, in feet, between the measured change in altitude and the actual change. By performing this calculation for the total number of samples across a floor, a distribution of error can be gathered. An example of such a distribution can be seen in Fig. 3.1 and Fig. 3.2.

Fig. 3.1 displays a distribution with a mean of approximately -5 ft and a variance of 3.27 ft for a particular day on which measurements were taken. With a negative mean of error, this dictates that in this instance, the pressure sensor calculated its altitude to be continuously lower (by 5 ft) than the ideal altitude difference between floors. Since the floors are separated by 14 ft, the absolute error must be less than 14ft or ± 7 ft to ensure an accurate floor estimate. With a mean of 5 ft in either the positive or negative direction, the handset can be said to only be one floor away from ground. The distribution of error while one floor above the ground-floor displays a Gaussian behavior which allows for simple prediction or calibration of error for the pressure sensor.

The distribution or error for a two floor change in altitude (measurements taken on the same day as in Fig. 3.1) can be seen in Fig. 3.2. This distribution displays that the statistical mean for error is approximately -7.5 ft with a variance of 5.56 ft. The error measurements

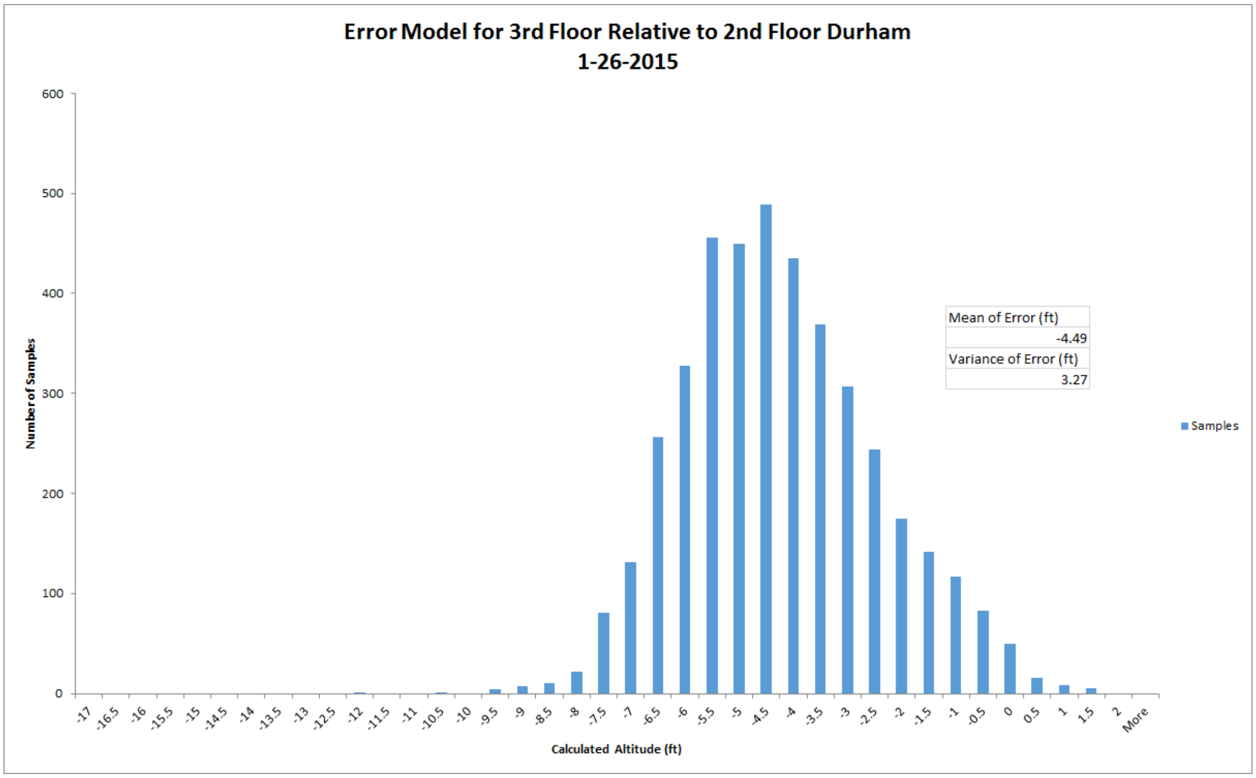

Figure 3.1: Distribution of Error between 3rd and 2nd Floors of Durham Hall

from the 4th floor are found by subtracting the ground floor reference altitude and then subtracting 28 ft. The actual distance between floors is 28 ft in this case and thus the mean is -7.5 ft below this value. As was mentioned before, the mobile handset was held at waist height, therefore this mean would be considered on the boundary of acceptable for being able to determine a certain floor. A distance of 7 ft above or below waist height while on a floor would "place" the mobile somewhere in the ceiling or floor if the measurement were to be translated to a location relative to the ground floor. Overall, on the particular day displayed in Fig. 3.1, the error measurements would not distinguish the appropriate floor given a comparison raw barometric pressure sensor data to the ground floor data.

By taking all of the error measurements from several days, a cumulative distribution of error is capable of been calculated. These cumulative distributions display the percentage or probability that a certain amount of error in the difference measurement between floors

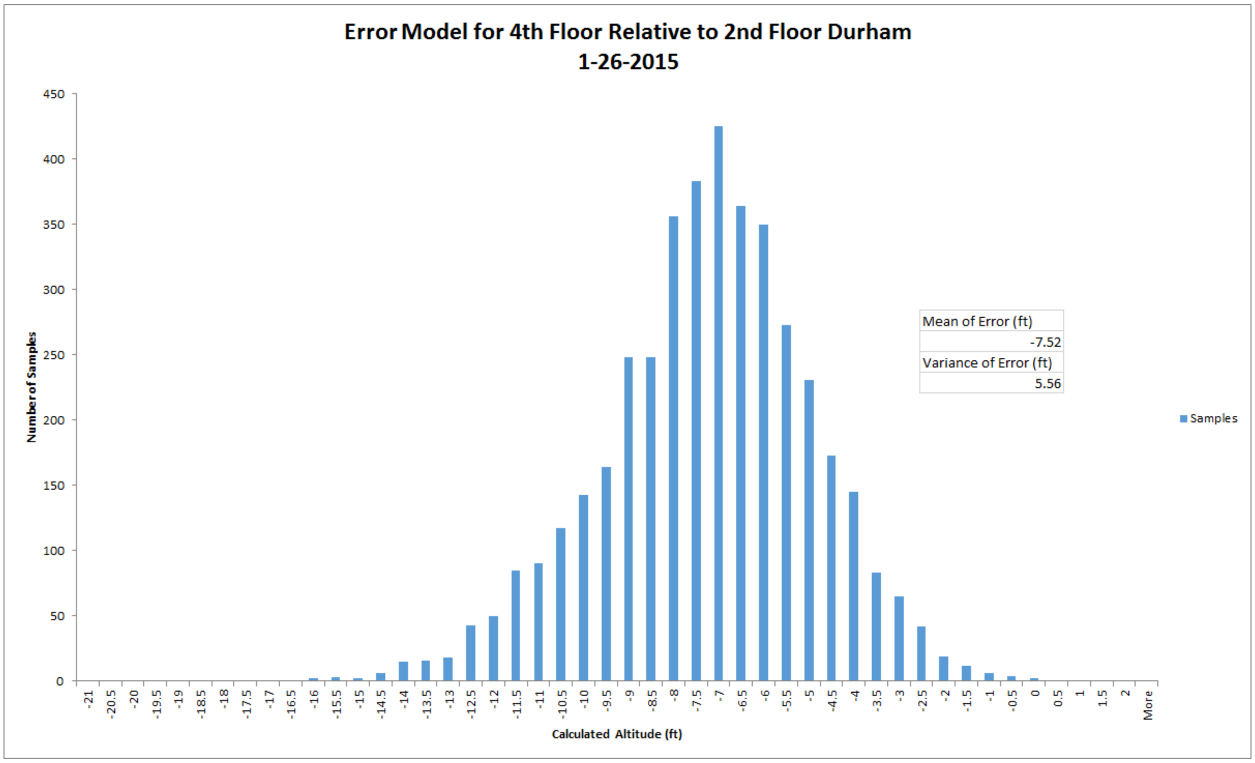

Figure 3.2: Distribution of Error between 4th and 2nd Floors of Durham Hall

will occur. This error still represents the amount of distance that the altitude measurements differ from the actual change in altitude. The ideal separation for a single floor change is 14 ft and the cumulative distribution for the measurements taken in this case can be seen in Fig. 3.3. Following the need for 67% of calls needing to be within 3 m or 10 ft accuracy, being able to resolve the floor a handset is on should meet the third dimension aspect of this requirement. Considering that the height error measurements can be $\pm X$, where X is some value of error, the absolute error must be taken into consideration. To correctly distinguish a floor 67% of the time, the error measurement must fall between ± 7 ft for 67% of the time. Looking at Fig. 3.3, the data that occurs between ± 7 ft accounts for the percentages between 15% and 85%. As a result it can be stated that a UE is capable of being located through the use of pressure measurements when it is one floor away from the reference ground floor.

The cumulative distribution for the two floor separation case can be seen in Fig. 3.4. The error yield for ± 7 accuracy spans from 30% – 55% of the data for two floor difference

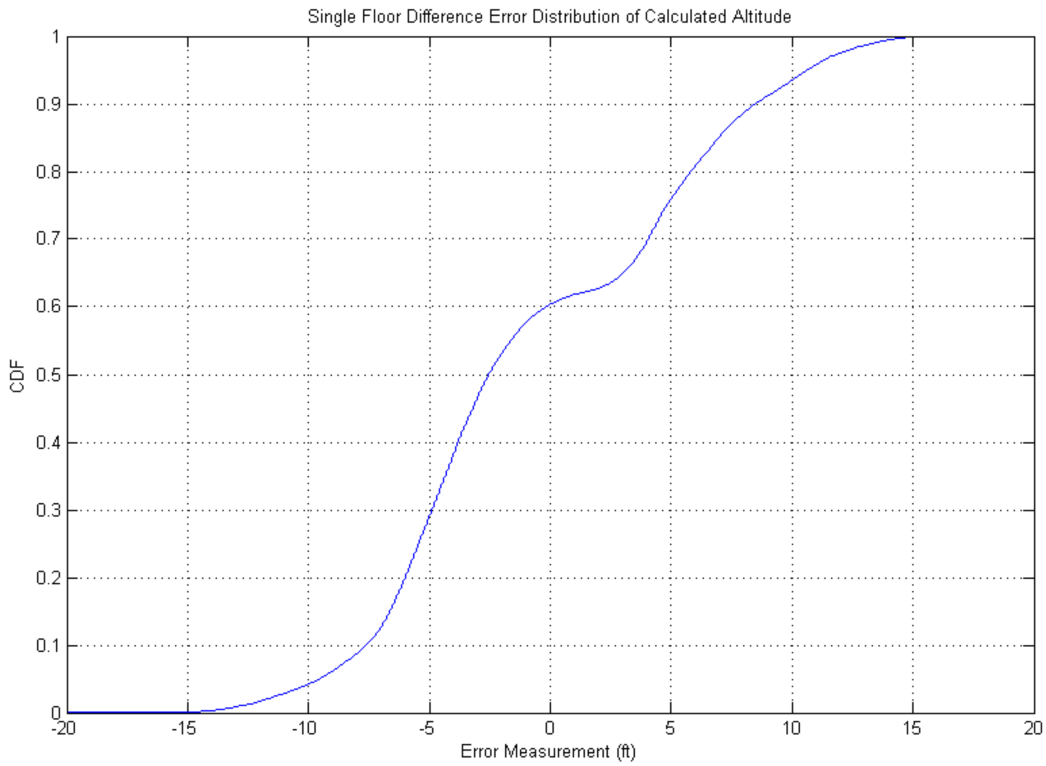

Figure 3.3: Cumulative Distribution of Error between 3rd and 2nd Floors of Durham Hall

measurements. Therefore, the correct floor will be distinguished approximately 25% of the time when two floors away from the reference floor. In this instance, 67% of the error measurement data spans from approximately -14 ft to +14 ft. Such errors would have the potential to miscalculate or wrongly determine the exact floor of handset; reporting that the UE is one floor away from it's true location for a majority of the time. Overall both cumulative distributions display calculated errors in altitude from raw barometric pressure data across several days. While the reference floor for each day is taken in account, the absolute measurement error and sensor drift is not considered. With proper budgeting for inherent sensor error as well as corrections for drift, the accuracy of floor resolution could be improved.

In order to simulate for the measurement error when moving in an indoor environment, an

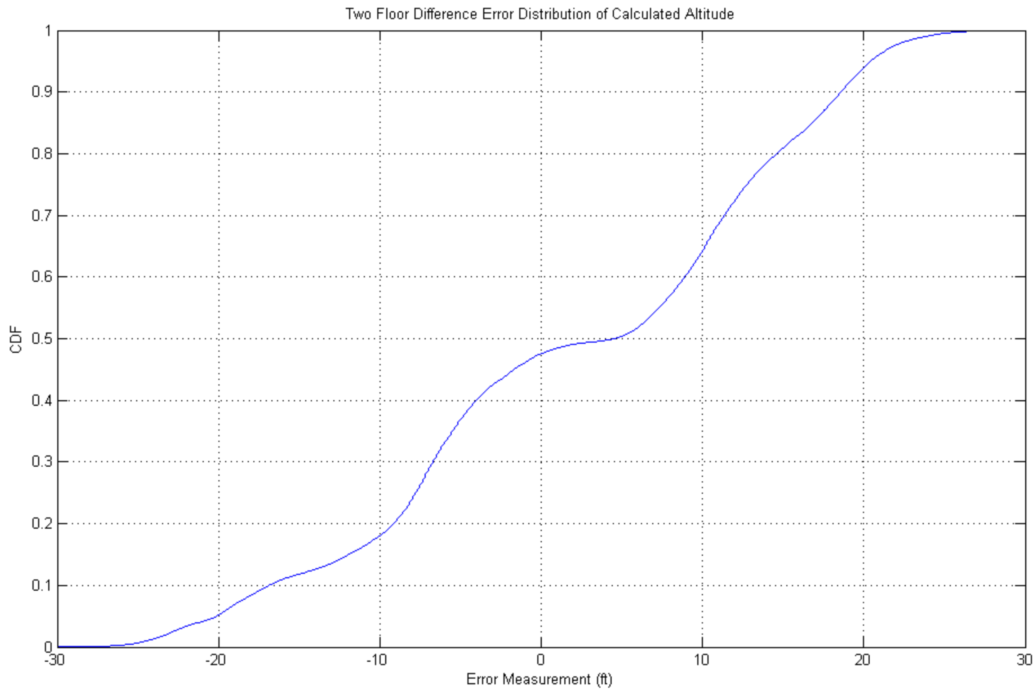

Figure 3.4: Cumulative Distribution of Error between 4th and 2nd Floors of Durham Hall

error model is to be applied to the barometric pressure sensor upon entering a building. The proposed single floor difference error model for the barometric pressure sensor, LPS25H, used in the Galaxy S5 and for the majority of pressure tests is:

$$e = \mu + \sigma * N \tag{3.5}$$

where μ is a uniformly distributed mean value of floor to floor difference, σ is the standard deviation, and N is a normally distributed random variable. Within this error model, σ does not vary, but μ is fixed for one day and will have to be reevaluated daily to account for the alterations in pressure. Then. the quantity for N will vary from measurement to measurement. This model is based upon testing and the resulting averages of error in floor to floor measurements seen in Fig. 3.3. To most closely match the distribution of errors with Eq. 3.5, $\mu = [-10, 10]$, $\sigma^2 = 5$ and the resulting proposed error model for when a pressure sensor has changed one floor can be seen in Fig. 3.5.

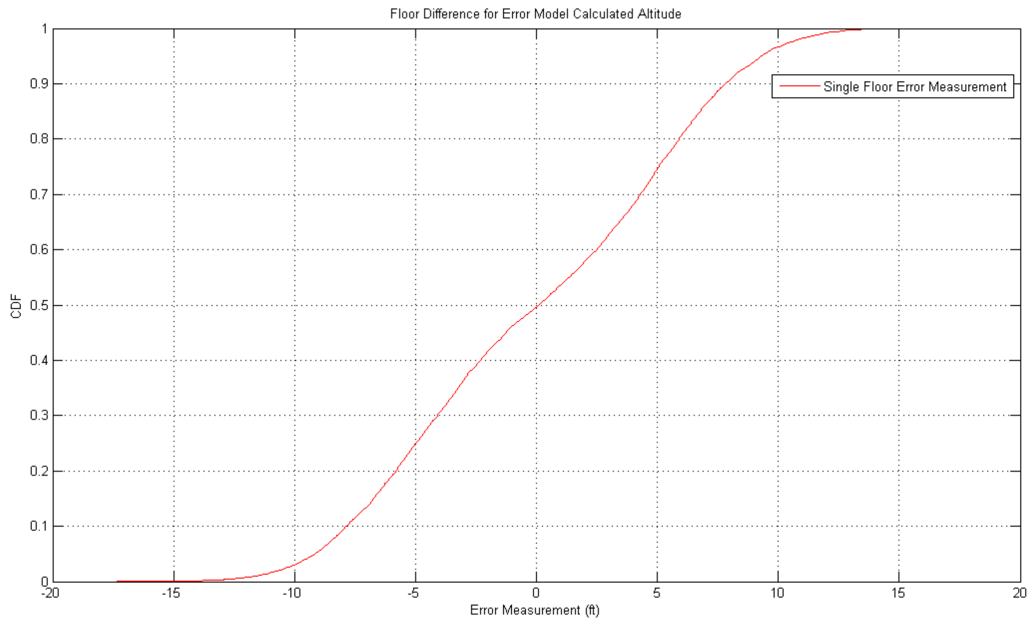

Figure 3.5: Error Model for UE Pressure Sensor based Altitude Inside of a Building

Fig. 3.6 shows the proposed single floor error model (Fig. 3.5) overlaying the single floor error measurements from Fig. 3.3. While the curves do not perfectly align, they do overlap at several points including both tails of the distributions. The high percentage of error measurements occurring from approximately -2 ft to +2 ft is not replicated by the error model. However, the percentage of errors that occur between -7 ft and +7 ft is closely matched. Therefore, with the use of the error model for a single floor, the probability that the correct floor is chosen can be estimated. The gradual distribution of the actual error measurements can be expected due to sensor error and drift. The error model for the single floor difference error measurements attempts to do the same by closely matching the distribution. The raw barometric pressure sensor data was shown to correctly distinguish a single floor difference 67% of the time in 3.3. The error model for the pressure sensor matches this percentage in the case of a change in one floor.

Due to the different spread of error measurements when accounting for a two floor change in

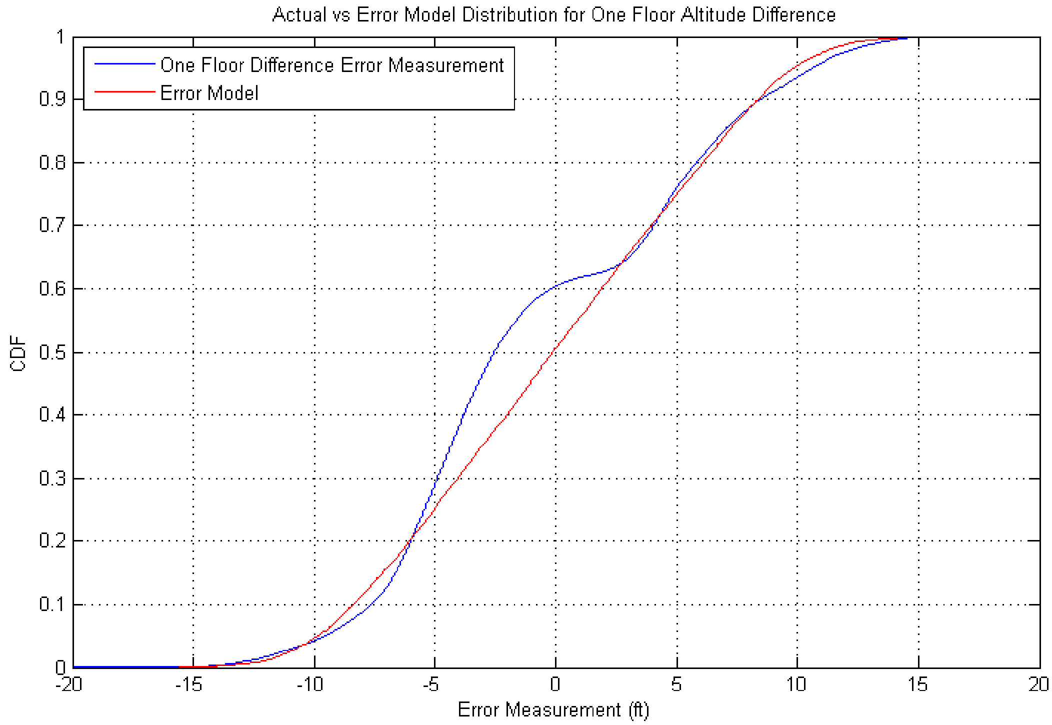

Figure 3.6: Single Floor Error Model for UE Pressure Sensor based Altitude Inside of a Building

altitude, a new error model had to be constructed. The distribution of data, being mentioned earlier, has a wider range of error and only correctly defines the floor for 25% of the time. In order to model this new case, two floor change in altitude from ground, $\mu = [-20, 20]$ and $\sigma^2 = 5$. The new resulting model can be seen overlaying the two floor difference error measurement distribution in Fig. 3.7. The cumulative distribution for a two floor difference has uneven plateaus that cause the error model to be slightly offset. Despite this fact, the tails of both plots align and the percentage of data occurring between ± 7 ft in error is comparable between plots, the discrepancy being in the error model due to the large plateau in the measured data.

Given the required change in μ to more accurately model the error of the pressure sensor for a two floor change, it is a logical assumption that a new error model would have to be proposed for each additional change in floor. As seen the variance would be kept constant but the distributed mean would have to double for each added floor. As a result of this, the potential for error, or an incorrect floor distinction, at any number of floors above two floors will continue to increase. It must be noted that such behavior is given the use of the particular LPS25H pressure sensor in the Galaxy S5 and its raw data measurements; without calibration or budgeting of any source of error. With a better understanding of how the pressure sensor operates, the scenarios previously mentioned are capable of being explored.

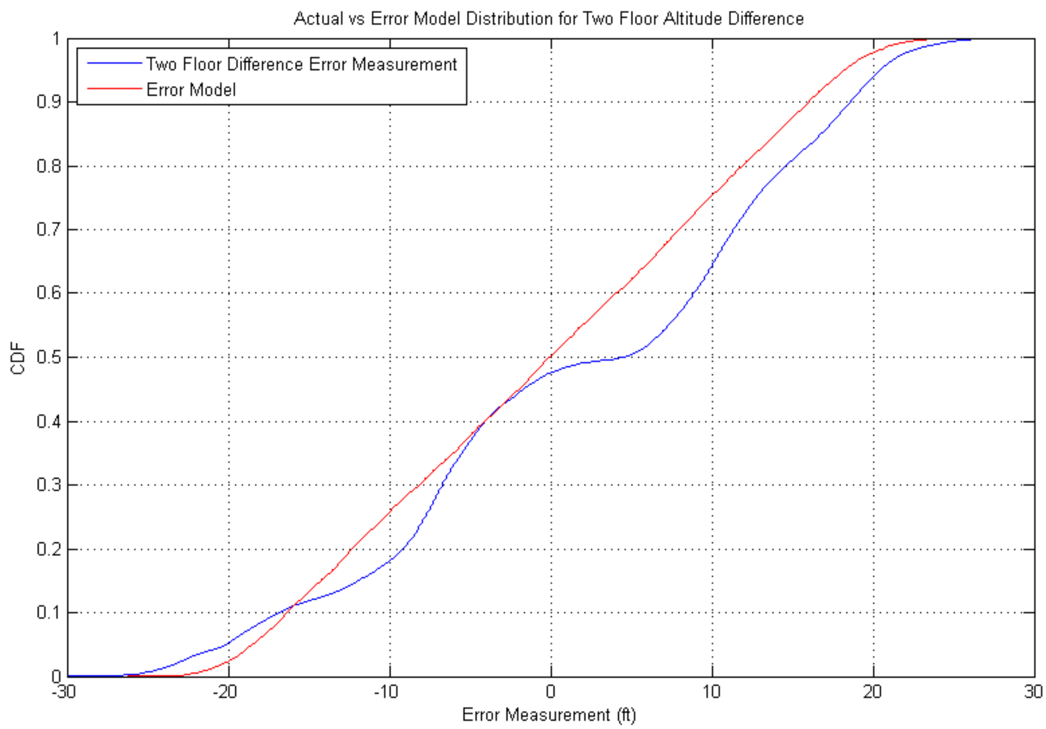

Figure 3.7: Two Floor Error Model for UE Pressure Sensor based Altitude Inside of a Building

3.4.2 Potential Use Case with a Single UE without *a priori* Information

For this scenario, there is a UE in a building and the floor on which it resides is unknown. The pressure recorded from its sensor will be able to be received by other individuals (handsets in the vicinity), but no other indoor references will be provided. The UE is capable of entering the building from any level and then can make its way throughout the building; pressure readings are not being recorded. At some arbitrary point in time, an emergency can occur and the UE will need to resolve the floor on which it is located. In this instance the phone has to locate itself whilst acting alone; there are no indoor nor outdoor references. To test the feasibility of this use case, a series of measurements were made over the course of a week from the exact same locations; recording pressure for five minutes for every trial. The mean, median, and variance of these measurements can be seen in Table 3.1. The actual altitude of the reporting location in Durham Hall is 2057 ft above sea level according to [23]. For further comparison of the day to day trend, the outdoor pressure as reported by a local weather station is also shown. Despite the offset, the general fluctuation of increasing or decreasing from day to day is seen in both readings.

Table 3.1: Mobile UE Elevation Measurements from One Location over the course of a week

Phone	Date	Location	Mean of Calculated Altitudes (ft)	Median of Calculated Altitudes (ft)	Variance of Altitudes (ft)	Outside Pressure based Altitudes (ft)
Galaxy S5	1/23/2015	Dur-Whit 2nd Floor	2020.24	2019.95	6.06	-210.65
Galaxy S5	1/24/2015	Dur-Whit 2nd Floor	2352.97	2353.05	5.08	233.11
Galaxy S5	1/25/2015	Dur-Whit 2nd Floor	2322.70	2322.46	2.30	103.07
Galaxy S5	1/26/2015	Dur-Whit 2nd Floor	2448.48	2448.34	2.74	214.70
Galaxy S5	1/27/2015	Dur-Whit 2nd Floor	2124.23	2124.07	2.96	66.13
Galaxy S5	1/28/2015	Dur-Whit 2nd Floor	1854.00	1853.79	4.43	-256.47
Galaxy S5	1/29/2015	Dur-Whit 2nd Floor	1987.46	1987.25	2.20	-201.42

From this compiled data it is observed that, despite being in the same location for measuring barometric pressure, the pressure will fluctuate even inside a building. While some variation is expected due to the absolute pressure variation of the sensor, the observable differences from day to day are much more significant. Again, this can be expected based upon the reaction of the indoor environment to that of the outdoor environment acting upon the building at a particular time. Further, the indoor HVAC system could be set for maintaining a different temperature and pressure in accordance with the outdoor temperature.

It can be seen that a single UE, acting alone, cannot resolve its location in the vertical plane without any memory or outside references of pressure measurements to reduce the discrepancy between pressure sensors. Pressure is highly sensitive to the weather conditions at the specific time of the required measurement and a single UE displays different altitudes based on not only the day of the week but the actual time of day despite being at the same physical location. Since a person, with their handset, still need to be located according to E911, other methods need to be explored. A handset needs some sort of reference barometric pressure in order to localize itself.

3.4.3 Potential Use Case with a UE and Weather Station

The first means of both reference and calibration when considering the effects of weather and elevation is a local weather station. Following Bosch, the first point to be addressed lies in resolving the discrepancy between being at an altitude above sea level and the base altitude at sea level. To ideally eliminate this difference between the weather station instruments and the handset pressure sensor, a local weather station and a collocated UE should be monitored simultaneously. A test was run for a total of five minutes in which the pressure sensor record approximately 1000 pressure values. The weather station was monitored via a website [58] and its pressure value and elevation were recorded at the beginning and end of the time interval of the experiment coinciding with the UE pressure sensor recording. The resulting data can be observed in Table 3.2 and Table 3.3 below.

Table 3.2: Weather Station Pressure and Elevation for 5min Experiment

Actual Weather Station Report		
Reported Elevation of Site (ft)	**Pressure at 2:45pm (mbar)**	**Pressure at 2:49pm (mbar)**
2086	1028.44	1028.44
	Calculated Barometric Altitude (ft)	**Calculated Barometric Altitude (ft)**
	-412.24	-412.24

Table 3.3: Mobile UE Elevation for 5min Experiment

Mobile UE Report (over 5min sample time)		
Mean of Altitudes (ft)	**Median of Altitudes (ft)**	**Variance of Altitudes (ft)**
1892.31	1892.50	38.86

Both of the elevations or altitudes in Table 3.2 are referenced to sea level being 0 ft. The weather station is physically located at 2086 ft above sea level, while its pressure translates to an altitude 412 ft below sea level. This difference in pressure based altitude can be directly attributed to the multitude of outdoor variables which affect pressure such as weather conditions, temperature and wind. The UE reported a mean elevation of 1892 ft above sea level which is a 2304 ft difference from the base station. Despite this large disagreement between measurements, with the inclusion of some other information a handset can be calibrated and referenced to a local weather station.

With the weather station always recording and reporting pressure that is referenced to sea level, if a handset calibrates to it then the barometric pressure sensor contained in it can accurately relay its own pressure based on sea level. However, every building will not be at the same altitude as the local weather station and by extension nor will a UE. For this reason, the geographically measured altitude of both the weather station and the ground floor of the building need to be known. With this information, the difference between pressure recorded by a local weather station and the handset (located indoors) can be compared and the handset can be calibrated. The offset between the altitude of the local weather station and the ground floor of the building is factored in and then the expected pressure of the ground floor can be calculated. For example, the local weather station is at 2086 ft above sea level and reports a 102.404 kPa pressure. Using Eq. 3.1, this corresponds to -293.3 ft. If the ground floor of a building is 2075 ft then an offset of 11 ft would be applied and a pressure corresponding to -304.3 ft would be the calibrated ground floor barometric pressure.

Despite the ability to calibrate to sea level and then calculate the appropriate floor, this case requires a great deal of information to be known beforehand in order to function. The ground floor pressure reference to the local weather station would also have to be updated often. The test shown in Table 3.2 and Table 3.3 shows that taking the pressure values from a weather station to compare against the pressure values of a UE beside it will not always be equal; this will almost always be the case when calibration has not been performed. The unpredictable nature of the indoor environment incites another variable that would cause further discrepancies between the calculated altitudes. UEs cannot be expected to be calibrated in the time of an emergency and, as such, it must be noted for all scenarios that a local baseline measurement from a weather station is not beneficial in regards to a handset trying to locate itself indoors. The indoor environment of a building can be considered as isolated from the outdoors and thus utilizing a local weather station for a reference to sea level or even for the geographic location will not help identify the floor on which the "lost" UE resides.

3.4.4 Potential Use Case with a Single UE with Infrastructure Based Assistance

As a means of collaboration with a "lost" UE, pressure sensors can be built into the infrastructure of newly developed buildings. This practice actually has been implemented in certain circumstances mainly for future technology building sensor systems [60]. While this could not be considered with the tests conducted for this research, due to the lack of pressure sensors being included in the infrastructure of a building at Virginia Tech at the time, it has the potential to be the most sophisticated and unique approach to solving the third dimension issue for E911.

With pressure sensors installed on each floor of a multi-story building, there is not only a ground-floor reference, but there is also a reference pressure for each floor. If a mobile handset is able to synchronize with these pressure sensors within the building upon entry, then a continuous comparison can be made. The physical separation between infrastructure pressure sensors will be known and thus the measured pressure by these sensors will always be relative to one another and accurately represent the altitude difference between floors. With such a system in place, barometric pressure sensors within a UE can measure pressure while moving within the building. To identify the floor the UE is located on, a simple exchange of pressure information would take place with the sensors in the building. It is to be expected that this comparison would display an offset between measurements due to sensor drifts and relative measurement error. However, if the relative pressure differences are tracked, through multiple measurement comparisons with infrastructure sensors, then any offset could be calculated and accounted for. Following this, any UE in this building with the ability to communicate with the pressure sensors of the infrastructure would also be capable of accurately locating itself in the vertical plane, on the Z-axis. This technique would require either building practices or applicable building codes mandating that sensors be placed on every floor within a multi-story structure. These sensors would be able to tell the UE which floor it is on. At this time no such mandates could be found. Thus, although this technique seems to provide an accurate means to calculate the elevation of the UE, without such a mandate the added building costs would tend to undermine adoption of sensor installations. Further, the pressure sensors in the handset are ultimately not required. If communication with the infrastructure pressure sensors can be performed then the building sensors can relay to the phone which floor it is on. This case would accurately place any handset, but the complexity and cost severely hinder its feasibility.

3.4.5 Proposed Use Case with a Single UE with Memory

The challenge to accurately determine the vertical height above ground level of a "lost" UE remains. In order to ascertain this information a new method needs to be implemented to overcome the shortcomings of the previous examples. The pressure needs to be known and reported by the "lost" UE given that it has set its own reference. Here, the UE will need to read and store the barometric pressure when it is on the first floor of a building. It is assumed in this case that the handset always enters on the ground floor. It is also assumed that the distance between floors of buildings is always 14 ft. With this information, and the knowledge of the translation to altitude, a differential calculation can be performed as the UE moves up or down in the building holding the first floor as "ground-zero". In order to evaluate the possibility of success for such a method, the following scenario was established. To ensure that pressure holds relatively steady while maintaining elevation and increases or decreases following elevation, a mobile handset moved from the 1st floor of Durham to the 4th floor. The travel time to walk the length of the hallway on each floor was approximately one minute and then stairs were used to ascend floors. The results of this can be seen in Figure 3.8

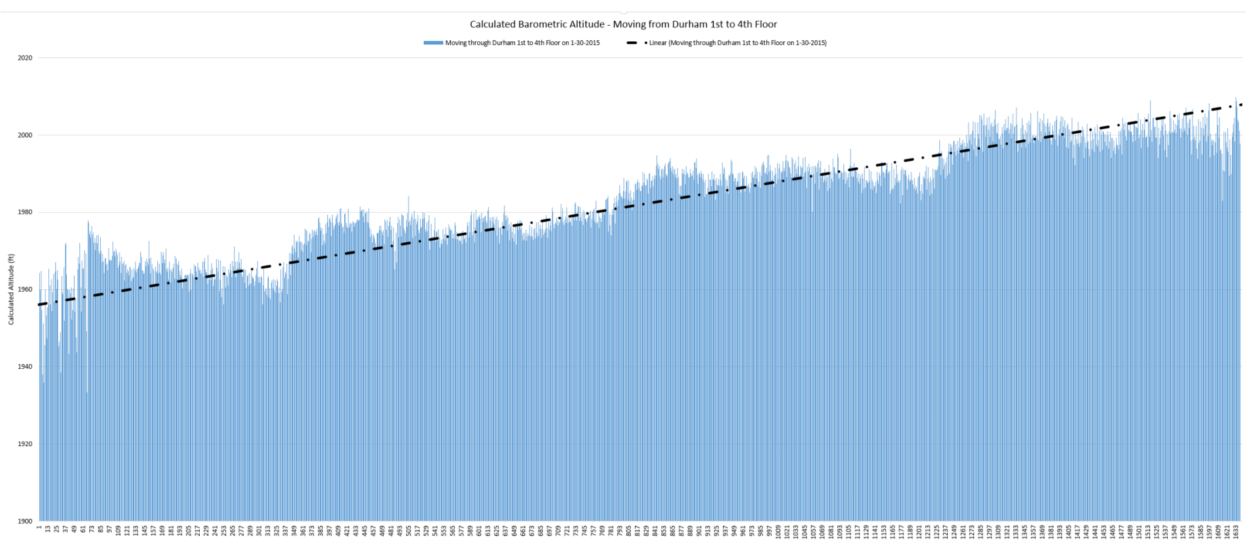

Figure 3.8: Gradual Elevation Changes while Walking through Building 1st to 4th floor

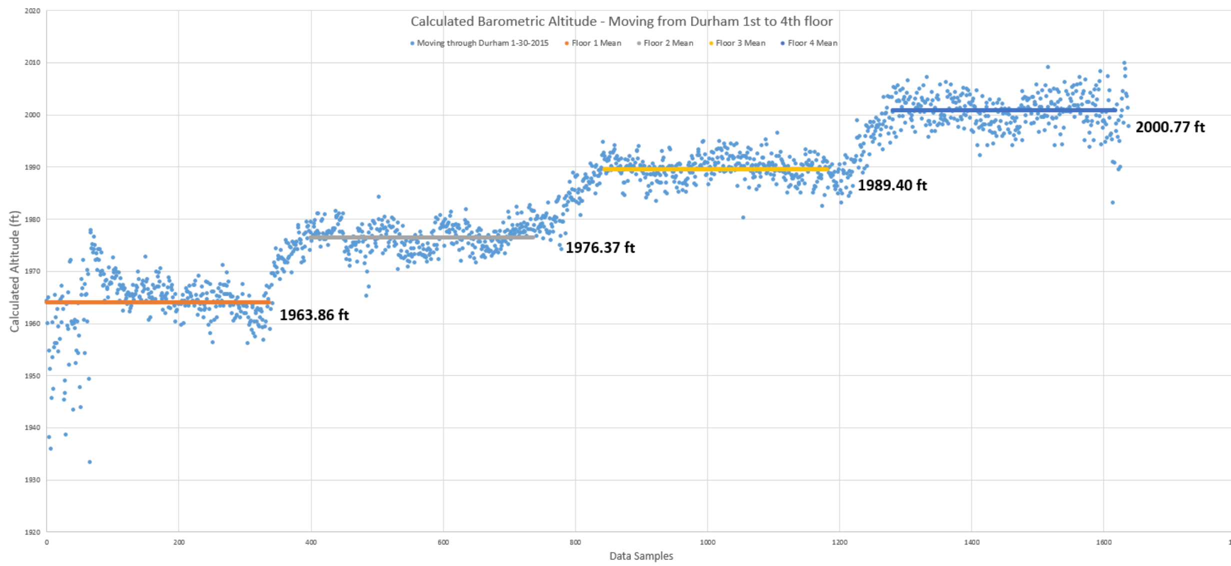

Figure 3.9: Mean of Floor Altitudes while Walking through Building 1st to 4th floor

With the trend-line in place, it is seen that there is a natural linear rise in the elevation and there are also four distinct plateaus during which the UE is on the same floor. The same data was plotted again and displays four calculated means for altitude during which pressure readings were taken while walking the length of the hallways in Durham. The resulting plot can be seen in Fig. 3.9. The distances between the average for floors 1 & 2 and then 2 & 3 is approximately 13 ft; the approximate distance between floors 3 & 4 is 11 ft. The actual separation is 14 ft, the averages do not discount pressure variation nor any sort of error. These displacements between floors are valid as the averages would still be able to determine one floor from another as the values are not below 10 ft; assuming long averaging is used. Given this data, signaling to the handset when it is on the first floor of a building and storing its pressure value at that time would be feasible for locating in the third dimension, the vertical height above ground level, when required. Noting that pressure even inside buildings will alter over the course of time, the first floor pressure will have to be stored upon entering the building each time. The pressure value stored for reference would be void for the following day. With a valid ground-floor pressure or altitude reference, a simple difference calculation can be made at the time of an emergency for any floor that the UE is located on to discover the altitude of the handset and therefore the floor of the building that it resides on.

The error models seen in Fig. 3.6 and 3.7 were generated utilizing thise proposed use case; using a ground floor pressure reference to attempt to accurately distinguish the floor the UE is actively on. The ability to resolve the correct floor is highest when there is only a single floor change in altitude. As the number of floors increases, the ability to register this change, given the barometric pressure sensor used for experimentation, becomes increasingly more difficult. Again, it must be noted that calibrating the pressure sensor and accounting for other sources of error could improve the probability of correct floor detection. With environment variables such as stack-effect and the outdoor weather as well as inherent sensor error, there is potential for a large discrepancy in data measurements.

3.4.6 Potential Use Case with a UE and Collaborator

An anchor, on any floor, with known location and its measured pressure could provide a reference for indoor pressure. Other mobile devices can be in the same building as the "lost device" and report the pressure given their location is already known in the X-Y dimensions. The UE, being located on the first floor of the building and knowing its location, could act as a reference for barometric pressure from the first floor of the building to which compare the pressure reading of the unknown mobile device. As a real application for this, the first floor pressure reading could be gathered quickly by emergency response members upon arrival at the scene of an emergency. The pressure reading of the unknown device could then be referenced to the readings made by the emergency response team, acting as a collaborator. In another instance of collaboration via emergency response teams, if they are able to communicate with any functioning UE, with known location, then information can be gathered about the pressure on various floors of a building. With this information and the corresponding altitude, the work of finding the unknown UE can potentially be simplified.

Other UEs that do not know their floor in the building could also act as collaborators. Any additional unknown UE on the same floor as the original "lost" UE can work in tandem to try and identify the floor they are both on. The devices have their own ground floor reference and therefore an estimate altitude based on their pressure sensor readings. If the individual estimates, being independent with respect to inherent error, are averaged then a common floor may be able to be distinguished.

In order to test the potential for collaboration between UEs, pressure was recorded across four different phones and the phone used for the majority of testing was held as the control for the experiment to which all data would be compared against. The phones consisted of 3x Galaxy S5s, 1x Galaxy S4, and 1x HTC One M8. Barometric pressure was recorded simultaneously on all five handsets at three locations on two different floors. For each of the three locations, pressure sensor information was collected for a total of five minutes. Given this amount of time, a large sample of data was collected on each phone. The pressure values were then averaged and then Eq. 3.1 was used to calculate the average height. On both floors, each of the handsets displayed mean altitudes with low variances and high precision; altitudes did not vary while on the same floor. When the floor on which measurements were taken was changed, all altitudes altered and displayed the same consistent pressure behavior. The comparison of these sets of data against the control phone holds the information in question and this can be seen below in Table 3.4.

Table 3.4: Indoor Elevation Comparison Measurements against Control Galaxy S5

Pressure Readings for Collaboration Testing			
HTC One M8	*Galaxy S4*	*Galaxy S5 #2*	*Galaxy S5 #3*
Floor 1	**Floor 1**	**Floor 1**	**Floor 1**
-48.93 ft	-7.54 ft	20.61 ft	-3.36 ft
-52.28 ft	-8.35 ft	18.67 ft	-3.24 ft
-49.54 ft	-7.46 ft	18.45 ft	-3.16 ft
Floor 2	**Floor 2**	**Floor 2**	**Floor 2**
-48.66 ft	-7.37 ft	17.95 ft	-4.20 ft
-49.25 ft	-7.83 ft	18.20 ft	-3.24 ft
-48.44 ft	-6.98 ft	18.78 ft	-2.88 ft

As seen from test results, pressure sensors can have a discrepancy between one another based on their relative measurement error and individual sensor drift despite being colocated. All of the data points, for three positions on each floor, are altitudes differentiated with the control handset; being either higher or lower than the control device's recorded altitude. For each handset it can observed that, given a small variance, there is a distinguishable offset relative to the control handset. The fact that the pressure differences are quite robust across devices has been shown in other similar tests as well [16]. This trend suggests that the pressure sensors could relay what would be considered “ideal” pressure measurements provided the offset between sensors was known a priori. The collaborating phone could act as a reference from a different floor if its sensor was calibrated to be equivalent with the “lost” UE. However, in most cases, this offset will not be known as all phones would have to have prior knowledge of the other devices.

The case of multiple ”lost” devices to account for variation in performance of pressure sensors was also explored. Table 3.5 shows the measurement errors calculated by each phone when trying to distinguish a one floor difference. The measurement errors made by each phone are within the bounds of ± 7 and therefore can distinguish the floor they are located on. If the measurement errors across several phones on the same floor were to be averaged there would be an increased potential to accurately distinguish the appropriate number of floors away from the ground floor. Due to the independent calculations of the collaborating devices referencing to ground, the pressure sensor offset mentioned earlier is taken care of and budgeted out. As a result, phones on the same floor can compare their floor location estimation without an inherent offset between the measurements. Through collaboration, phones on the same floor can average their altitudes with each other and attempt to identify their floor with more accuracy than a singular phone. A group of phones could not be acquired to test this scenario, but a simulation based around the pressure sensor error model could be done and this will be discussed in a later section.

Table 3.5: Average Measurement Error Across Collaborating Phones from Single Day Test

Measured Change in Altitude for Different Handsets	
HTC One M8	
1st to 2nd Floor Difference	2nd Floor Measurement Error
20.64 ft	6.64 ft
Galaxy S4	
1st to 2nd Floor Difference	2nd Floor Measurement Error
19.57 ft	5.57 ft
Galaxy S5 #2	
1st to 2nd Floor Difference	2nd Floor Measurement Error
18.25 ft	4.25 ft
Galaxy S5 #3	
1st to 2nd Floor Difference	2nd Floor Measurement Error
19.00 ft	5.00 ft

Chapter 4

Simulation Results

4.1 Localization Accuracy

Localizability is defined as the ability of a UE to be uniquely localized without ambiguity. A UE is localizable when it is connected to at least three non-collinear ENodeBs. The definition of localizability changes for a cooperative network. A UE is localizable in a cooperative network if it has at least three disjoint paths to three non-collinear ENodeBs [34]. In order to ensure localizability, connectivity thresholds have to be set based on SINR for ENodeBs and SNR for collaborating UEs. The SINR of each base station relative to a UE is dependent on the geometry of the link in the network; with variables such as shadowing and pathloss affecting the signal. The SNR between UEs is also dependent on the same variables, but there is no interference between devices. In this simulation the threshold for connectivity to the base stations is set to -27 dB. This parameter is set to match the SNR for a high detection probability as seen in [6]. The connectivity threshold for UE links is assumed to be -6 dB as also seen in [34]. Given the CDF plot in Fig. 4.1 and the stated threshold, it can be expected that at least five base stations sectors will be available for connections a majority of the time. Given the CDF plot in Fig. 4.2, it can also be expected that more than five UEs will be connected and are thus available for collaboration.

Before performing the TDOA calculation across the connected base stations for a particular UE and its collaborators, bias and a TOA range error are associated with each link. To simulate UTDOA, the distances associated with each link measurement from the unknown UE to all of the base stations have noise, η, and a bias, α, applied to them. The lookup table established in the link layer simulations associates a SRS range error based on the SINR of connected base station. One range error from the 1000 iterations at a respective SINR value is chosen to add to the link. Fig. 4.4, 4.5, and 4.6 show the dispersion of range errors for SNR values of -27, 0, and 25 dB. The mean range errors in the three cases are 675.63 m, 58.86 m, and 59.60 m respectively. The average TOA range error displayed diminishing returns as the SNR was increased from -15 dB to 25 dB. The average range errors for this range of SNR values was approximately between 50 m and 60 m. With each of the anchor to source links established, a differential of the TOA is performed, referencing to one ENodeB. and then a localization estimation can be calculated.

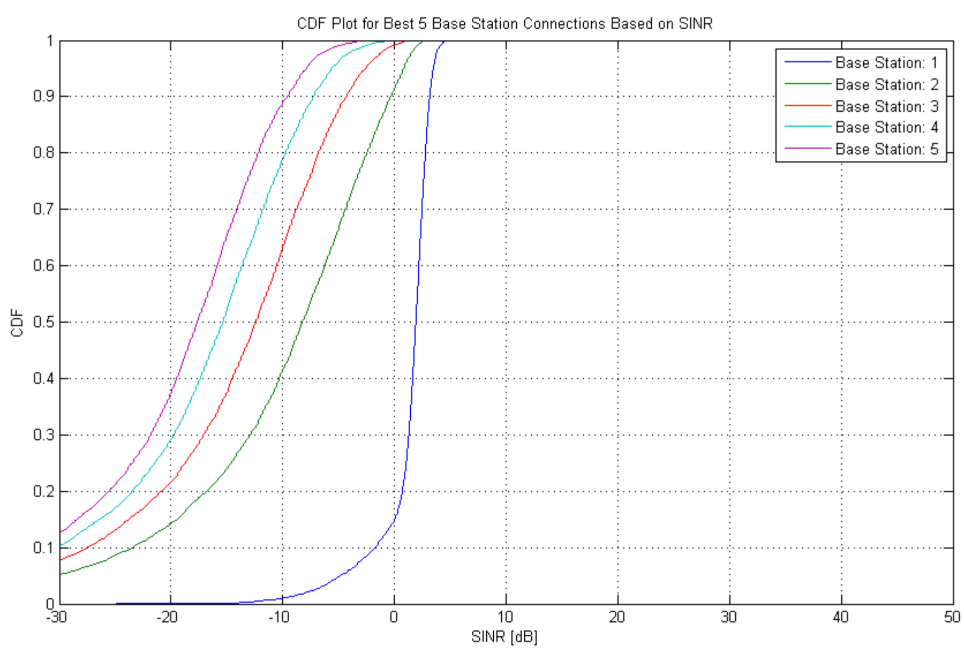

Figure 4.1: SINR of the Best 5 Connected Base Stations in the Network

Fig. 4.7 shows the CDF for the localization error versus the number of collaborators. The

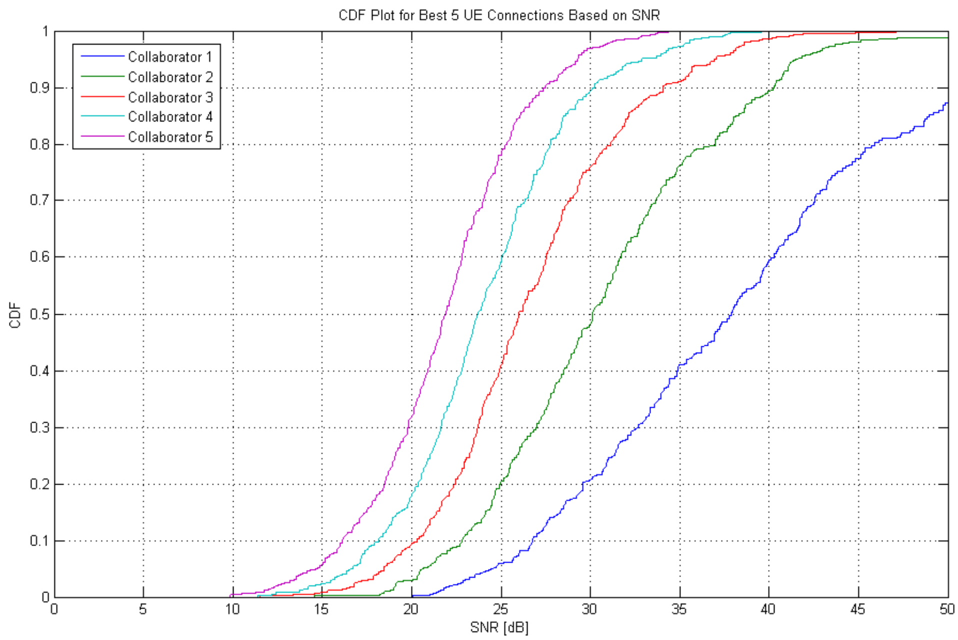

Figure 4.2: SNR of the Best 5 Connected Collaborators in the Network

zero or non-collaborator case utilizes only ENodeB-UE connections and any collaborators are other UE-UE connections. As with the base stations, the connectivity to potential collaborating UEs is established after calculating the SNR to the devices within range and setting a threshold. In most cases, the more connections that are available to the target UE the better its location estimation will be. Collaborating UEs and their uniquely connected base station will provide more position references for resolving the location of the unknown UE. With the additional connections, issues such as bad geometry with ENodeBs as well as large noise error can be combated [34]. Fig. 4.3 displays the number of unique base stations that are included in the geometry of connections for a varying number of collaborators. From this figure it is evident that the number of connected base stations increases as more collaborative UEs are associated with the target UE. As mentioned, in order to be localizable, the UE must have at least three disjoint paths to three non-collinear ENodeBs. Fig. 4.3 shows that three paths occur only 45% of the time in the non-collaborative case but 90% of the time for five collaborating UEs. Therefore, there is a demonstrable benefit to having

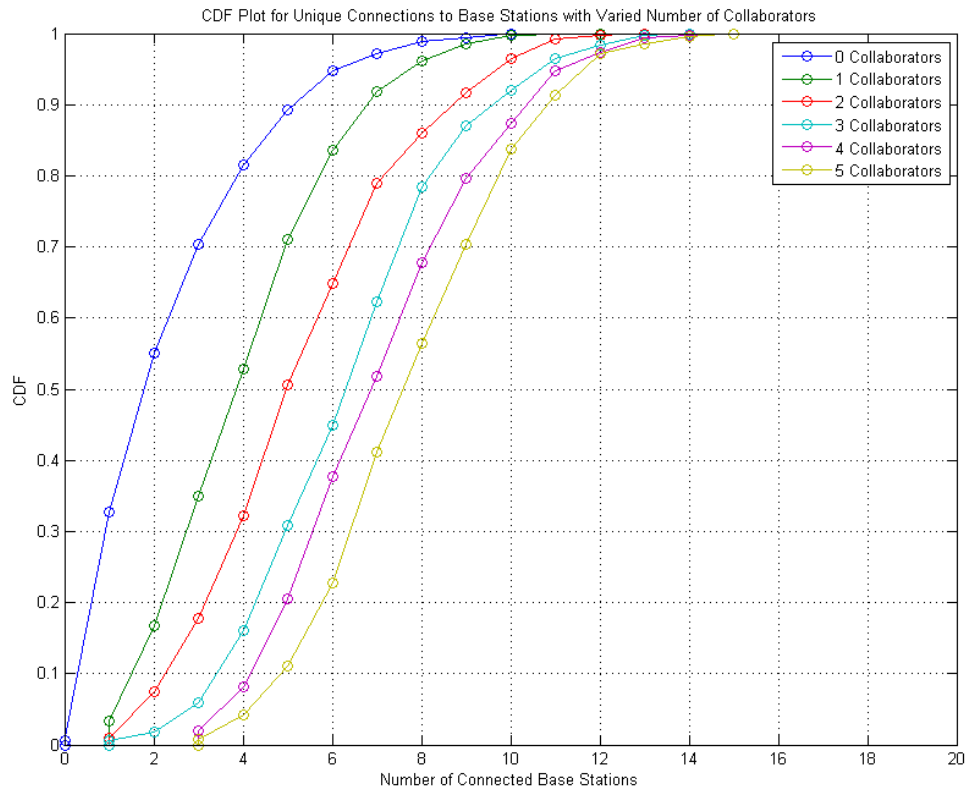

Figure 4.3: The Probability for Number of Connected Unique ENodeBs as Number of Collaborators Changes

collaborating UEs.

The non-cooperative localization estimation in Fig. 4.7 closely matches the high load ETU case I for SRS only measurements made by TruePosition in [12]. The error measurement is less than 100 m for 73.6% of the time and matches the UTDOA accuracy of 300 m for 93.1% of the time. The same SRS assumptions, system assumptions, and interference model that are used in [12] are also used for the simulations in this thesis. With the addition of collaborators, the TruePosition performance is improved upon. It can be seen that, given a -6 dB SNR threshold, with one collaborating UE, performance is improved nearly 15%; the location error estimation for zero collaborators is 100 m for 78% of the time and 85m for the equivalent probability for one collaborator. The February 2015 FCC x,y location accuracy

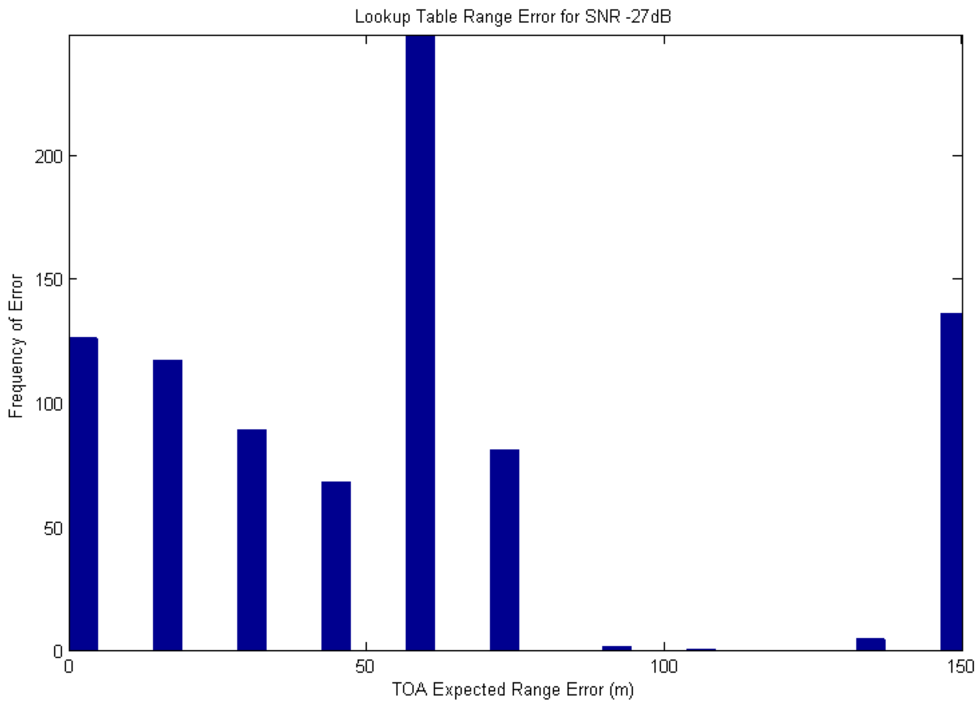

Figure 4.4: Histogram of TOA Range Error for -27dB

requirements for wireless 911 calls state that a UE must be located within 50 m 40% of the time within two years after publication and up to 80% of the time within six years [4]. The collaboration results shown in Fig. 4.7 meet the FCC 5 year requirements where the location accuracy must be within 50 m 70% of the time. It must be noted, however, that the collaborative UTDOA results do not exceed the position estimation accuracy of collaborative OTDOA as seen in [34].

It is seen in Fig. 4.7 that additional collaborators continue to improve the error measurement performance until the use of four or more collaborators. Diminishing returns in performance improvement are expected as the number of anchors used for the Levenberg-Marquardt algorithm becomes excessively large and does not help to the error of the location estimate. Fig. 4.8 shows the result of collaborative localization with an altered ENodeB connectivity threshold. In order to observe more collaborative improvement, raising the threshold for ENodeB connectivity from -27 to -12 dB reduces the number of connections to the UE.

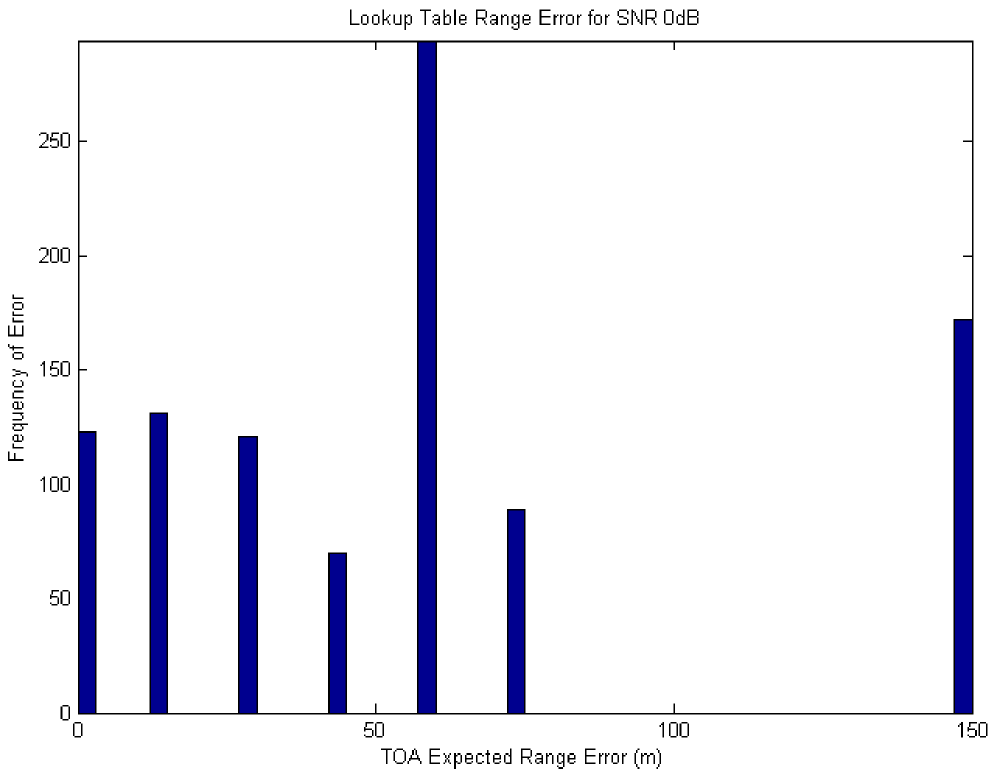

Figure 4.5: Histogram of TOA Range Error for 0dB

With less points for use in the Levenberg-Marquardt algorithm, the localization estimation will display an overall lower accuracy. This result can be seen in the 0 collaborating case in Fig. 4.8 which is significantly lower than that of the one in Fig. 4.7. However, in this case , adding connections via collaborators improves the localization with a much greater impact. Adding one collaborator improves the location estimation at 150 m from approximately 64% to 71%. With 3 collaborators, the probability of error measurement of 150m is 80%. Clearly, the use of collaborators provides a more pronounced benefit in position estimation when there are fewer ENodeB connections supported by the target UE.

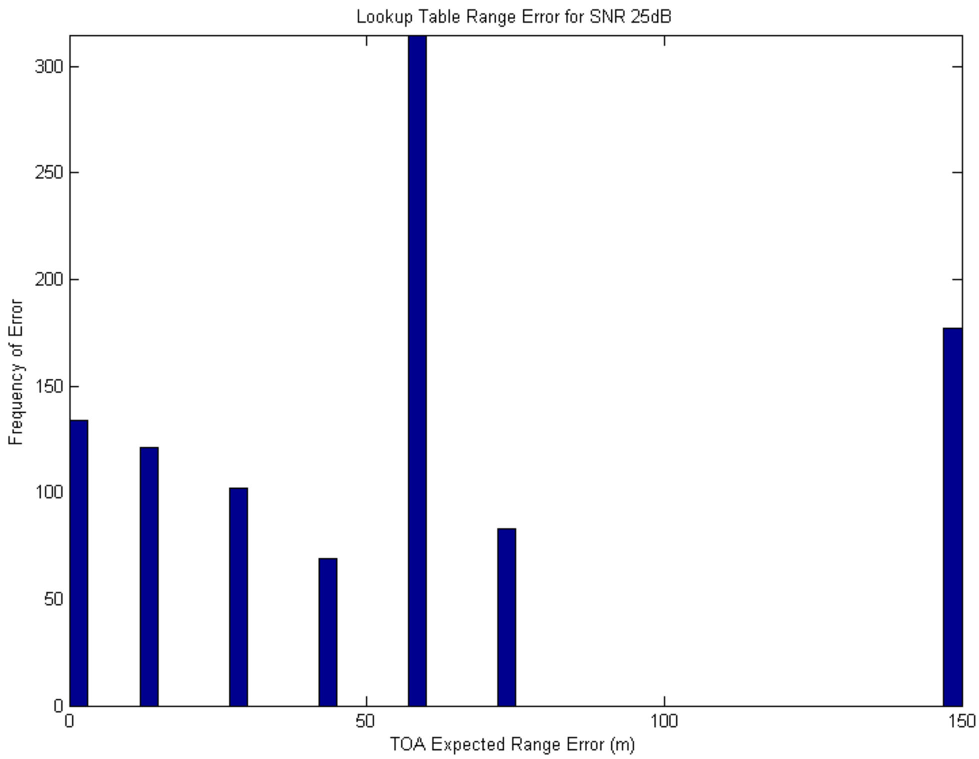

Figure 4.6: Histogram of TOA Range Error for 25dB

4.2 Conclusion of UTDOA Localization

In order to accurately locate a handset in two dimensions, X and Y, with an uplink LTE signal, UTDOA and collaboration prove to be a feasible option for localization. Link and network layer simulations are established following the base references outlined in [9]. The SRS sequence is generated and then passed through pieces of a transmitter as a part of the LTE uplink transmission scheme. Following the fading ETU Case I channel model, a correlation of received signal sequences is performed to isolate the range error associated with each SINR. With range error estimates from 50 accumulations of the SRS sequence and then the nonlinear position estimator algorithm, it can be seen that the TruePosition 3GPP specifications are matched for the non-cooperative case. Further, with the use of collaboration, the localization accuracy is capable of meeting current FCC horizontal location requirements

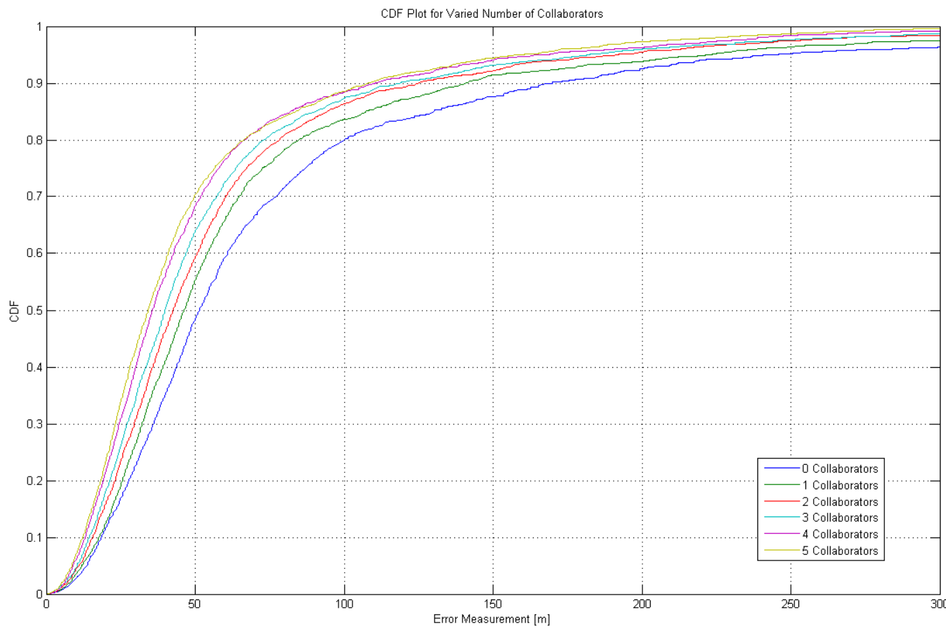

Figure 4.7: The CDF of Localization Error Versus the Number of Collaborators

for wireless 911 calls [4]. Through the use of one collaborator, the two-dimensional location error is within 50 m for 55% of the time. This performance exceeds the two and three year time frame requirements. By using five collaborators the requirements to be met within five years can also be met. Overall, with the use of cooperating mobile devices, the estimation of the position of an unknown UE is improved.

4.3 Pressure Sensor Localization

With any inherent offset between barometric pressure sensors of phones, resolving the exact floor on which the phone in question resides and the collaborating phone is on will be a complex matter. If the pressure readings from the barometric sensor differ by a mere 35 Pa this indicates a more than 10 ft difference meaning that the two UEs are not on the same floor. However, given a building with a multitude of floors, for example more than ten, the offset could still be used to provide a reasonable estimate which group of floors a UE could

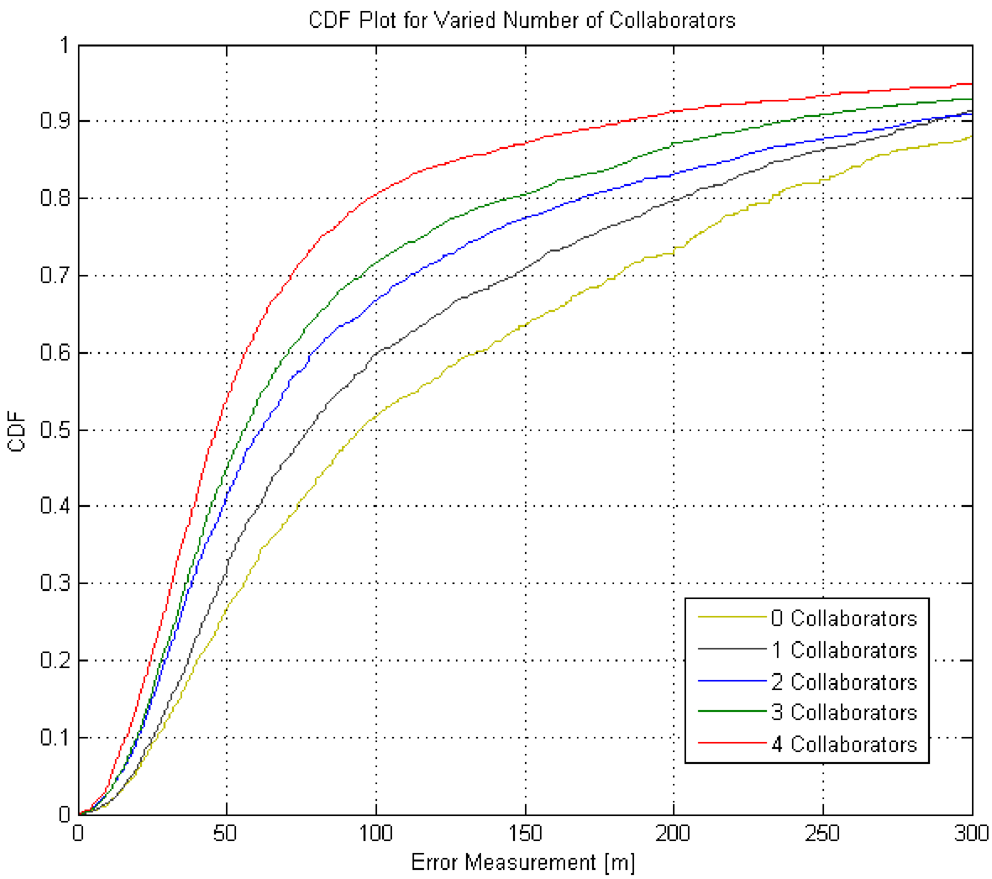

Figure 4.8: The CDF of Localization Error Versus the Number of Collaborators with Higher ENodeB Connectivity Threshold (-12 dB)

be located on. Given no other information relative to altitude or floor of the building, this could be utilized in the operational application to benefit emergency response teams. In a 75 story building, rather than searching every floor, a grouping of just a few floors could be chosen relative to the UE's reported, calculated altitude. Ultimately, having a handset from a specific user or an emergency team record the pressure upon arrival of the first floor of a building will not provide a good reference for finding the floor of the UE in question.

Instead, collaborating UEs located on the same floor as the unknown UE could be used. The standing offset between the phones is not a concern in such a scenario as each phone makes altitude measurements based on a ground reference. If these measurements are then averaged across several co-located UEs, there may an increased potential to correctly identify the proper floor. In order to test this, a simulation was run following the use of the error models for different users and given the geometry of Durham Hall at Virginia Tech. This simulation assumes the same error models for measurements between floors as seen in Fig. 3.6 and Fig. 3.7. There are assumed to be 100 randomly placed users on the same floor as the "lost" device and then a random sample of these users are chosen to act as collaborators. Each device has their own measured pressure as well as ground reference pressure. The resulting error measurements with collaboration can be seen in Fig. 4.9 and Fig. 4.10. With the probability of correctly identifying the floor residing in the ± 7 ft range of error measurements, it can be seen that in both instances collaboration improves the performance. When averaging measurements with one collaborating UE, the error measurement falls between ± 7 ft for $5\% - 90\%$ of the data. This is a 20% improvement with the use of one collaborator as the data for ± 7 ft with a single user, single floor difference is $15\% - 85\%$. With the use of three collaborating UEs the probability of correctly distinguishing a single floor difference is approximately 98%. A summary of the probabilities for correctly distinguishing the floor the "lost" UE is located on can be seen in Table 4.1.

Table 4.1: Probability of Correctly Identifying Floor Location Given a Single Floor Change

Single Floor Difference Case	
Number of Collaborators	Probability of Correct Floor Detection
0	69.65%
1	88.70%
2	95.80%
3	97.75%
4	99.25%
5	99.60%

In the two floor difference case, the absolute error for ± 7 ft falls between 30% and 65% for the error model with one device. When averaged with one collaborating UE, the absolute error range is improved to cover between 20% and 80% of the data. Therefore approximately 20% more of the data resides between ± 7 ft and the probability of correctly estimating a two floor difference is equally improved. With the use of five collaborating devices, the desired absolute error is seen from $5\% - 95\%$. A summary of the probabilities for correct floor detection for the two floor case can be seen in Table 4.2.

Table 4.2: Probability of Correctly Identifying Floor Location Given a Two Floor Change

Two Floor Difference Case	
Number of Collaborators	Probability of Correct Floor Detection
0	36.25%
1	56.85%
2	69.10%
3	74.90%
4	79.10%
5	86.15%

As more UEs collaborate, their potential for correctly finding the floor they are on relative to the ground floor increases. As mentioned before, the distribution of error measurements seen in the pressure sensor increases with the number of floors away from ground. As such, the ability to correctly find the floor a user is on becomes harder and harder as the number of floors increases. However, with the use of collaborators the spread of error measurements can be reduced and the probability of finding the floor regardless of distance from ground can be enhanced.

4.4 Conclusion of Pressure Sensor based Geolocation

As a means to accurately locate a UE in three planes, X, Y and Z, while indoors, use of the barometric pressure sensor that is included in modern day phones is a promising solution in determining elevation. The barometric pressure can be used to calculate altitude and then a difference measurement from the ground-floor can be performed to determine offset or height in the building. As can be seen from the error models, when differentiating calculated altitude between various numbers of floors, there is potential to correctly identify the current

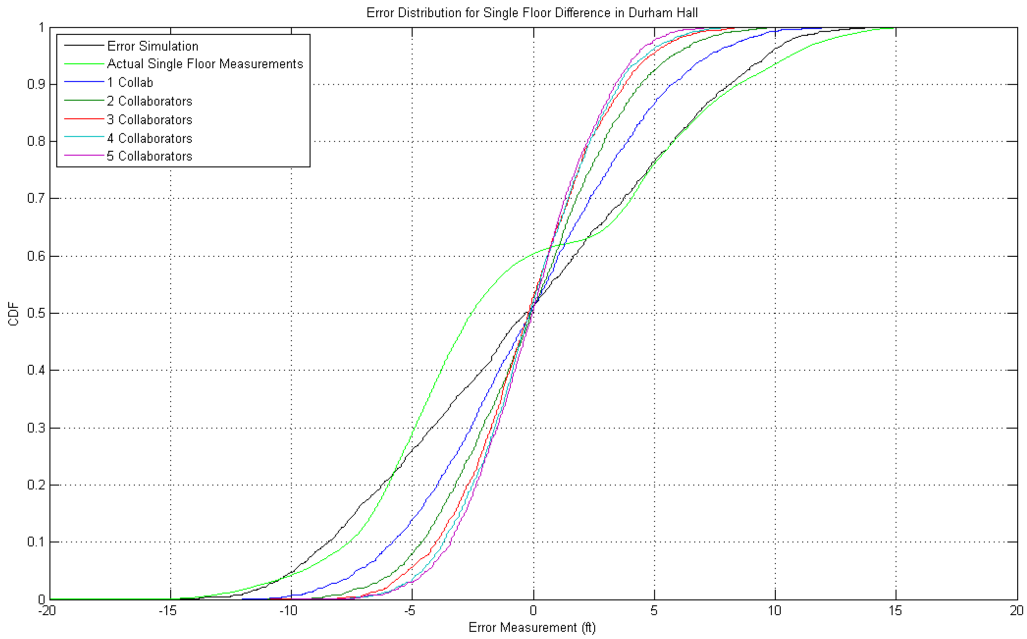

Figure 4.9: Simulation of Single Floor Difference Measurements when Collaborating with other UEs

floor of the device. Multiple methods were evaluated to test as feasible options of using a pressure sensor inside of a building. Ultimately, there are two methods proposed for Z-axis localization. First, having a UE with memory of pressure readings is the preferred choice for being able to ascertain differences in pressure from floor to floor. In order to discount the change of the indoor pressure from day to day and still ensure that the ground-floor reference measurement is valid, the barometric pressure will have to be recorded and stored each time the UE enters the building. A means of detecting the change of environment from outdoors to indoors will have to be put in place. Based on the ground reference measurement, the differential can be calculated, extrapolated to an elevation above the ground floor and, finally, it can be estimated what floor the UE is located on. This method is the most realistically attainable yet unique solution as the technology is already in place and the overall expenditures required for implementation are not unreasonable. To improve the probability of correction floor detection, this method could be paired with the use of other UEs as

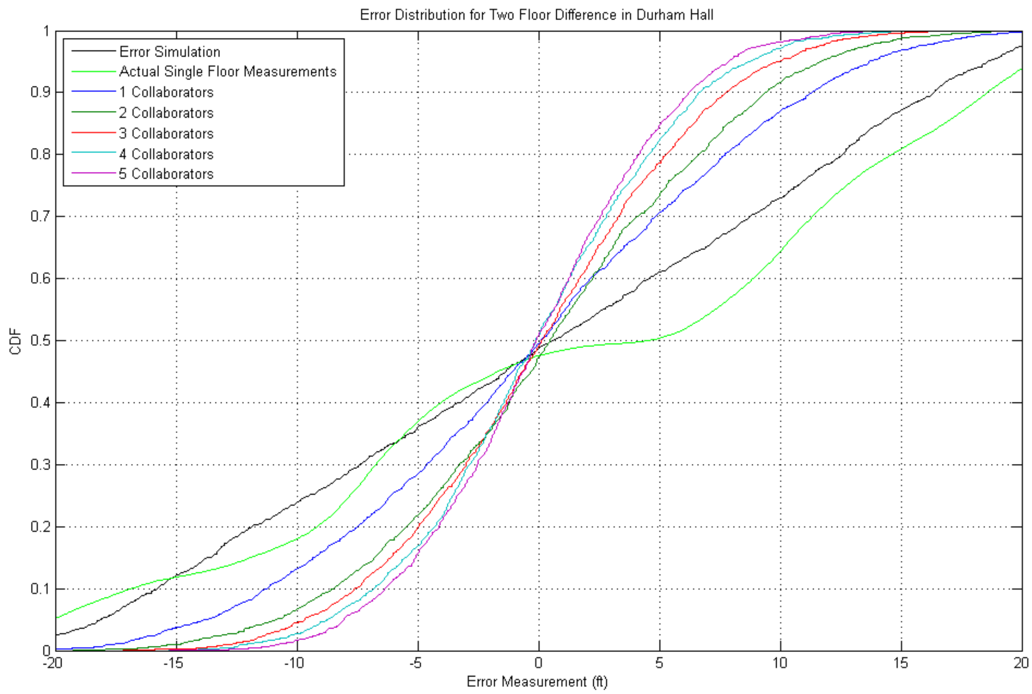

Figure 4.10: Simulation of Two Floor Difference Measurements when Collaborating with Users

collaborators. By averaging predicted altitudes with independent ground references, all cooperating UEs could minimize their potential for errors due to the environment, while also improving their chance of correctly identifying their floor location. Finally, the next and more sophisticated but expensive solution has mobile handsets synchronize with pressure sensors that are built into the infrastructure of the building. Through constant communication, the mobile handset would be able to identify it's location in a building given that its measured pressure, accounting for bias, matched that of the pressure sensors within the building on the same floor. The infrastructure sensors will continuously know the floor they are located on and as such the "lost" device simply has to verify it can observe a pressure close to that of the building sensor. The potential for error in such a case is minute as the building could almost tell the user which floor they are located on.

Chapter 5

Conclusion and Future Work

In this thesis cooperative positioning in LTE systems was studied for both the two-dimensional and three-dimensional case. A cooperative technique was proposed for uplink LTE systems where the UTDOA measurement method is used to estimate position between bases stations and UEs. Overall RTT was used as the measurement method between collaborating UEs. Through the use of computer simulations in Matlab, the benefits of cooperative localization over non-cooperative localization were determined. The zero collaborator case is capable of matching the UTDOA performance for SRS only transmissions achieved by TruePosition [12]. Overall, through the cooperation with other UEs, the ability to accurately localize a UE in a LTE network with UTDOA was improved, and it is capable of meeting current FCC horizontal location requirements for wireless 911 calls [4]. Through the use of one collaborator, the two-dimensional location error is within 50 m for 55% of the time. This performance exceeds the two and three year time frame requirements. By using five collaborators the requirements to be met within five years can also be met. Therefore, the proposed cooperative positioning technique significantly improves the positioning accuracy in comparison with non-cooperative localization and meets FCC wireless 911 location accuracy requirements currently set to be met within five years.

The use of barometric pressure sensors was studied to resolve the floor a handset is located on. Multiple test scenarios were shown, and the least complex and feasible method was proposed; taking a ground floor measurement and referring to it when moving up in the building. The correct floor was shown to be capable of being resolved more than 67% of the time give a single floor change, but this decreased given a larger change in altitude. Through the use of one collaborator and a one floor change in altitude, performance was improved by 20% in both the one and two floor change cases. In order to identify the correct floor 67% of the time with a two floor change from the ground reference there must be at least 2 collaborators. For future work regarding pressure sensors use in localization, it must be noted that the results here were dictated by the singular barometric pressure sensor model in the T-Mobile Galaxy S5 mobile handset. The error model for other pressure sensors could be characterized by better performance; having an absolute measurement error, e, less than 7 ft for a higher percentage of time. To further improve performance other methods of altitude measuring would have to be employed. Constant tracking of the pressure sensor could be done through the internet cloud and several complex algorithms or the building could relay the floor information to the mobile handset given infrastructure based pressure sensors. Complexity as well as cost become a larger burden that would need to be addressed for the most efficient means of achieving a desired third dimension accuracy required by the FCC.

Bibliography

[1] R. Zekavat, and R. M. Buehrer, Handbook of Position Location: Theory, Practice and Advances. John Wiley and Sons, 2011.

[2] C. Bokath, "Technical and Environmental Factors Affecting Indoor E911 Location Accuracy," Blind Tiger Communications.

[3] H. Tang, Z. Ding, and B. Levy, "Enabling D2D Communications Through Neighbor Discovery in LTE Cellular Networks," *IEEE Transactions on Signal Processing*, Vol. 62, No. 19, Oct. 1, 2014.

[4] Federal Communications Commission, "In the Matter of: Wireless E911 Location Accuracy Requirements," Ps Docket No. 07-114, Feb. 3 2015.

[5] "Basic LTE: Understanding Basic Concepts for LTE," SRS, http://lteshare.blogspot.com/2013/12/SRSLTE.html March 2015.

[6] R1-092998, 3GPP TSG RAN WG1 58 "Results for UTDOA Positioning Simulations," TruePosition. Aug. 2009.

[7] R1-094327, 3GPP TSG RAN WG1 58-bis "Network Based Positioning Support for LTE Rel9," Andrew Solutions. Oct. 2009.

[8] R1-094485, 3GPP TSG RAN WG1-59, "Uplink Signals for LTE Network Based Positioning," Andrew Solutions. Nov. 2009.

[9] R1-103410, 3GPP TSG RAN WG1-61, "Chairman's note on simulation assumptions

for UTDOA," NTT DOCOMO. May 2010.

[10] R1-105227, 3GPP TSG RAN WG1-62bis. "Aspects of Simulation Parameter for Network Based Positioning," Andrew Corporation. Oct. 2010.

[11] R1-104420, 3GPP TSG RAN WG1-62. "Further Evaluation of Network Based Positioning," Andrew Corporation. Aug. 2010.

[12] R1-106003, 3GPP TSG RAN WG1-63. "UTDOA Evaluation Summary," TruePosition. Nov. 2010.

[13] 3GPP Technical Specification 36.211, "Evolved Universal Terrestrial Radio Access (E-UTRA); Physical Channels and Modulation (Release 11)," Ver. 11.5.0, 2014.

[14] 3GPP Technical Specification 36.101, "Evolved Universal Terrestrial Radio Access (E-UTRA); User Equipment (UE) Radio Transmission and Reception (Release 11)," Ver. 11.8.0, 2014.

[15] W. Song; J. Lee; B. Lee; Schulzrinne, H., "Finding 9-1-1 callers in tall buildings," A World of Wireless, *Mobile and Multimedia Networks (WoWMoM)*, 2014 IEEE 15th International Symposium, pp.1,9, 19-19 June 2014.

[16] K. Muralidharan, A. Khan, A. Misra, R. Balan, and S. Agarwal, "Barometric Phone Sensors – More Hype Than Hope!," *Proceedings of the 15th Workshop on Mobile Computing Systems and Applications* Article No. 12, 2014.

[17] H. Ye, T. Gu, X. Tao, and J. Lu, "B-Loc: Scalable Floor Localization using Barometer on Smartphone," *Mobile Ad Hoc and Sensor System* IEEE 11th International Conference 2014.

[18] W. Namiki, M. Ichino, H. Yoshiura, "Altitude Estimation Using Mobile Terminal's Pressure Sensor and External Weather Information," *The 18th IEEE International Symposium on Consumer Electronics*, pp.1-3, 22-25 June 2014.

[19] A. Moschevikin, R. Voronov, A. Galov, A. Soloviev, "Using Pressure Sensors for Floor

Identification in Wireless Sensors Networks," *IEEE 1st International Symposium on Wireless Systems*, pp.2,6, 20-21 Sept. 2012

[20] J.Parviainen, J. Kantola, and J. Collin, "Differential Barometry in Personal Navigation," *IEEE Position, Location and Navigation Symposium*,pp.148,152, 5-8 May 2008.

[21] C. Bollmeyer, T. Esemann, H. Gehring, H. Hellbruck, "Precise Indoor Altitude Estimation Based on Differential Barometric Sensing for Wireless Medical Applications," *IEEE International Conference on Body Sensor Networks*,pp.1-6, 6-9 May 2013.

[22] Binghao Li; Harvey, B.; Gallagher, T., "Using barometers to determine the height for indoor positioning," *International Conference on Indoor Positioning and Indoor Navigation*, pp.1-7, 28-31 Oct. 2013.

[23] R. Niemi, TopoQuest. Apr. 2015. ¡https://www.topoquest.com/place-detail.php?id=2110657¿

[24] Torbjörn Wigren, "LTE Fingerprinting Localization with Altitude," Ericsson.

[25] "Atmospheric Pressure, Winds, and Circulation Patterns," Cengage. Ch.5. pp. 113-137.

[26] D. Green. "Pressure, Barometers, and Barometric Pressure," http://www.challengers101.com/Pressure.html 2015.

[27] M. Mahmood Shakir and Dr. S. Abdul-Mawjoud, "U-TDOA Position Location Technique for WCDMA". *Tikrit Journal of Engineering Sciences*, vol.20, No.1, pp 29-41, Mar. 2013.

[28] R. Mardeni , K. Anuar, P. Shahabi, and M, Riahimanesh, "Efficient Uplink Time Difference of Arrival Mobile Device Localization in Cellular Networks," *Asia-Pacific Microwave Conference Proceedings* pp. 1124-1126, Nov. 2013.

[29] R. Mardeni , P. Shahabi, and M, Riahimanesh, "Mobile Station Localization in Wireless Cellular Systems Using UTDOA," Vol. 5, pp. 1-4, May 2012.

[30] Yehia R. Hamdy and Dr. Sami A. Mawjoud, "Performance Assessment of U-TDOA

and A-GPS Positioning Methods," *International Conference on Future Communication Networks*, 2012.

[31] A. Hatami, B. Alavi, K.h Pahlavan, and M. Kanaan, "A Comparative Performance Evaluation of Indoor Geolocation Technologies," *Interdisciplinary Information Sciences*, Vol. 12, No. 2, pp. 133–146. April 2006.

[32] N. Patwari, J. N. Ash, S. Kyperountas, A. O. Hero III, R. L. Moses, and N. S. Correal, "Locating the nodes: Cooperative localization in Wireless Sensor Networks," *IEEE Signal Process. Mag.*, Vol. 22, No. 4, pp. 54–69, Jul. 2005.

[33] N. Patwari, A. Hero, M. Perkins, N. Correal, and R. J. O'Dea, "Relative Location Estimation in Wireless Sensor Networks," *IEEE TRANSACTIONS ON SIGNAL PROCESSING*, Vol. 51, No. 8, Aug. 2003.

[34] R. M. Vaghefi and R. M. Buehrer, "Improving Positioning in LTE through Collaboration". 2014.

[35] Y.T. Chan and K. C. Ho "A Simple and Efficient Estimator for Hyperbolic Location," *IEEE TRANSACTIONS ON SIGNAL PROCESSING*, Vol. 42, No. 8. Aug. 1994.

[36] W.H. Foy "Position-Location Solutions by Taylor-Series Estimation," *IEEE Transactions on Aerospace and Electronic Systems*, Vol.AES-12, No.2, pp.187-194, March 1976.

[37] D.J. Torrieri "Statistical Theory of Passive Location Systems," *IEEE Transactions on Aerospace and Electronic Systems*, Vol.AES-20, No.2, pp.183-198, Mar. 1984.

[38] 3GPP Technical Specification 36.305, "Evolved Universal Terrestrial Radio Access Network (E-UTRAN); Stage 2 functional specification of User Equipment (UE) positioning in E-UTRAN (Release 9)," 2009.

[39] A. Asadi, Q. Wng, and V. Meancuso, "A Survey on Device-to-Device Communication in Cellular Networks," *IEEE Communications Surveys and Tutorials*, Vol.16, No.4, pp.1801-1819, 2014.

[40] L. Xingqin; J. Andrews; A. Ghosh; R. Ratasuk, "An Overview of 3GPP Device-to-Device Proximity services," *IEEE Communications Magazine*, Vol.52, No.4, pp.40-48, April 2014.

[41] F. Benedetto, G. Giunta, E. Guzzon, "Enhanced TOA-based Indoor-Positioning Algorithm for Mobile LTE Cellular Systems," *8th Workshop on Positioning Navigation and Communication (WPNC)*, pp.137-142, 7-8 April 2011.

[42] P. Yi, M. Yu, Z. Zhou, W. Xu, Q. Zhang, and T. Zhu, "A Three-Dimensional Wireless Indoor Localization System," *Journal of Electrical and Computer Engineering*, Vol. 2014, Article ID 149016, 2014.

[43] Calin, D.; Kaya, A.O.; Petrut, I., "On the In-Building Performance and Feasibility of LTE Small Cells with Beamforming Capabilities," *Globecom Workshops*, pp.1211-1216, 8-12 Dec. 2014.

[44] A.O. Kaya and D. Calin, "Modeling Three Dimensional Channel Characteristics in Outdoor-to-Indoor LTE Small Cell Environments," *IEEE Military Communications Conference*, MILCOM,pp.933-938, 18-20 Nov. 2013.

[45] V. Torres, F. Esparza, F. Falcone, "Simulation and Analysis of Performance of LTE in Indoor Environments," *Mediterrannean Microwave Symposium (MMS)*, pp.1-5, 15-17 Nov. 2009.

[46] R. Surgiewicz, N. Strom, A. Ahmed and Y. Ai." LTE Uplink Transmission Scheme," Apr. 2014. ¡http://www.mehrpouyan.info/Projects/Group%201.pdf¿.

[47] "SC-FDMA Single Carrier FDMA in LTE," IXIA Nov. 2009.

[48] H. Gavin "The Levenberg-Marquardt Method for Nonlinear Least Squares Curve-Fitting Problems," Oct. 2013.

[49] S. Gezici and H.V. Poor, "Position Estimation via Ultra-Wide-Band Signals," *Proceedings of the IEEE*, Vol.97, No.2, pp.386-403, Feb. 2009.

[50] J. Bull, ”Wireless Geolocation: Advantages and Disadvantages of the Two Basic Approaches for E-911,” *IEEE Vehicular Technology Mag.*, Dec. 2009.

[51] ”Positioning With LTE,” Ericsson, Sept. 2011.

[52] M. Abo-Zahhad, Sabah M. Ahmed, and M. Mourad ”Hybrid Uplink-Time Difference of Arrival and Assisted-GPS Positioning Technique,” *Int. J. Communications, Network and System Sciences*, pp. 303-312, May 2012.

[53] Mike Thorpe, M. Kottkamp, A. Rössler, and J. Schütz, ”LTE Location Based Services Technology Introduction,” Apr. 2013.

[54] Hui Liu, H. Darabi, P. Banerjee, and J. Liu ”Survey of Wireless Indoor Positioning Techniques and Systems,” *IEEE TRANSACTIONS ON SYSTEMS, MAN, AND CYBERNETICS—PART C: APPLICATIONS AND REVIEWS*, Vol. 37, No. 6, Nov. 2007.

[55] ”LTE Positioning Technology for Mobile Devices: Test Challenges and Solutions,” White Paper. Spirent. Rev. A. Feb. 2012.

[56] Ana-Maria Roxin, J. Gaber, M. Wack, and A. Nait Sidi Moh ”Survey of Wireless Geolocation Techniques,” *IEEE Globecom Workshops*, Nov. 2007, Washington, DC, United States. pp.9.

[57] A. Kangas and T. Wigren ”Location Coverage and Sensitivity with A-GPS,” *Ericsson AB, SE-164 80.* 2004. pp. 361-363.

[58] WeatherUnderground. http://www.wunderground.com/personal-weather-station/dashboard?ID=MD8443.

[59] Bosch LLC, ”Comments of Bosch Sensortec,” FCC. PS Docket No. 07-114, Washington DC, May 2014.

[60] Shwetak N. Patel, M. Reynolds, and G. Abowd, ”Detecting Human Movement by Differential Air Pressure Sensing in HVAC System Ductwork: An Exploration in Infrastructure Mediated Sensing”. Springer. 2008.

[61] W. Bauer and G. Westfall, "University Physics," McGraw-Hill. Ch. 13, pp. 435. Copyright 2011.

[62] "High and Low Pressure," Met Office. <http://www.metoffice.gov.uk/learning/learn-about-the-weather/how-weather-works/highs-and-lows/pressure>. Sept. 3 2013. Jan. 2015.

[63] U.S. Climate and Data <http://www.usclimatedata.com/map.php?location=USVA0068>. Jan. 2015.

[64] Pressure Altitude <http://www.srh.noaa.gov/images/epz/wxcalc/pressureAltitude.pdf>. Jan. 2015.

[65] Rick Quirouette and B.Arch. "Air Pressure and the Building Envelope," Nov. 2004.

[66] R1-105998, 3GPP TSG RAN WG1-63, "Specification Impact Analysis of UTDOA," Alcatel-Lucent. Nov. 2010.

Chapter 6

Appendix

Appendix A: Bosch BMP280 Pressure Sensor

http://www.mouser.com/ds/2/621/BST-BMA280-DS000-11_published-471424.pdf

Used under fair use, 2015.

Data sheet

BMA280
Digital, triaxial acceleration sensor

Bosch Sensortec

BOSCH
Invented for life

BMA280: Data sheet

Document revision	1.8
Document release date	01 August 2014
Document number	BST-BMA280-DS000-11
Technical reference code(s)	0 273 141 148
Notes	Data in this document are subject to change without notice. Product photos and pictures are for illustration purposes only and may differ from the real product's appearance. Not intended for publishing

BMA280

14 BIT, DIGITAL, TRIAXIAL ACCELERATION SENSOR WITH INTELLIGENT ON-CHIP MOTION-TRIGGERED INTERRUPT CONTROLLER

Key features

• Ultra-Small package	LGA package (12 pins), footprint 2mm x 2mm, height 0.95mm
• Digital interface	SPI (4-wire, 3-wire), I²C, 2 interrupt pins V_{DDIO} voltage range: 1.2V to 3.6V
• Programmable functionality	Acceleration ranges ±2g/±4g/±8g/±16g Low-pass filter bandwidths 500Hz - <8Hz up to an max. output data read out of 2kHz (unfiltered)
• On-chip FIFO	Integrated FIFO with a depth of 32 frames
• On-chip interrupt controller	Motion-triggered interrupt-signal generation for - new data - any-motion (slope) detection - tap sensing (single tap / double tap) - orientation recognition - flat detection - low-g/high-g detection - no-motion / inactivity detection
• Ultra-low power	Low current consumption, short wake-up time, advanced features for system power management
• Temperature sensor	
• RoHS compliant, halogen-free	

Typical applications

- Display profile switching
- Menu scrolling, tap / double tap sensing
- Gaming
- Pedometer / step counting
- Free-fall detection
- E-compass tilt compensation
- Drop detection for warranty logging
- Advanced system power management for mobile applications

General description

The BMA280 is a triaxial, low-g acceleration sensor with digital output for consumer applications. It allows measurements of acceleration in three perpendicular axes. An evaluation circuitry (ASIC) converts the output of a micromechanical acceleration-sensing structure (MEMS) that works according to the differential capacitance principle.

Package and interfaces of the BMA280 have been defined to match a multitude of hardware requirements. Since the sensor features an ultra-small footprint and a flat package it is ingeniously suited for mobile applications.

The BMA280 offers a variable V_{DDIO} voltage range from 1.2V to 3.6V and can be programmed to optimize functionality, performance and power consumption in customer specific applications. In addition it features an on-chip interrupt controller enabling motion-based applications without use of a microcontroller.

The BMA280 senses tilt, motion, inactivity and shock vibration in cell phones, handhelds, computer peripherals, man-machine interfaces, virtual reality features and game controllers.

1. Specification

Unless stated otherwise, the given values are over lifetime, operating temperature and voltage ranges. Minimum/maximum values are ±3σ.

Table 1: Parameter specification

OPERATING CONDITIONS						
Parameter	**Symbol**	**Condition**	**Min**	**Typ**	**Max**	**Units**
Acceleration Range	g_{FS2g}	Selectable via serial digital interface		±2		g
	g_{FS4g}			±4		g
	g_{FS8g}			±8		g
	g_{FS16g}			±16		g
Supply Voltage Internal Domains	V_{DD}		1.62	2.4	3.6	V
Supply Voltage I/O Domain	V_{DDIO}		1.2	2.4	3.6	V
Voltage Input Low Level	V_{IL}	SPI & I²C			$0.3V_{DDIO}$	-
Voltage Input High Level	V_{IH}	SPI & I²C	$0.7V_{DDIO}$			-
Voltage Output Low Level	V_{OL}	I_{OL} = 3mA, SPI & I²C			$0.2V_{DDIO}$	-
Voltage Output High Level	V_{OH}	I_{OH} = 3mA, SPI	$0.8V_{DDIO}$			-
Total Supply Current in Normal Mode	I_{DD}	T_A=25°C, $ODR_{max.}$ $V_{DD} = V_{DDIO}$ = 2.4V		130		µA
Total Supply Current in Suspend Mode	I_{DDsum}	T_A=25°C $V_{DD} = V_{DDIO}$ = 2.4V		2.1		µA
Total Supply Current in Deep Suspend Mode	I_{DDdsum}	T_A=25°C $V_{DD} = V_{DDIO}$ = 2.4V		1		µA
Total Supply Current in Low-power Mode 1	I_{DDlp1}	T_A=25°C, unfiltered $V_{DD} = V_{DDIO}$ = 2.4V sleep duration = 25ms		6.5		µA

Total Supply Current in Low-power Mode 2	I_{DDlp2}	T_A=25°C, unfiltered $V_{DD} = V_{DDIO}$ = 2.4V sleep duration = 25ms		66		µA
Total Supply Current in Standby Mode	I_{DDsbm}	T_A=25°C $V_{DD} = V_{DDIO}$ = 2.4V		62		µA
Wake-Up Time 1	$t_{w,up1}$	from Low-power Mode 1 or Suspend Mode or Deep Suspend Mode, $ODR_{max.}$		1.3	1.8	ms
Wake-Up Time 2	$t_{w,up2}$	from Low-power Mode 2 or Stand-by Mode, $ODR_{max.}$		1	1.2	ms
Start-Up Time	$t_{s,up}$	POR, $ODR_{max.}$			3	ms
Non-volatile memory (NVM) write-cycles	n_{NVM}				15	cycles
Operating Temperature	T_A		-40		+85	°C

OUTPUT SIGNAL

Parameter	Symbol	Condition	Min	Typ	Max	Units
Sensitivity	S_{2g}	g_{FS2g}, T_A=25°C		4096		LSB/g
	S_{4g}	g_{FS4g}, T_A=25°C		2048		LSB/g
	S_{8g}	g_{FS8g}, T_A=25°C		1024		LSB/g
	S_{16g}	g_{FS16g}, T_A=25°C		512		LSB/g
Sensitivity Temperature Drift	TCS	g_{FS2g}, Nominal V_{DD} supplies		0.015		%/K
Zero-g Offset	Off	g_{FS2g}, T_A=25°C, nominal V_{DD} supplies, over life-time		±50		mg
Zero-g Offset Temperature Drift	TCO	g_{FS2g}, Nominal V_{DD} supplies		±1.0		mg/K
Bandwidth	bw_8	2nd order filter, bandwidth programmable		8		Hz
	bw_{16}			16		Hz
	bw_{31}			31		Hz
	bw_{63}			63		Hz
	bw_{125}			125		Hz
	bw_{250}			250		Hz
	bw_{500}			500		Hz
Output Data Rate	$ODR_{max.}$	unfiltered		2000		Hz
Nonlinearity	NL	best fit straight line, g_{FS2g}		±0.5		%FS

Output Noise Density	n_{rms}	g_{FS2g}, T_A=25°C Nominal V_{DD} supplies Normal mode		120		µg/√Hz
Temperature Sensor Measurement Range	T_S		-40		85	°C
Temperature Sensor Slope	dT_S			0.5		K/LSB
Temperature Sensor Offset	OT_S			±2		K

MECHANICAL CHARACTERISTICS

Parameter	Symbol	Condition	Min	Typ	Max	Units
Cross Axis Sensitivity	S	relative contribution between any two of the three axes		1		%
Alignment Error	E_A	relative to package outline		±0.5		°

2. Absolute maximum ratings

Table 2: Absolute maximum ratings

Parameter	Condition	Min	Max	Units
Voltage at Supply Pin	V_{DD} Pin	-0.3	4.25	V
	V_{DDIO} Pin	-0.3	4.25	V
Voltage at any Logic Pin	Non-Supply Pin	-0.3	V_{DDIO}+0.3	V
Passive Storage Temp. Range	≤ 65% rel. H.	-50	+150	°C
None-volatile memory (NVM) Data Retention	T = 85°C, after 15 cycles	10		y
Mechanical Shock	Duration ≤ 200µs		10,000	g
	Duration ≤ 1.0ms		2,000	g
	Free fall onto hard surfaces		1.8	m
ESD	HBM, at any Pin		2	kV
	CDM		500	V
	MM		200	V

Note:
Stress above these limits may cause damage to the device. Exceeding the specified electrical limits may affect the device reliability or cause malfunction.

Appendix B: STMicroElectronics LPS25H Pressure Sensor

http://www.st.com/web/catalog/sense_power/FM89/SC1316/PF255230

Used under fair use, 2015.

LPS25H

MEMS pressure sensor: 260-1260 hPa absolute digital output barometer

Datasheet - production data

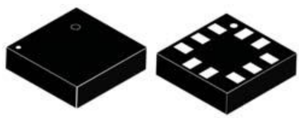

HCLGA-10L
(2.5 x 2.5 x 1.0 mm)

Features

- 260 to 1260 hPa absolute pressure range
- High-resolution mode: 1 Pa RMS
- Low power consumption:
  – Low resolution mode: 4 µA
  – High resolution mode: 25 µA
- High overpressure capability: 20x full scale
- Embedded temperature compensation
- Embedded 24-bit ADC
- Selectable ODR from 1 Hz to 25 Hz
- SPI and I²C interfaces
- Embedded FIFO
- Supply voltage: 1.7 to 3.6 V
- High shock survivability: 10,000 *g*
- Small and thin package
- ECOPACK® lead-free compliant

Applications

- Altimeter and barometer for portable devices
- GPS applications
- Weather Station Equipment
- Sport Watches

Description

The LPS25H is an ultra compact absolute piezoresistive pressure sensor. It includes a monolithic sensing element and an IC interface able to take the information from the sensing element and to provide a digital signal to the external world.

The sensing element consists of a suspended membrane realized inside a single mono-silicon substrate. It is capable to detect the absolute pressure and is manufactured with a dedicated process developed by ST.

The membrane is very small compared to the traditionally built silicon micromachined membranes. Membrane breakage is prevented by an intrinsic mechanical stopper.

The IC interface is manufactured using a standard CMOS process that allows a high level of integration to design a dedicated circuit which is trimmed to better match the sensing element characteristics.

The LPS25H is available in a cavity holed LGA package (HCLGA). It is guaranteed to operate over a temperature range extending from -30 °C to +105 °C. The package is holed to allow external pressure to reach the sensing element.

Table 1. Device summary

Order codes	Temperature range [°C]	Package	Packing
LPS25HTR	-30 to +105	HCLGA-10L	Tape and reel
LPS25H		HCLGA-10L	Tray

2 Mechanical and electrical specifications

2.1 Mechanical characteristics

V_{DD} = 2.5 V, T = 25 °C, unless otherwise noted.

Table 3. Mechanical characteristics

Symbol	Parameter	Test condition	Min.	Typ.[1]	Max.	Unit
Top	Operating temperature range		-30		105	°C
Tfull	Full accuracy temperature range		0		80	°C
Pop	Operating pressure range		260		1260	hPa
Pbits	Pressure output data			24		bits
Psens	Pressure sensitivity			4096		LSB/ hPa
Paccrel	Relative accuracy over pressure[2]	P = 800 to 1100 hPa T = 25°C		± 0.1		hPa
PaccT	Absolute accuracy pressure over temperature[3]	P = 260 to 1260 hPa T = 20 ~ +60 °C		± 0.2		hPa
		P = 260 to 1260 hPa T = 0 ~ +80 °C		± 1		
Pnoise	Pressure noise[4]	without embedded filtering		0.03		hPa RMS
		with embedded filtering		0.01		
Tbits	Temperature output data			16		bits
Tsens	Temperature sensitivity			480		LSB/°C
Tacc	Absolute accuracy temperature	T= 0 ~ +65 °C		± 2		°C

1. Typical specifications are not guaranteed.
2. Characterization data. Parameter not tested at final test
3. Embedded quadratic compensation.
4. Pressure noise RMS evalueted in a controlled environment,based on the average standard deviation of 32 measurements at highest ODR.

2.2 Electrical characteristics

VDD = 2.5 V, T = 25 °C, unless otherwise noted.

Table 4. Electrical characteristics

Symbol	Parameter	Test condition	Min.	Typ.[1]	Max.	Unit
VDD	Supply voltage		1.7		3.6	V
VDD_IO	IO supply voltage		1.7		3.6	V
Idd	Supply current @ ODR 1 Hz, highest resolution			25		µA
IddPdn	Supply current in power-down mode T = 25 °C			0.5		µA

1. Typical specifications are not guaranteed.